

Gradu Amaierako Lana/Trabajo Fin de Grado

Fisikako Gradua/Grado en Física

Classical and Quantum Artificial Life

Asier Izquierdo

Director:

Prof. Enrique Solano

Codirector:

Dr. Mikel Sanz

Department of Physical Chemistry
Faculty of Science and Technology
University of the Basque Country UPV/EHU

Leioa, June 2018

Contents

Contents	2
1 Introduction and objectives	4
1.1 Categorization	5
1.2 Objectives and relevance	6
2 Classical artificial life	7
2.1 Definition of cellular automata	7
2.2 Cellular automata example: the game of life	8
2.3 Implementation of game of life	8
2.3.1 Code	8
2.3.2 Results	8
2.4 Transition from classical to quantum artificial life	9
2.4.1 Probabilistic picture of measurements	10
2.4.2 Quantum implementation of GoL rules (without phase difference $e^{i\phi}$)	10
2.4.3 A more quantum-like implementation of GoL rules (with phase difference $e^{i\phi}$)	13
3 Fundamentals of quantum artificial life	14
3.1 Qubits	14
3.1.1 Bloch representation	15
3.1.2 Single qubit quantum logic gates	17
3.2 Controlled-NOT quantum logic gate (\hat{U}_{CNOT})	18
3.3 No-cloning theorem	19
3.3.1 General no-cloning theorem	19
3.3.2 No-cloning theorem for approximate cloning	20
4 Quantum artificial life model	21
4.1 Finite lifetime ($\langle \hat{\sigma}_z \rangle_{\hat{\rho}_p}(t)$), time constant genotype ($\langle \hat{\sigma}_z \rangle_{\hat{\rho}_g} \neq \langle \hat{\sigma}_z \rangle_{\hat{\rho}_g}(t)$) and relative trophic roles ($\langle \hat{\sigma}_z \rangle_{\hat{\rho}_g} \leq \langle \hat{\sigma}_z \rangle_{\hat{\rho}_g}$)	21
4.2 Reproduction: self-replication	22
4.2.1 Quantum partial cloning operator \hat{U} as self-replication operator	24
4.2.2 Genotype creation	26
4.2.3 Phenotype creation	27
4.2.4 Preservation of $\langle \hat{\sigma}_z \rangle$ after self-replications	28
4.3 Phenotype change	29
4.3.1 Environment	30
4.3.2 Inter-individual interaction	31
4.4 Experimental implementation	32
4.4.1 Experimental implementation of self-replication	33
4.4.2 Experimental implementation of environment's decoherence	34
5 Conclusions	35
Bibliography	37
Appendix A Codes	38

A.1	Game of life implementation	38
A.2	Quantum GoL implementation	41
A.2.1	Quantum GoL without phase $e^{i\phi}$	41
A.2.2	Quantum GoL with phase $e^{i\phi}$	41
A.3	Quantum artificial life code	44
Appendix B Calculations		50
B.1	Why did we choose $t \uparrow$, $\langle \hat{\sigma}_z \rangle_{\hat{\rho}_p} \uparrow$?	50
B.2	If $\hat{\sigma}_z$ is the observable whose expectation value in the genotype subspace is chosen to be preserved by Eq. (4.2), and $\hat{\rho}_A = 0\rangle\langle 0 $, why $\hat{U} = \hat{U}_{\text{CNOT}}$?	51
B.3	Calculations of $\hat{\rho}_{g_1}$, Eq. (4.8), and \hat{U}_{CNOT} , Eq. (4.9)	53
B.4	Calculations of Eq. (4.15-4.17)	53
B.5	Why is $\hat{\rho}_A$ the steady state of our Lindbladian?	55
B.6	Calculations of $\hat{\rho}_{p_0}(t)$, Eq. (4.21)	57
B.7	Calculations of Eq. (4.22-4.23)	59
B.8	Proof of Eq. (4.30)	59
B.9	Proof of Eq. (4.31)	60
B.10	Calculations of $\langle \tilde{H}_k \rangle_{\hat{\rho}_g^\alpha \otimes \hat{\rho}_g^\beta _{k=\alpha}}$, Eq. (4.26)	61

1 Introduction and objectives

Mimicking how classical computers are built from electrical circuits, quantum computers (QC) can be built from quantum circuits [1, p. 17, l. 30-32]. Regarding the former, classical bits are stored on capacitors: uncharged (charged) capacitors register the bit 0 (1). Concerning the latter, in contrast to pure abstraction's hegemony in classical computation, QCs process information by patent physical means such as photons, spins or atoms: respectively, superposition of photons (particle of light) in the arms of an interferometer¹; the two different polarizations of a photon or, more broadly, the alignment of the up $|\uparrow\rangle$ and down $|\downarrow\rangle$ states of a spin-1/2 particle; or the superposition of two atomic energy levels [1, p. 14, l. 16-17].

For instance, digging into the last physical device, the one based on atomic energy levels, an ion in its ground, or lowest energy, state $|g\rangle \equiv |0\rangle$ (in one of its excited states $|e\rangle \equiv |1\rangle$) can be identified with an uncharged (charged) capacitor [2, p. 1073, l. 8-19]. Here, independent manipulation of each atom or 2-level subsystem is accomplished by laser beams.

Quantum computation studies this sort of systems. Combining physics, mathematics and computer science, it is an *abstract paradigm* for information processing encoded in quantum mechanical variables that may have plenty of applications (Section 1.2) in technology [1, p. 50, l. 36-37]. It takes its power from exploiting the following features, which have no classical analog: quantum **superposition** and **entanglement**².

Superposition consists on the weighted sum of two or more states. It allows more efficiency in terms of memory (for example, a 2-level state like the aforementioned ions in paragraph 2 can be represented by a single quantum bit or **qubit**³, instead of two classical bits) and time (superposition allows following various computation paths simultaneously, exploiting what is called *quantum parallelism*).

Superposition classically corresponds, for instance, to the state of the air when two or more music tones simultaneously sound, to the classical interference of their waves. However, conventional interferences like playing n music tones at once can only yield classical superpositions of n states.

On the other hand, a quantum superposition of n quantum bits, is defined by means of 2^n complex numbers or amplitudes, so it takes 2^n resources in a classical computer. In other words, if we measure this quantum state, the output will be one of the 2^n possible classical bits. For instance, a 2-qubit pure state $|\psi\rangle$ is described by $2^{(n=2)} = 4$ linearly independent complex numbers or, equivalently, $2^{(n=2)} = 4$ base states –basis $\{|0\rangle, |1\rangle\}^{\otimes(n=2)}$ –: $|\psi\rangle = a|00\rangle + b|01\rangle + c|10\rangle + d|11\rangle$.

Then, a conventional computers needs more than a million numbers (2^{20} , concretely) to describe only 20 qubits. In a QC, however, performing the evolution of a quantum system with n two-dimensional systems requires only n quantum bits! [2, p. 1074, l. 1] Thus, although a conventional computer can be programmed (even when inefficient, as seen) to *represent* a quantum superposition, this is different from its classical memory actually *being* in this quantum superposition of qubits.

Moreover, QCs are able to perform classical logic gates – f functions from some fixed number m of input

¹See an **example** on the author's web page. Links to the author's web are meant to help make a more global perspective of the work, but they can be skipped. However, we earnestly recommend reading the work on a computer, so that hyperlinks to calculations (Appendix B) and bibliographic references can be employed.

²For additional information the reader is referred to **entanglement**, on the author's website.

³For more information about the *qubit* approach, see Section 3.1.

bits to some fixed number n of output bits, $f : \{0, 1\}^m \rightarrow \{0, 1\}^n$ – as well as quantum ones. Quantum logic gates are generalizations of classical logic gates. They use qubits in quantum superposition of classical bits 0 and 1. Since QCs are capable of using both classical and quantum gates, they are at least as efficient as conventional computers.

If the advantages pointed so far are not sufficient to persuade you, we can sell it better: Moore’s law is presumably reaching its asymptote and, at microscopic scale, quantum effects become important and classical computation theory becomes fundamentally inadequate. The (medium-term) future is quantum!

In particular, let us name, as examples, three main classes of quantum algorithms which excel those belonging to classical computers: algorithms that provide quantum versions of the Fourier transform, quantum search algorithms and **quantum simulations** [1, p. 37, l. 4-10] [2, p. 1073, l. 65-68].

Algorithms are precise recipes for performing particular tasks and constitute the key concept of computer science. The last type described in the previous paragraph entails mimicking quantum mechanical systems, by engineering Hamiltonians which effectively resemble the dynamics of the system to emulate, beyond classical limitations [1, p. 39, l. 6-10], which allows us to manipulate rather than merely observe quantum phenomena. Engineering Hamiltonians means having one system simulate another *directly* and classical limitations refer to the use of amounts of resources, computer time and memory space, that grow as exponential functions with the number of variables (particles, lattice sites, etc.) required to characterize the system of interest [2, p. 1073, l. 89-95].

In this bachelor thesis, we will develop the idea of *Artificial life* (AL) – the study of biological phenomena by means of simulations –, a prototypical branch of the mentioned quantum simulations. It serves as a source to gain a deeper understanding about the complex systems which characterize living beings or, with a wider connotation, *living systems* (cells -either nerve cells, named neurons, or tumor cells-, tissues, organisms, ecosystems, human societies or financial markets). [4, p. 47]

1.1 Categorization

We will follow a scheme fitting the two categories into which the field of Artificial Life can be split:

Section 2, **Classical Artificial Life** (CAL): we introduce John Conway’s popular cellular automaton, *Game of Life* (GoL), invented in 1970 [4, p. 40], which provides CAL’s most notable example. It consists of a 2D grid or lattice of square cells that can be in one of two states: populated (*alive*) or not (*dead*). Its evolution is determined by discrete time step interactions with each cell’s Moore neighborhood.

The importance of Conway’s automaton system resides in the fact that simple individual cells’ interaction rules are able to produce patterns of great complexity. It even has the power to create an universal Turing machine [6, p. 520, Fig. 26.1], a classical computing device capable of efficiently carrying out any algorithm –in computational space (memory) and time (steps) that scale polynomially with the input size–, according to the Church-Turing thesis [1, p. 125, l. 10-13] –in its quantitative or strong form [3, p. 2, Thesis. 1.1]–.

Roughly speaking, some aspects belonging to the field of *deterministic chaos* could be identified in this CAL example. Id est, the laws of the system are well known and strict – besides, straightforward, in the case of GoL– and its evolution depends only on the initial state (*deterministic*), but the result of iterating these

simple steps many times cannot be precisely determined and, despite the lack of randomness, it recalls *chaos*. This special coexistence among order and disorder plays a relevant role in understanding some basic features of quantum systems, such as entanglement². Due to the extraordinary complexity of these results, presently, *the computer has become our new telescope* [4, p. 17-18], even for the relatively simple code in Appendix A.1.

Section 4, **Quantum Artificial Life** (QAL), constitutes the second part of this work. It is mainly based on Ref. [7], where *the first experimental realization of a QAL algorithm in a QC* [7, p. 1, l. 1-2] was presented. Here, biological behaviors such as self-replication (used as a reproduction mechanism), mutation, interaction (feeding on predator-prey ecological subsistence relationships), aging and death (finite lifetime), consistent with the mechanisms of evolution (Darwinian laws of natural selection, such as partial preservation of the genetic information and survival of better adapted living beings), were mimicked based on quantum information protocols.

1.2 Objectives and relevance

Along with the goal proposed in Ref. [7, p. 2, l. 15-16] –reproducing the characteristic processes of natural selection, adapted to the language of quantum computing and, more precisely, quantum simulation–, intellectually appealing by itself, we also want to emphasize the importance of AL.

For instance, the cohabitation of predators and preys in the just mentioned QAL example could be replaced in another seemingly different field such as a medical context by cancerous and healthy cells [4, p. 49]; within an ecological framework, as polluted and clean air; or even the development of inventions –why do forks have 4 tines?–, since as the paleobiologist Niles Eldredge proposes, both the evolution of the species and technology have the propagation of some information as a common point [4, p. 129, l. 12-13].

The value of QAL relies upon the fact that experimental implementation of QAL might notably contribute to understand quantum mechanics and the emergency of life and complex systems. Although achievable with current QCs [15, p. 1, l. 6-7], constructing QAL experimental setups constitutes a great challenge per se, and simulating the described QAL model can only be done for a small number of individuals and generations, for the moment, which limits the results. As Richard Feynman said [4, p. 69, l. 30-31]: *What I cannot create, I do not understand*. In this case, both parts of the quote feedback: knowledge and an unending number of attempts are needed in order to tackle the technological difficulties that await the realization of experimental implementation of QCs, and, at the same time, empirical results are expected to shed new light on the foundations of quantum physics.

In fact, this is exactly one of our objectives: processing information quantum mechanically is a utterly new field for us, so we hope this work signifies a remarkable widening of scope in the applications of quantum mechanics seen, so far, in our Physics degree.

Moreover, we will argue that quantum computing, based on lifeless microscopic matter (atoms, photons, etc.) that follows the laws of quantum mechanics, is the most appropriate tool to simulate the evolution of (here, living or biological, AL) systems with complex outputs. To this end, we compare both Classical (GoL, here) and Quantum Artificial Life systems. That’s where the title of our essay comes from.

We have considered that the most adequate path is making a gradual transition from CAL to QAL. On top of this, GoL can be seen as a *less abstract* representation of classical computation, in a parallelism with QCs, which have a mathematical perspective, but can also be physically built in experimental setups!

2 Classical artificial life

Let us begin from the abstract part of CAL, the mathematical definition of cellular automata:

2.1 Definition of cellular automata

A Cellular Automaton (CA) of dimension $d \in \mathbb{N} - \{0\}$ is defined mathematically by a 5-tuple $(T, L, S, N(\mathbf{x}), f)$ where [6, p. 136]

- T is the Timeline. In GoL, $T = \mathbb{Z}$ is the discrete timeline.
- L is the d -dimensional grid or Lattice. For *continuous* CA, $L = \mathbb{R}^d$, where \mathbb{R}^d denotes the d -dimensional Euclidean space of column vectors with d real components, or d -dimensional real vector space. On the other hand, $L = \mathbb{Z}^d$ for *discrete* ones. In GoL, $L = \mathbb{Z}^2$ is the two-dimensional ($d=2$) discrete ($L = \mathbb{Z}^d$) grid.
- S is a finite *set of States*. In GoL, $S = \{0, 1\} = \{\text{unpopulated (dead), populated (alive)}\}$ is the set of each cell's possible states.
- $N(\mathbf{x}) = \{\mathbf{x} + \mathbf{n} : \mathbf{x}, \mathbf{n} \in \mathbb{R}^d\}$ is the Neighborhood of the site $\mathbf{x} \in L$, a finite ordered subset of L . In GoL, $d = 2$, and
 - ◊ $\mathbf{x} = (x, y) \in \mathbb{Z}^{d=2}$.
 - ◊ $n = \{-1, 0, 1\}^{d=2}$. The notation $\{-1, 0, 1\}^2$ means the set of two-dimensional vectors with each component either -1, 0 or 1. [1, p. 16, l. 27-28]
 - ◊ $N(\mathbf{x})$ is the 8-site Moore neighborhood in the Chebyshev or *chessboard* metric. The points at a Chebyshev distance of $\mathbf{n} = (0, 0)$ from the *cell*-site $\mathbf{x} = (x, y)$ are the site \mathbf{x} itself. Any other combination of $n = \{-1, 0, 1\}^2$ represents one of the 8 Moore neighbors.
- $f : S^{|N|} \rightarrow S$ is the deterministic *local transition rule* or function, space- and time-homogeneous. In GoL, $f : S^{8+1} \rightarrow S$. The domain is S^{8+1} due to the 9 possible combinations allowed in the Moore neighborhood: 8 neighbors + the reference cell $-\mathbf{n} = (0, 0)$ – itself. Every site's state, which forms the codomain S , output of the map f , is updated *simultaneously* according to the following local rule:

$$C(t + \Delta t, \mathbf{x}) = \begin{cases} 1 & \text{if } C(t, \mathbf{x}) = 1 \wedge \sum S(t, \mathbf{x}) \in \{2, 3\}, \quad \mathbf{x} \in N(\mathbf{x}) \text{ (survival)} \\ 1 & \text{if } C(t, \mathbf{x}) = 0 \wedge \sum S(t, \mathbf{x}) = 3, \quad \mathbf{x} \in N(\mathbf{x}) \text{ (reproduction)} \\ 0 & \text{otherwise (death by underpopulation/overpopulation)} \end{cases} \quad (2.1)$$

where we define the mapping $C(t, \mathbf{x}) : T \wedge L \rightarrow S$ as the Configuration or *pattern* (i.e., the collection of S states over the whole L grid) of site $\mathbf{n} = (0, 0)$ at time or generation $t \in T$. That is, $S(t, \mathbf{x})|_{\mathbf{n}=(0,0)} = C(t, \mathbf{x})$. In GoL, $\mathbf{x} = (x, y)$, $T = \mathbb{Z}$, $L = \mathbb{Z}^2$ and $S = \{0, 1\}$, so, $C(t, (x, y)) : (\mathbb{Z}^3) \rightarrow \{0, 1\}$. [6, p. 136]

2.2 Cellular automata example: the game of life

Furthering with our GoL example, as mentioned in Section 1.1, interactions occur at discrete time steps. These are determined by the following simple set of rules, mathematically defined in Eq. (2.1). $n \in \mathbb{N}$ is the number of populated nearest (orthogonally adjacent) and next-nearest (diagonally adjacent) neighbors or, equivalently, the number of populated cells in a determined Moore neighborhood. All births and deaths must occur *synchronously* and together make up a single so-called *generation* [5, p. 2, l. 16-17] [6, p. 73].

- **Death:** (Eq. (2.1), line 3)
 - ◊ by overpopulation: populated cells $-C(t, \mathbf{x}) = 1-$ with $n > 3$ $-\sum S(t, \mathbf{x}) \in [4, 8]$, $\mathbf{x} \in N(\mathbf{x})-$ at time t depopulate at time $t + \Delta t$: $C(t + \Delta t, \mathbf{x}) = 0$.
 - ◊ by underpopulation: populated cells $-C(t, \mathbf{x}) = 1-$ with $n < 2$ $-\sum S(t, \mathbf{x}) \in \{0, 1\}$, $\mathbf{x} \in N(\mathbf{x})-$ at time t depopulate at time $t + \Delta t$: $C(t + \Delta t, \mathbf{x}) = 0$.
- **Survival** (for the next generation): populated cells $-C(t, \mathbf{x}) = 1-$ with $n = 2, 3$ $-\sum S(t, \mathbf{x}) \in \{2, 3\}$, $\mathbf{x} \in N(\mathbf{x})-$ at time t do not change state at time $t + \Delta t$: $C(t + \Delta t, \mathbf{x}) = 1$. See Eq. (2.1), line 1.
- **Reproduction:** unpopulated cells $-C(t, \mathbf{x}) = 0-$ with $n = 3$ $-\sum S(t, \mathbf{x}) = 3$, $\mathbf{x} \in N(\mathbf{x})-$ at time t populate at the next move (time $t + \Delta t$): $C(t + \Delta t, \mathbf{x}) = 1$. See Eq. (2.1), line 2.

Apart from its conspicuous biological analogies, GoL also bears some resemblance to physical laws through the concept of maximum attainable velocity [5, p. 4, l. 1-2]. Namely, we can define a *speed of light* c , or the upper bound on the speed of any pattern, as one cell-step across Moore's neighborhood per generation or time step Δt . Notwithstanding, no pattern is capable of moving, unassisted, one cell every generation—at least classically. We shall see what occurs when we implement superposition and a relative phase $e^{i\phi}$ in Section 2.4.3. Objects can only travel at the defined *speed of light* through trails (stripes of populated cells) and not if, reminiscent of *vacuum* ($\mu_r = \epsilon_r = 1$), the medium is an empty space formed by unpopulated cells, contrary to the situation in nature, where in materials ($\mu_r, \epsilon_r > 1$) it is always less: $c = \frac{1}{\sqrt{\mu \epsilon}} = \frac{1}{\sqrt{\mu_0 \mu_r \epsilon_0 \epsilon_r}} < c_0 = \frac{1}{\sqrt{\mu_0 \epsilon_0}}$.

2.3 Implementation of game of life

Now we will materialize GoL, our CAL example, abstractly described so far:

2.3.1 Code

GNU Octave is a convenient environment for deploying GoL, since its universe is a matrix. Details can be found in Appendix A.1.

2.3.2 Results

Let us introduce some illustrative results obtained by the corresponding *GNU Octave* code shown in Appendix A.1:⁴

⁴See the corresponding videos on the author's page: [Glider](#), [Tetromino1](#) and [Tetromino2](#).

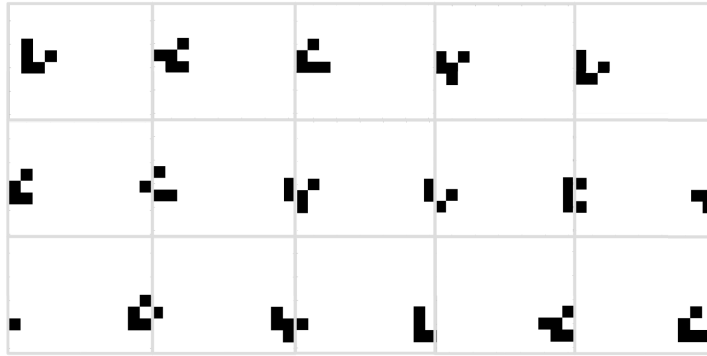


Figure 2.1: *Glider*, created using the classical GoL code in Appendix A.1. The first 15 generations are displayed. Notice the implementation of periodic boundary conditions (PBCs).



Figure 2.2: The first 6 generations of an example of the so-called *Tetromino* (shape formed by 4 connected populated (black) cells) [5, p. 4, l. 9-10], displayed via the classical GoL code in Appendix A.1. As it can be observed, it becomes an stable pattern or *still-life* after the 3rd generation.

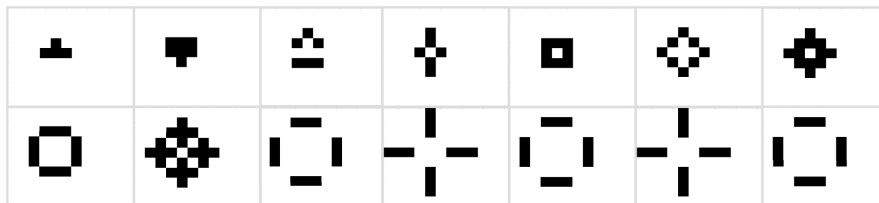


Figure 2.3: The first 14 generations of another example of a *Tetromino* [5, p. 4, l. 10-11], displayed using the classical GoL code in Appendix A.1. After the 9th generation, it becomes 4 isolated period-2 figures or oscillators known as *traffic lights*.

Continuing with our gradual transition from CAL to QAL, we will add some quantum mechanical characteristics to GoL.

2.4 Transition from classical to quantum artificial life

We will give a semi-classical (with no entanglement, locally quantum) version of GoL. We will use the Schrödinger picture, in which quantum states –the ensemble of cells in the grid, here– evolve in time according to time-independent operators acting on them. This operators would be, in our case, the GoL transition rules, which are, as mentioned, time-homogeneous (Section 2.1). Nevertheless, in practice, two problems arise: some of this operators will not be unitary and, withal, synchronous update of all cells cannot be carried in current QCs. However, even if experimental implementation is not possible, this section is valuable for a better comprehension of the following sections of our work.

2.4.1 Probabilistic picture of measurements

Continuing with GoL, quantum mechanical features can be implemented, such as the probability of measuring the system in a particular state, Eq. (2.3-2.4). As it is well known, quantum mechanical algorithms work with this probability distributions over various states, which come into play due to the impossibility of making definite predictions.

Suppose that we consider GoL a finite quantum mechanical system that can be exactly imitated by a physical register that at each point in space-time has solely two possible base states: either occupied (alive or, e.g., spin 1/2 down $|\downarrow\rangle$), or unoccupied (dead or, e.g., spin 1/2 up $|\uparrow\rangle$) [8, p. 475, l. 27-31]. Then, the state of each cell can be represented applying the idea of quantum *superposition* of states: [9, p. 1, Eq. (1)]

$$|\psi\rangle = a|1\rangle + b|0\rangle, \quad (2.2)$$

where $|1\rangle \equiv |\text{alive}\rangle$ and $|0\rangle \equiv |\text{dead}\rangle$, subject to the normalization condition $|a|^2 + |b|^2 = 1$. $a, b \in \mathbb{C}$ are the complex vectorial *amplitudes* in each state. In the *reverse order* computational basis $\{|\mp\rangle_z\} \equiv \{|1\rangle, |0\rangle\}$ [1, p. 13, l. 23], $|\psi\rangle = a|1\rangle + b|0\rangle \doteq \begin{pmatrix} a \\ b \end{pmatrix}$.

Thus, the probability [10, p. 24, Eq. (1.4.4)] of measuring the cell as *alive* or *dead* is, respectively,

$$\Pr_{|\psi\rangle}(|1\rangle) = |\langle 1|\psi\rangle|^2 \doteq \left| \begin{pmatrix} 1 & 0 \end{pmatrix} \begin{pmatrix} a \\ b \end{pmatrix} \right|^2 = \left| \begin{pmatrix} a \\ 0 \end{pmatrix} \right|^2 = \begin{pmatrix} a^* & 0 \end{pmatrix} \begin{pmatrix} a \\ 0 \end{pmatrix} = a^*a = |a|^2, \quad (2.3)$$

$$\Pr_{|\psi\rangle}(|0\rangle) = |\langle 0|\psi\rangle|^2 \doteq \left| \begin{pmatrix} 0 & 1 \end{pmatrix} \begin{pmatrix} a \\ b \end{pmatrix} \right|^2 = \left| \begin{pmatrix} 0 \\ b \end{pmatrix} \right|^2 = \begin{pmatrix} 0 & b^* \end{pmatrix} \begin{pmatrix} 0 \\ b \end{pmatrix} = b^*b = |b|^2, \quad (2.4)$$

where, $\langle\phi| = |\phi\rangle^\dagger$, and the *Hermitian conjugate* (\dagger) is obtained by transposing and complex conjugating the operator or matrix [1, p. 18, l. 28]). As usual, due to the normalization of the wave function, the total probability is 1 [11, p. 107, Eq. (3.48)]: $\Pr_{\text{tot}} = \Pr_{|\psi\rangle}(|1\rangle) + \Pr_{|\psi\rangle}(|0\rangle) = |a|^2 + |b|^2 = 1$, where the last equality $|a|^2 + |b|^2 = 1$ follows from the normalization condition of Eq. (2.2)⁵.

2.4.2 Quantum implementation of GoL rules (without phase difference $e^{i\phi}$)

We apply the GoL rules by means of linear combinations of the following birth (\hat{B}), death (\hat{D}) and survival (\hat{S}) operators: [9, p. 2, Eq. (3)]

$$\hat{B}|\psi\rangle = |1\rangle, \quad \hat{D}|\psi\rangle = |0\rangle, \quad \text{and} \quad \hat{S}|\psi\rangle = |\psi\rangle, \quad (2.5)$$

with, in the $\{|1\rangle, |0\rangle\}$ basis,

$$\hat{B} \doteq \frac{1}{a+b} \begin{pmatrix} 1 & 1 \\ 0 & 0 \end{pmatrix}, \quad \hat{D} \doteq \frac{1}{a+b} \begin{pmatrix} 0 & 0 \\ 1 & 1 \end{pmatrix}, \quad \hat{S} \doteq \begin{pmatrix} 1 & 0 \\ 0 & 1 \end{pmatrix} = \hat{1}_2. \quad (2.6)$$

Hence, $\hat{B}|\psi\rangle \doteq \frac{1}{a+b} \begin{pmatrix} 1 & 1 \\ 0 & 0 \end{pmatrix} \begin{pmatrix} a \\ b \end{pmatrix} = \frac{1}{a+b} \begin{pmatrix} a+b \\ 0 \end{pmatrix} = \begin{pmatrix} 1 \\ 0 \end{pmatrix} \doteq |1\rangle$, $\hat{D}|\psi\rangle \doteq \frac{1}{a+b} \begin{pmatrix} 0 & 0 \\ 1 & 1 \end{pmatrix} \begin{pmatrix} a \\ b \end{pmatrix} = \frac{1}{a+b} \begin{pmatrix} 0 \\ a+b \end{pmatrix} = \begin{pmatrix} 0 \\ 1 \end{pmatrix} \doteq |0\rangle$, and $\hat{S}|\psi\rangle \doteq \begin{pmatrix} 1 & 0 \\ 0 & 1 \end{pmatrix} \begin{pmatrix} a \\ b \end{pmatrix} = \begin{pmatrix} a \\ b \end{pmatrix} \doteq |\psi\rangle$. Thus, Eq. (2.5) is fulfilled.

⁵See a more complete study, via the *density operator* ($\hat{\rho}$) approach, for Eq. (2.3-2.4) on the author's [page](#).

In addition, the matrix representation of \hat{S} is diagonal when $|1\rangle$ and $|0\rangle$ are used as the base kets. Then, we can infer that these are the eigenkets⁶ of \hat{S} [10, p. 22, l. 3-5 & p. 36, l. 5-7]. These two eigenfunctions share the same eigenvalue ($S = 1$, degeneration $g = 2$), so any linear combination of them ($|\psi\rangle$ defined in Eq. (2.2), for instance) is itself an eigenfunction, with the same eigenvalue (obvious from $\hat{S}|\psi\rangle = 1|\psi\rangle$, Eq. (2.5)). [11, p. 102, l. 6-8]

\hat{B} and \hat{D} are not unitary since their Hermitian conjugate (\dagger) is not equal to their inverse –respectively, $\hat{B}^\dagger \neq \hat{B}^{-1}$ and $\hat{D}^\dagger \neq \hat{D}^{-1}$ –, or, equivalently, [10, p. 36, Eq. (1.5.2)]

$$\hat{B}\hat{B}^\dagger \doteq \frac{1}{a+b} \begin{pmatrix} 1 & 1 \\ 0 & 0 \end{pmatrix} \frac{1}{a^*+b^*} \begin{pmatrix} 1 & 1 \\ 0 & 0 \end{pmatrix}^T = \frac{1}{|a+b|^2} \begin{pmatrix} 1 & 1 \\ 0 & 0 \end{pmatrix} \begin{pmatrix} 1 & 0 \\ 1 & 0 \end{pmatrix} = \frac{1}{|a+b|^2} \begin{pmatrix} 2 & 0 \\ 0 & 0 \end{pmatrix} \neq \hat{1}_2, \quad (2.7)$$

$$\hat{D}\hat{D}^\dagger \doteq \frac{1}{a+b} \begin{pmatrix} 0 & 0 \\ 1 & 1 \end{pmatrix} \frac{1}{a^*+b^*} \begin{pmatrix} 0 & 0 \\ 1 & 1 \end{pmatrix}^T = \frac{1}{|a+b|^2} \begin{pmatrix} 0 & 0 \\ 1 & 1 \end{pmatrix} \begin{pmatrix} 0 & 1 \\ 0 & 1 \end{pmatrix} = \frac{1}{|a+b|^2} \begin{pmatrix} 0 & 0 \\ 0 & 2 \end{pmatrix} \neq \hat{1}_2. \quad (2.8)$$

A quantum gate (or, more generally, quantum evolution operator) is said to be feasible if its matrix representation is unitary ($\hat{U}\hat{U}^\dagger = \hat{U}^\dagger\hat{U} = 1$, or, equivalently, $\hat{U}^\dagger = \hat{U}^{-1}$), so that probability, defined in the same manner as Eq. (2.3-2.4), is conserved,

$$\Pr_{|\psi\rangle}(|\phi\rangle) = \frac{|\langle\phi|\psi\rangle|^2}{\langle\phi|\phi\rangle\langle\psi|\psi\rangle} = \frac{|\langle\phi|\hat{U}^\dagger\hat{U}|\psi\rangle|^2}{\langle\phi|\hat{U}^\dagger\hat{U}|\phi\rangle\langle\psi|\hat{U}^\dagger\hat{U}|\psi\rangle} = \Pr_{\hat{U}|\psi\rangle}(\hat{U}|\phi\rangle). \quad (2.9)$$

Then, from Eq. (2.7-2.8), \hat{B} and \hat{D} cannot be empirically implemented in a QC, at least if some accuracy is wanted.

Besides unitary, quantum logic gates must be reversible, with the exception of measurement ones, but GoL is not: information is lost, input (original state at a certain time t) cannot be fully deduced from output (state at time $t + \Delta t$). Nevertheless, not as non-unitarity of \hat{B} and \hat{D} , irreversibility can be overcome keeping spare qubits (second lines of Fig. 2.4) in order to divert information that helps recover the input from the output and otherwise would be lost.

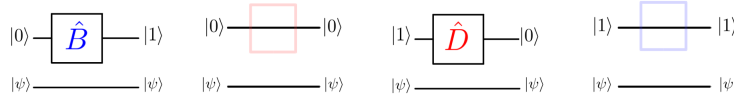


Figure 2.4: Realizing \hat{B} (blue squares) and \hat{D} (red squares), Eq. (2.6), reversibly; that is, in a way that, thanks to the spare qubit $|\psi\rangle$, the output can be fully inferred from the input.

Obviously, \hat{S} is unitary [10, p. 36, Eq. (1.5.2)], $\hat{S} = \hat{1}_2 = \hat{S}^{-1} = \hat{S}^\dagger$, so $\hat{S}\hat{S}^\dagger = \hat{S}^\dagger\hat{S} = \hat{1}_2$. Furthermore, \hat{S} is a Hermitian operator ($\hat{S} = \hat{S}^\dagger \equiv (\hat{S}^*)^T$) [10, p. 15, Eq. (1.2.25)], so its eigenvalues ($S = 1$, as we have already seen) are real [11, p. 101, Theo. 1] ($S \in \mathbb{R}$). Notice that, since they do not represent observables or measurable quantities, they are just used to apply the GoL rules, the birth (\hat{B}), death (\hat{D}) and survival (\hat{S}) operators are not required to be Hermitian [11, p. 97, Eq. (3.18)], which, as just said, would ensure the

⁶In the 3-dimensional real vector space \mathbb{R}^3 , eigenvectors can be seen as vectors that are transformed into scalar multiples of themselves by the θ angle rotation about some axis, applied by an operator $\hat{U}(\theta)$. Exempli gratia, vectors that lie *along* the rotation axis do not change at all ($\hat{U}(\theta)|\psi\rangle = |\psi\rangle$, eigenvalue= 1), and, for $\theta = \pi$, if they lie in the *equatorial* plane of the rotation axis, $\hat{U}(\pi)|\psi\rangle = -1|\psi\rangle$ (eigenvalue= -1).

reality of their eigenvalues. But, as we have also exposed, probability conservation in Eq. (2.9), cannot be ensured because of non-unitarity.

As mentioned, we apply the rules of GoL through linear combinations of the birth (\hat{B}), death (\hat{D}) and survival (\hat{S}) operators defined in Eq. (2.6). These linear combinations –which will also be operators, and we will call them \hat{G} , from *Generation*– depend on the value of the sum of the a coefficients in the $|\psi\rangle$ (Eq. (2.2)) states corresponding to each of the 8 Moore neighbors. If we define this sum as $a_{\text{Moore}} \equiv a_M \equiv \sum_{i=1}^8 a_i$, [9, p. 2, Eq. (7)]

$$\hat{G} \propto \begin{cases} \hat{D} & \text{if } 0 \leq a_M \leq 1, \\ C_1 (2 - a_M) \hat{D} + (a_M - 1) \hat{S} & \text{if } 1 < a_M \leq 2, \\ C_2 (3 - a_M) \hat{S} + (a_M - 2) \hat{B} & \text{if } 2 < a_M \leq 3, \\ C_3 (4 - a_M) \hat{B} + (a_M - 3) \hat{D} & \text{if } 3 < a_M \leq 4, \\ \hat{D} & \text{if } a_M > 4. \end{cases} \quad (2.10)$$

If $C_i = 1$, $i = 1, 2, 3$, we would have continuity of \hat{G} on the boundaries. For $a_M = 1, 2, 3, 4$, respectively,

$$\begin{aligned} \hat{G}(a_{M^-} = 1) &= \hat{D} = \hat{G}(a_{M^+} = 1) = (2 - 1)\hat{D} + (1 - 1)\hat{S} = \hat{D}, \\ \hat{G}(a_{M^-} = 2) &= (2 - 2)\hat{D} + (2 - 1)\hat{S} = \hat{S} = \hat{G}(a_{M^+} = 2) = (3 - 2)\hat{S} + (2 - 2)\hat{B} = \hat{S}, \\ \hat{G}(a_{M^-} = 3) &= (3 - 3)\hat{S} + (3 - 2)\hat{B} = \hat{B} = \hat{G}(a_{M^+} = 3) = (4 - 3)\hat{B} + (3 - 3)\hat{D} = \hat{B}, \quad \text{and} \\ \hat{G}(a_{M^-} = 4) &= (4 - 4)\hat{S} + (4 - 3)\hat{D} = \hat{D} = \hat{G}(a_{M^+} = 4) = \hat{D}. \end{aligned}$$

Nevertheless, we want a more logical behavior in the middle of each range in Eq. (2.10). That is, for $a_M = \frac{1}{\sqrt{2}} + x : x \in [1, 3]$, we want the contribution of both summands to be the same, $\frac{1}{\sqrt{2}}$. Then, e.g., if $a_M = 1 + \frac{1}{\sqrt{2}}$,

$$\begin{aligned} \frac{1}{\sqrt{2}}(\hat{D} + \hat{S}) &= C_1 \left(2 - \left(1 + \frac{1}{\sqrt{2}}\right) \right) \hat{D} + \left(\left(1 + \frac{1}{\sqrt{2}}\right) - 1 \right) \hat{S} = C_1 \frac{\sqrt{2} - 1}{\sqrt{2}} \hat{D} + \frac{1}{\sqrt{2}} \hat{S} \\ \Leftrightarrow \frac{1}{\sqrt{2}} \hat{D} &= C_1 \frac{\sqrt{2} - 1}{\sqrt{2}} \hat{D} \quad \Leftrightarrow \quad C_1 = \frac{1}{\sqrt{2} - 1} = \frac{1}{(\sqrt{2} - 1)(\sqrt{2} + 1)} = \frac{\sqrt{2} + 1}{(\sqrt{2})^2 - 1^2} = \sqrt{2} + 1. \end{aligned} \quad (2.11)$$

We would obtain the same for $a_M = 2 + \frac{1}{\sqrt{2}}$ and $a_M = 3 + \frac{1}{\sqrt{2}}$. Thus, $C_i = \sqrt{2} + 1$. On the other hand, for $a_M \in \mathbb{N}$, \hat{G} is equal to \hat{B} , \hat{D} or \hat{S} (solely one out of these three operators, not a linear combination of two of them, as in Eq. (2.10)). Then, the rules of the classical GoL are recovered!

In the new *generation* or time step, the state of the cell is

$$|\psi'\rangle = \hat{G}|\psi\rangle \doteq \hat{G} \begin{pmatrix} a \\ b \end{pmatrix} = \begin{pmatrix} a' \\ b' \end{pmatrix} \doteq a'|1\rangle + b'|0\rangle, \quad (2.12)$$

in the $\{|1\rangle, |0\rangle\}$ basis, where the new state $|\psi'\rangle$ requires renormalization so that $|a'|^2 + |b'|^2 = 1$. That is, after applying \hat{B} , \hat{D} , \hat{S} , or some mixture of them, the probabilities of being dead or alive must still sum up to unity. Because of this *renormalization*, overall factors in Eq. (2.10) have no effect [9, p. 3, Eq. (10)], but

relative constants, of course, would matter.

Without phase difference $e^{i\phi}$, we should obtain the same results as in Section 2.3.2. See the code belonging to this section in Appendix A.2.1.

2.4.3 A more quantum-like implementation of GoL rules (with phase difference $e^{i\phi}$)

We can additionally introduce a phase difference $e^{i\phi}$, $\phi \in \mathbb{R}$, with the aim of achieving a different behavior from the classical GoL and allow *interference* –the reinforcement or cancellation between states of different relative phases–, which is a fundamental quantum property, along with the uncertainty or probabilistic picture introduced in Section 2.4.1. The *phase* has no classical counterpart and it comes about in quantum mechanics, because amplitudes are complex numbers [12, p. 2, l. 64-67].

Similar to the consequences of renormalizing Eq. (2.12), while relative phase constants (in a superposition) are important, the *global* phase factor of the wave function is physically irrelevant; in this case, however, because it cancels out whenever we measure a quantity [11, p. 39, l. 14-16] [1, p. 15, Eq. (1.3) & p. 93, l. 10-17], rather than by renormalization. In other words, the *overall* phase of a quantum state is not measurable, has no quantum physical significance: $|\psi\rangle$ is the same as $e^{i\phi}|\psi\rangle$, both yield the same density matrix $\hat{\rho}$.

Now, instead of Eq. (2.5), we have [9, p. 3]

$$\hat{B}|\psi\rangle = \frac{a + be^{i\phi}}{\sqrt{|a + be^{i\phi}|^2}}|1\rangle, \hat{D}|\psi\rangle = \frac{ae^{i\phi} + b}{\sqrt{|ae^{i\phi} + b|^2}}|0\rangle, \hat{S}|\psi\rangle = |\psi\rangle, \quad (2.13)$$

where

- $|a + be^{i\phi}|^2 = (a + be^{i\phi})(a^* + b^*e^{-i\phi}) = |a|^2 + ab^*e^{-i\phi} + a^*be^{i\phi} + |b|^2 = |a|^2 + |b|^2 + 2\text{Re}(a^*be^{i\phi}) = |a|^2 + |b|^2 + 2\text{Re}(a^*b) \cos \phi$.
- $|ae^{i\phi} + b|^2 = (ae^{i\phi} + b)(a^*e^{-i\phi} + b^*) = |a|^2 + ab^*e^{i\phi} + a^*be^{-i\phi} + |b|^2 = |a|^2 + |b|^2 + 2\text{Re}(ab^*e^{i\phi}) = |a|^2 + |b|^2 + 2\text{Re}(ab^*) \cos \phi$.

Therefore, Eq. (2.13) becomes

$$\hat{B}|\psi\rangle = \frac{a + be^{i\phi}}{\sqrt{|a|^2 + |b|^2 + 2\text{Re}(a^*b) \cos \phi}}|1\rangle, \hat{D}|\psi\rangle = \frac{ae^{i\phi} + b}{\sqrt{|a|^2 + |b|^2 + 2\text{Re}(ab^*) \cos \phi}}|0\rangle, \hat{S}|\psi\rangle = |\psi\rangle. \quad (2.14)$$

In addition to that, instead of $a_M \equiv \sum_{i=1}^8 a_i$, we will use $a_M \equiv \sum_{i=1}^8 a_i e^{i\phi}$ [9, p. 3, Eq. (12)]. We will multiply $|0\rangle$ or $|1\rangle$ by the same phase ($e^{i\phi}$) which appears in a_M (the sum of the a coefficients of the surrounding nearest 8 cells), but just if the state has changed ($|0\rangle \leftrightarrow |1\rangle$) in the last time step; in other words, if the current cell is alive (dead) and in the previous generation was dead (alive): $\hat{B}|1\rangle = |1\rangle$, $\hat{B}|0\rangle = e^{i\phi}|1\rangle$, $\hat{D}|1\rangle = e^{i\phi}|0\rangle$, $\hat{D}|0\rangle = |0\rangle$ and $\hat{S}|\psi\rangle = |\psi\rangle$.

Equation (2.10) is applied in the same way as before, substituting a_M with $|a_M|$. Nonetheless, now, the phase ($e^{i\phi}$) in $a_M \equiv \sum_{i=1}^8 a_i e^{i\phi}$ allows for interference effects! For instance, a cell with $a_i = e^{\pm i(\phi=\pi)} = -1$ still has a unit probability of being measured in the live state ($\text{Pr}_{\cdot|\psi\rangle}(|1\rangle) \stackrel{(2.3)}{=} |a_i|^2 = |-1|^2 = 1$), but its effect on the a_M sum will cancel (destructive *interference*) that of a cell with $a_i = e^{i(\phi=0)} = 1$. See the associated code in Appendix A.2.2.

3 Fundamentals of quantum artificial life

Before describing our QAL model, we will briefly introduce some basic concepts that shall be referenced later.

3.1 Qubits

Qubits (or quantum bits [1, p. 4, l. 2]) constitute the minimal representative of a quantum mechanical system [1, p. 80, l. 30-31]. They are 2-level quantum systems (2LS) $\in \mathcal{H}_2 \subset \mathbb{C}^2$, where \mathcal{H}_2 is the 2-dimensional Hilbert subspace [1, p. 43, l. 11-12], a complex vector space over the complex numbers \mathbb{C}^2 , with inner product defined.

Then, since \mathbb{C}^2 , a qubit takes two real numbers $-\theta$ and φ in Eq. (3.2)– to fully describe it. Precisely, they can represent a 0 or 1 state, as classical bits, but also a linear combination of both, which is the property mentioned in Section 1, known as *quantum superposition*. More generally, they are named *qutrits* for \mathbb{C}^3 and *qudits* for \mathbb{C}^d . They are usually described in the $\{|\pm\rangle_z\} \equiv \{|0\rangle, |1\rangle\}$ basis, called *computational basis* (or standard basis or *Z* basis, which is the basis that diagonalizes $\hat{\sigma}_z$), as the following vectors: [1, p. xxix, l. 20-21]

$$|0\rangle \doteq \begin{pmatrix} 1 \\ 0 \end{pmatrix} \quad \text{and} \quad |1\rangle \doteq \begin{pmatrix} 0 \\ 1 \end{pmatrix}. \quad (3.1)$$

Defining basis kets (or *measurement directions*, in a more quantum physical terminology) is a tool borrowed from linear algebra. Once the basis is chosen, any other vector can be constructed from a linear combination of these basis kets or vectors. Another basis examples are the *superposition basis* or *X* basis (because it diagonalizes $\hat{\sigma}_x$) $\{|\pm\rangle_x \equiv |\pm\rangle \equiv \frac{1}{\sqrt{2}}(|0\rangle \pm |1\rangle)\}$, and the *Y* basis (because it is formed by the eigenkets of $\hat{\sigma}_y$) $\{|\pm\rangle_y \equiv \frac{1}{\sqrt{2}}(|0\rangle \pm i|1\rangle)\}$ [10, p. 9, Eq. (1.1.14)].

Nevertheless, quantum computing spans beyond linear algebra: qubits are not to be thought just abstractly, they are decidedly real! As mentioned in Section 1, they can be realized in diverse physical apparatus (1/2-spins, photons, ions, etc.).

Qubits or quantum registers can be modified by operations or gates described by *unitary* operators \hat{U} , being unitarity the *only* constraint imposed upon valid quantum logic gates [1, p. 18, l. 30][19, p. 76, l. 19-20]. As a matter of fact, unitarity is the requirement that the norm of the vectors (single qubits) in the Bloch sphere be preserved –i.e., unitary matrices leave the length of a complex vector unchanged [18, l. 4]– and then probability is conserved, Eq. (2.9) [1, p. 21, l. 12].

These quantum logic gates are described by $2^n \times 2^n$ unitary matrices, where n is the number of qubits they act on [1, p. 18, l. 22]. Since unitary matrices are square ($\hat{U}^T = \hat{U}$), logic gates ($\hat{U} \doteq \sum_i |\text{in}^{(i)}\rangle \langle \text{out}^{(i)}|$) can only have the same number of inputs (rows, $|\text{in}\rangle$) as outputs (columns, $\langle \text{out}|$). Quantum gates are also *local*, that is, they act on a restricted number of qubits [3, p. 6, l. 11-12] [19, p. 88, l. 1].

On top of this, because of the fact that the inverse of a unitary matrix is also a unitary matrix, unitary matrices –unitary quantum gates, here– are *always* invertible [18, l. 10]. That is, a quantum gate \hat{U} can always be inverted by another quantum gate \hat{U}^{-1} [1, p. 21, l. 21-23]. In this sense, as mentioned in Fig. 2.4, quantum logic gates are *reversible* because, given the output, the input is uniquely determined and can be recovered, no information is ever erased during the computation. Hence, we can say gates

follow the laws of physics, since they are reversible [3, p. 8, l. 5-6], with the possible exception of quantum measurements that collapse the wave function to the eigenket of the output observable [1, p. 157, l. 1-2].

To sum up, qubits serve as information registers and, on the other hand, logic gates represented by \hat{U} unitary operators process information and, for instance, make up the time-evolution operator $\hat{U}(t, t_0)$ [10, p. 67, Eq. (2.1.5)] present in the Schrödinger equation.

A priori, akin to conventional computation, any general n -qubit unitary transformation operation \hat{U} could be constructed as a product of several elements of a universal set of gates. The universal set of quantum logic gates is formed by the CNOT gate between two qubits (3.2) and 1-qubit rotations (2 bit transformations) [1, p. 22, l. 5-6] [3, p. 6, l. 25-27]. The latter can be implemented by relatively simple physical systems [3, p. 6, l. 17]. Nevertheless, in practice, limitations arise by the errors originated from the fact that qubits and gates are said to be an approximation (closed or totally isolated systems) of open quantum systems (Section 4.3.1, paragraph 1).

3.1.1 Bloch representation

The state of the quantum system is a point represented by a unit-length (if normalized) vector in the mentioned $d = 2^n$ -dimensional (this is, with 2^n basis kets, for n qubits) complex vector space with inner product defined, known as *Hilbert space* $\mathcal{H} \subset \mathbb{C}^d$ [3, p. 5, l. 29-30]. Quantum logic gates produce rotations of these vectors and, measurements, probabilistic projections to the chosen basis.

A simpler geometrical picture useful in thinking about single qubits is the so-called *Bloch sphere* representation, a one-to-one correspondence or bijection between pure [mixed] one-qubit states (\mathbb{C}^3) and the points on the surface of [inside] a unit sphere (\mathbb{R}^3) [1, p. 15]. If we suppose that the Bloch sphere represents a $s = 1/2$ spin system (or any other 2-state or 2-level quantum system, 2LS), the spin-up state $|\uparrow\rangle$ may represent the $|0\rangle$ bit, and, the spin-down state $|\downarrow\rangle$, the $|1\rangle$ bit. It is a form of representing complex vectors in a viewable way, Fig. 3.1, but, due to this simplification, misleading interpretations could come up. For instance, $|0\rangle$ and $|1\rangle$ might seem antiparallel, whereas they are orthogonal, $\langle 0|1\rangle = 0$.

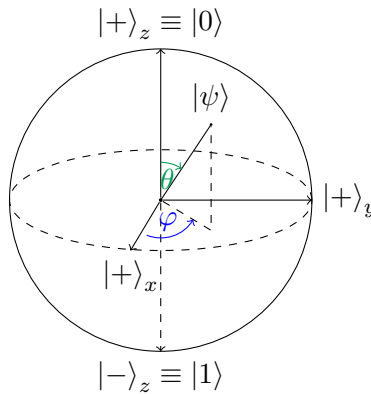


Figure 3.1: Bloch sphere representation of the *qubit* $|\psi\rangle$, Eq. (3.2), as a function of the angles θ and φ .

Any point or state⁷ $|\psi\rangle$ on the Bloch sphere can be defined via the polar, θ , and azimuth, φ , angles,

⁷See the proof for Eq. (3.2) on the author's page.

[1, p. 15, Eq. (1.4)]

$$|\hat{\sigma} \cdot \hat{r}; \pm\rangle \equiv |\psi(\theta, \varphi)\rangle = \cos(\theta/2) |0\rangle + \sin(\theta/2)e^{i\varphi} |1\rangle \doteq \begin{pmatrix} \cos(\theta/2) \\ \sin(\theta/2)e^{i\varphi} \end{pmatrix}, \quad (3.2)$$

where $\varphi \in [0, 2\pi)$ and $\theta \in [0, \pi]$.

- For instance, for $\varphi = 0$ and $\theta = \begin{Bmatrix} 0 \\ \pi \end{Bmatrix}$ we obtain [1, p. xxix, l. 24]

$$\begin{aligned} |\hat{\sigma}_z; \pm\rangle &\equiv |\pm\rangle_z \equiv |\psi(\begin{Bmatrix} 0 \\ \pi \end{Bmatrix}, 0)\rangle \stackrel{(3.2)}{=} \cos\left(\begin{Bmatrix} 0 \\ \pi \end{Bmatrix}/2\right) |0\rangle + \sin\left(\begin{Bmatrix} 0 \\ \pi \end{Bmatrix}/2\right) e^{i0} |1\rangle \\ &= \begin{Bmatrix} 1 \\ 0 \end{Bmatrix} |0\rangle + \begin{Bmatrix} 0 \\ 1 \end{Bmatrix} |1\rangle = \begin{Bmatrix} |0\rangle \\ |1\rangle \end{Bmatrix}, \end{aligned} \quad (3.3)$$

which clearly agrees the computational basis $\{|\pm\rangle_z\} \equiv \{|0\rangle, |1\rangle\}$ from Fig. 3.1!

- Another useful example corresponds to $\theta = \pi/2$ and $\varphi = \begin{Bmatrix} 0 \\ \pi \end{Bmatrix}$. Taking into account Eq. (3.2),

$$|\hat{\sigma}_x; \pm\rangle \equiv |\pm\rangle_x \equiv |\psi(\pi/2, \begin{Bmatrix} 0 \\ \pi \end{Bmatrix})\rangle \stackrel{(3.2)}{=} \cos((\pi/2)/2) |0\rangle + \sin((\pi/2)/2) e^{i\begin{Bmatrix} 0 \\ \pi \end{Bmatrix}} |1\rangle = \frac{|0\rangle \pm |1\rangle}{\sqrt{2}} \equiv |\pm\rangle, \quad (3.4)$$

which form the mentioned $\{|\pm\rangle_x \equiv |\pm\rangle\}$ or X basis, whose base kets are the eigenvectors of $\hat{\sigma}_x$. These states, as $\{|\pm\rangle_y\}$ in the following paragraph, lie in the *equator* of the Bloch sphere.

- Finally, the base states of the $\{|\pm\rangle_y\}$ or Y basis are

$$|\hat{\sigma}_y; \pm\rangle \equiv |\pm\rangle_y \equiv |\psi(\pi/2, \begin{Bmatrix} \pi/2 \\ 3\pi/2 \end{Bmatrix})\rangle \stackrel{(3.2)}{=} \cos(\pi/4) |0\rangle + \sin(\pi/4) e^{i\begin{Bmatrix} \pi/2 \\ 3\pi/2 \end{Bmatrix}} |1\rangle = \frac{|0\rangle \pm i|1\rangle}{\sqrt{2}} \equiv |\pm\rangle_y. \quad (3.5)$$

Besides, in the same depiction, an arbitrary density operator $\hat{\rho}$ for a mixed state⁸ can be written as

$$\hat{\rho} = \frac{1}{2}(\hat{1}_2 + \vec{r} \cdot \vec{\sigma}), \quad (3.6)$$

where $\vec{r} = \langle \hat{\sigma}_i \rangle_{\hat{\rho}} \vec{n}_i$ is a real three-dimensional vector known as the *Bloch vector* [16, p. L222, l. 31-32] or *Polarization vector*, and \vec{n}_i is the unit vector $\hat{x}, \hat{y}, \hat{z}$ for $i = 1, 2, 3$, respectively. Then, given an arbitrary single qubit, calculating $\vec{r} = (\langle \hat{\sigma}_x \rangle_{\hat{\rho}}, \langle \hat{\sigma}_y \rangle_{\hat{\rho}}, \langle \hat{\sigma}_z \rangle_{\hat{\rho}})$ is an easy way of locating it on a point of Fig. 3.1. Moreover, $0 \leq |\vec{r}| \leq 1$, where the right-hand equality holds for a pure ensemble [1, p. 195, Eq. (2.175)]. Instead, for the left-hand equality $\vec{r} = 0$, the state is maximally disordered or mixed, $\hat{\rho} = \frac{\hat{1}_d}{d}$, for dimension $d = 2^1$ here, because it is a single qubit ($n = 1$), and lies in the center of the Bloch sphere, in analogy to maximally unpolarized light in the Poincaré sphere.

⁸See the proof for Eq. (3.6) on the author's page.

3.1.2 Single qubit quantum logic gates

In addition, as mentioned (Section 3.1.1, line 3), *single qubit gates* correspond to rotations (and reflections) of the Bloch sphere represented in Fig. 3.1. For instance, the action of the Hadamard gate we will later use in Eq. (4.31),

$$\hat{U}_{\text{Had}} \doteq \frac{1}{2} \begin{pmatrix} 1 & 1 \\ 1 & -1 \end{pmatrix}, \quad (3.7)$$

can be thought of as a π rotation around the $\frac{1}{\sqrt{2}}(\vec{x} + \vec{z})$ axis, which exchanges \vec{x} and \vec{z} : [1, p. 19, l. 11-14].

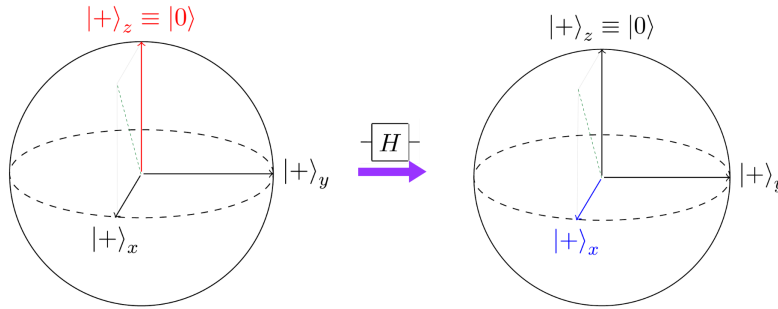


Figure 3.2: Hadamard gate acting on the input $|0\rangle$ to yield $(|0\rangle + |1\rangle)/\sqrt{2}$, in the Bloch sphere representation.

Even if experimentally we can only physically perform measurements in the OZ axis of the Bloch sphere –i.e., we can only measure in the computational basis $\{|\pm\rangle_z\} \equiv \{|0\rangle, |1\rangle\}$ –, we can use \hat{U}_{Had} to measure as if we could directly access other directions.

For instance, if we apply \hat{U}_{Had} before measuring, what previously pointed along OX – $|\pm\rangle_x$, Eq. (3.4)–, now points along OZ – $|\pm\rangle_z$, Eq. (3.3)– and vice versa: $\hat{M}_x \equiv \hat{U}_{\text{Had}} \hat{M}_z$, where \hat{M}_i denotes measurement in the i direction. This OX measuring direction is adequate, for example, to distinguish if the output qubit is either $|+\rangle_x$ or $|-\rangle_x$. This is because, taking into account Eq. (3.4), they are indistinguishable if measured in the computational basis, since we would obtain the classical bits 0 or 1 with %50 probability for both $|+\rangle_x$ or $|-\rangle_x$.

But how can we *experimentally* deploy quantum logic gates? We will briefly explain it for the case of single qubit rotations⁹ and CNOT gates, which comprise the mentioned universal set of quantum gates.

First, a multiqubit state like $|\psi\rangle = |0\rangle^{\otimes n} = |000\dots\rangle$ has to be manufactured. This can be accomplished, in an atomic physics experimental setup, for instance, putting the spins in a strong magnetic field \vec{B} which rises all of them to the spin-up state $|0\rangle \equiv |\uparrow\rangle$ in Fig. 3.1.

Then, the spins can be modified illuminating them with radiation that connects the upper state $|0\rangle \equiv |\uparrow\rangle$ with the lower state $|1\rangle \equiv |\downarrow\rangle$ [17, p. 4602, l. 43-52]. In other words, the oscillatory nature of this radiation induces a cyclic behavior between $|1\rangle$ and $|0\rangle$ known as *Rabi oscillation*.

If the pulse illuminates a qubit for $t = T/2$, where T is the Rabi oscillation period, a π tip is performed: for example, applying the radiation to the 2nd qubit, $|000\dots\rangle \rightarrow |010\dots\rangle$. On the other hand, for $t = T/4$ (a

⁹An additional example has already been given in footnote 1, for the particular case of the just introduced Hadamard single qubit rotation \hat{U}_{Had} . Now we give an explanation for general one-qubit rotations, using a setup based on 1/2-spins rather than photon interferometry.

$\pi/2$ spin rotation) it evolves as $|000\dots\rangle \rightarrow \frac{1}{\sqrt{2}}(|000\dots\rangle + |010\dots\rangle)$ [17, p. 4603, Eq. (2)].

In conjunction with 1-qubit gates, \hat{U}_{CNOT} can be implemented engineering an interaction Hamiltonian $\hat{H}_{\text{int}} = s\hbar\hat{\sigma}_z^i\hat{\sigma}_z^j$ ($s = 1/2$, here) which couples the control i and target j qubits and is turned on momentarily when the CNOT gate needs to act. Some experimental constraints can arise: e.g., IBM's quantum computer solely allows the CNOT act in the $i > j$ direction¹⁰, where $(i, j) = (\text{ctrl}, \text{target})$ and $|\rangle_{n-1} \dots |\rangle_2 |\rangle_1 |\rangle_0$ in IBM's notation¹¹, for $n \in \mathbb{N} - \{0\}$ qubits. This can be verified using its [editor](#).

Let us give a summarized explanation of the action of the latter quantum logic gate:

3.2 Controlled-NOT quantum logic gate (\hat{U}_{CNOT})

The *controlled*-NOT or CNOT gate ($\hat{U}_{\text{CNOT}} \equiv \hat{U}_{C_{\hat{\sigma}_x}}$) is the quintessential multi-qubit quantum logic gate. It is an example of a gate that performs the *conditional logic* (meaning the state of one qubit depends on the state of another) needed to make use of those the configurations (such as entanglement) that only arise in the quantum world, giving QCs features unseen on conventional computers.

It has two input qubits: the *control* qubit and the *target* [1, p. 20, l. 28-29]. The target qubit is flipped if the control qubit is 1. In other words, it performs a classical XOR (exclusive *or*) operation of both input qubits and stores the result in the output target qubit: if, for instance, we take the qubit on the left as the control, $\hat{U}_{\text{CNOT}}|x, y\rangle = |x, x \oplus y\rangle$, where \oplus is addition modulo 2 [1, p. 22, Eq. (1.18)]. Thus, apart from a two-qubit entangling gate, it can also be considered a *non-perturbing measurement gate*, in the sense that, if the target qubit is 0, it performs a perfectly accurate measurement of the control qubit [19, p. 75, l. 12-14]. In the $\{|0\rangle, |1\rangle\} \otimes \{|0\rangle, |1\rangle\} = \{|00\rangle, |01\rangle, |10\rangle, |11\rangle\}$ basis,

$$\hat{U}_{\text{CNOT}}|00\rangle \doteq \begin{pmatrix} \hat{1}_2 & \\ & \hat{\sigma}_x \end{pmatrix} \left[\begin{pmatrix} 1 \\ 0 \end{pmatrix} \otimes \begin{pmatrix} 1 \\ 0 \end{pmatrix} \right] = \begin{pmatrix} 1 & 0 & 0 & 0 \\ 0 & 1 & 0 & 0 \\ 0 & 0 & 0 & 1 \\ 0 & 0 & 1 & 0 \end{pmatrix} \begin{pmatrix} 1 \\ 0 \\ 0 \\ 0 \end{pmatrix} = \begin{pmatrix} 1 \\ 0 \\ 0 \\ 0 \end{pmatrix} \doteq |00\rangle, \quad (3.8)$$

and, in the same manner, $\hat{U}_{\text{CNOT}}|01\rangle = |01\rangle$, $\hat{U}_{\text{CNOT}}|10\rangle = |11\rangle$ and $\hat{U}_{\text{CNOT}}|11\rangle = |10\rangle$.

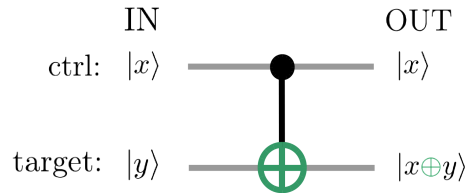


Figure 3.3: Schematic representation of CNOT gate. The control qubit is indicated by the line with the black dot. \oplus in the target qubit (second line) means addition modulo 2 and $x, y \in \{0, 1\}$.

¹⁰See the paragraph previous to Eq. (4.31).

¹¹See Eq. (4.29) for the $n = 4$ case.

3.3 No-cloning theorem

The *no-cloning theorem* is a no-go theorem that asserts that there are no physical means by which quantum information encoded in an arbitrary unknown *pure* quantum state can be copied (3.3.1), if it belongs to a *nonorthogonal* set (3.3.2).

It arose in year 1982, as the most relevant drawback that the quantum nature of information entails. It is remarkably curious that, given the relevance and simplicity of the no-cloning theorem, it was not discovered sooner.

3.3.1 General no-cloning theorem

The *no-cloning theorem* states that there is no unitary ($\hat{U}\hat{U}^\dagger = \hat{U}^\dagger\hat{U} = \hat{1}$, or $\hat{U}^\dagger = \hat{U}^{-1}$) transformation \hat{U} that can perform $|\Psi 0\rangle \rightarrow |\Psi\Psi\rangle$ for $\forall |\Psi\rangle$ [20, p. 39, l. 28-31]. This theorem is an immediate consequence of quantum physics limitation to **linearity** [7, p. 1, l. 33].

It turns out that the linear behavior is a general property of quantum mechanics. For instance, time-dependent Schrödinger equation, which describes the evolution of unitary operators $\hat{U}(t, t_0)$ ($= e^{\frac{i}{\hbar}\hat{H}(t-t_0)}$ if \hat{H} is t independent), is linear [1, p. 429, footnote 12]. Otherwise, furthering with this instance, we could not write $|\Psi\rangle$ quantum states as linear combinations of $|n\rangle$ eigenkets of the \hat{H} Hamiltonian, $|\Psi(t, t_0)\rangle = \sum_n \hat{U}(t, t_0) |n\rangle$, in order to describe their t evolution. Similarly, our cloning device must act linearly, and its effect is the following: [20, p. 39, Eq. (2.8)]

$$\hat{U} |\psi 0\rangle = \hat{U} |\psi\psi\rangle = \hat{U} |\psi\rangle^{\otimes 2} \quad \text{and} \quad \hat{U} |\phi 0\rangle = \hat{U} |\phi\phi\rangle = \hat{U} |\phi\rangle^{\otimes 2}, \quad (3.9)$$

where $|0\rangle$ is the state of the blank qubit used as a register. Taking into account the mentioned linearity,

$$\hat{U}(a|\psi\rangle + b|\phi\rangle)|0\rangle \stackrel{(\text{lin.})}{=} a\hat{U}|\psi 0\rangle + b\hat{U}|\phi 0\rangle \stackrel{(3.9)}{=} a|\psi\psi\rangle + b|\phi\phi\rangle, \quad (3.10)$$

or, which should be equivalent, taking the whole linear combination of $|\psi\rangle$ and $|\phi\rangle$ as the arbitrary input, [11, p. 429, Eq. (12.17)]

$$\hat{U}(a|\psi\rangle + b|\phi\rangle)|0\rangle \stackrel{(3.9)}{=} (a|\psi\rangle + b|\phi\rangle)(a|\psi\rangle + b|\phi\rangle) = a^2|\psi\psi\rangle + ab[|\psi\phi\rangle + |\phi\psi\rangle] + b^2|\phi\phi\rangle. \quad (3.11)$$

Thus, (3.10)=(3.11) $\leftrightarrow (a, b) = (0, \pm 1)$ or $(a, b) = (\pm 1, 0)$. That is, if and only if, the input is either $\pm|\phi\rangle$ (if $a = 0$) or $\pm|\psi\rangle$ (if $b = 0$), but not a linear combination of them. Notice that, if they are not summands of a linear combination, following Section 2.4.3, paragraph 2, $\pm|\psi\rangle = |\psi\rangle$ and $\pm|\phi\rangle = |\phi\rangle$, since $\pm 1 = e^{i\phi}$, where, respectively, $\phi = 0, \pi \in \mathbb{R}$.

With the aim of illustrating why quantum superpositions like $a|\psi\rangle + b|\phi\rangle$ cannot be cloned by using a real quantum gate, we may choose the just introduced CNOT gate, $\hat{U} = \hat{U}_{\text{CNOT}} = (3.8)$. Let us consider the task of duplicating a qubit in the particular unknown state $(a|0\rangle + b|1\rangle)$. That is, the input state of Eq. (3.10-3.11), but in the particular case $|\psi\rangle = |0\rangle$ and $|\phi\rangle = |1\rangle$.

If the target qubit is blank, $|0\rangle$, the control qubit can be seemed as cloned into there after applying the CNOT gate: $\hat{U}_{\text{CNOT}}|x0\rangle = |xx\rangle$, $x \in \{0, 1\}$. In our example, the input $(a|0\rangle + b|1\rangle)$ contains the *control* qubits, and the *target* is $|0\rangle$. Then applying linearly the CNOT gate, $\hat{U}_{\text{CNOT}}(a|0\rangle + b|1\rangle)|0\rangle = a\hat{U}_{\text{CNOT}}|00\rangle + b\hat{U}_{\text{CNOT}}|10\rangle = a|00\rangle + b|11\rangle$; i.e., the superposition $(a|0\rangle + b|1\rangle)$ is transformed into the unnormalized entangled state $a|00\rangle + b|11\rangle$. On the other had, even if we do not exploit the linearity of the cloning operator in Eq. (3.9), we should produce the same result as the CNOT, $\hat{U}(a|0\rangle + b|1\rangle)|0\rangle =$

$(a|0\rangle + b|1\rangle)(a|0\rangle + b|1\rangle) = a|00\rangle + ab|01\rangle + ab|10\rangle + b^2|11\rangle$ and we see once again that \hat{U} (here, \hat{U}_{CNOT} , when linearity is applied) does not copy the unknown input quantum state unless $(a, b) = (0, \pm 1)$ or $(a, b) = (\pm 1, 0)$ [1, p. 24, l. 8-19].

3.3.2 No-cloning theorem for approximate cloning

We will prove that even if we suppose that constraints related to linearity can be roughly overcome (approximate cloning), it is not possible duplicating *nonorthogonal* states [20, p. 40, l. 6-7]. Let us suppose that an unitary operation \hat{U} clones *approximately* both $|\psi\rangle$ and $|\phi\rangle$:

$$\hat{U}(|\psi 0\rangle) \approx |\psi\psi\rangle \quad \text{and} \quad \hat{U}(|\phi 0\rangle) \approx |\phi\phi\rangle. \quad (3.12)$$

Let us now introduce the relation between unitary operations \hat{U} and inner products (\cdot, \cdot) . First, we will define the latter. They are $(\cdot, \cdot) : \mathcal{H} \times \mathcal{H} \rightarrow \mathbb{C}$ maps, where \mathcal{H} is the Hilbert space, the aforementioned vector space over \mathbb{C} (complex vector space) equipped with inner product [1, p. 80, l. 15-16]. Id est, the inner product is the dot product generalized to the n -dimensional complex vector space \mathbb{C}^n .

Unitary operations \hat{U} preserve this inner products (\cdot, \cdot) , which is a crucial feature for probability conservation, Eq. (2.9). That is, the inner product of $\hat{U}|\psi\rangle$ and $\hat{U}|\phi\rangle$ gives the same result as the inner product of $|\psi\rangle$ and $|\phi\rangle$: respectively, $(\hat{U}|\psi\rangle, \hat{U}|\phi\rangle) = (\hat{U}|\psi\rangle)^\dagger(\hat{U}|\phi\rangle) \stackrel{(1)}{=} (|\psi\rangle^\dagger \hat{U}^\dagger)(\hat{U}|\phi\rangle) = \langle\psi| \hat{U}^\dagger \hat{U} |\phi\rangle = \langle\psi| \hat{1} |\phi\rangle = \langle\psi|\phi\rangle \stackrel{(2)}{=} (|\psi\rangle)^\dagger(|\phi\rangle) = (|\psi\rangle, |\phi\rangle)$, where in (1) we used the definition of *dual correspondence* (DC): $\hat{X}|\alpha\rangle \stackrel{\text{DC}}{\longleftrightarrow} |\alpha\rangle^\dagger \hat{X}^\dagger \equiv \langle\alpha| \hat{X}^\dagger$ [10, p. 15, Eq. (1.2.24)].

Besides, the inner product of two tensor products (\otimes) of states is the (ordinary) product of their inner products, subsystem by subsystem¹⁹ (id est, the inner product of the kets on the left of \otimes ,¹⁸ multiplied by the inner product of the kets on the right of \otimes): $(|\alpha\rangle|\psi\rangle, |\beta\rangle|\phi\rangle) = (|\alpha\rangle|\psi\rangle)^\dagger(|\beta\rangle|\phi\rangle) \stackrel{(1)}{=} (\langle\psi| \langle\alpha|)(|\beta\rangle|\phi\rangle) \stackrel{(2)}{=} \langle\psi| \langle\alpha|\beta\rangle |\phi\rangle = \langle\alpha|\beta\rangle \langle\psi|\phi\rangle$.¹² If we substitute $|\alpha\rangle = |\beta\rangle = \hat{U}$, and we replace $|\psi\rangle \rightarrow |\psi\rangle|0\rangle$ and $|\phi\rangle \rightarrow |\phi\rangle|0\rangle$:

$$\begin{aligned} (\hat{U}|\psi\rangle|0\rangle, \hat{U}|\phi\rangle|0\rangle) &= (\hat{U}|\psi\rangle|0\rangle)^\dagger(\hat{U}|\phi\rangle|0\rangle) \stackrel{(1)}{=} (\langle 0| \langle\psi| \hat{U}^\dagger)(\hat{U}|\phi\rangle|0\rangle) = \langle 0| \langle\psi| \hat{U}^\dagger \hat{U} |\phi\rangle |0\rangle \\ &= \langle 0| \langle\psi| \hat{1} |\phi\rangle |0\rangle = \langle 0| \langle\psi|\phi\rangle |0\rangle = \langle\psi|\phi\rangle \langle 0|0\rangle \stackrel{(\text{norm.})}{=} \langle\psi|\phi\rangle \cdot 1 = \langle\psi|\phi\rangle, \quad \text{or, using (3.12),} \end{aligned} \quad (3.13)$$

$$\begin{aligned} (\hat{U}|\psi\rangle|0\rangle, \hat{U}|\phi\rangle|0\rangle) &= (\hat{U}|\psi\rangle|0\rangle)^\dagger(\hat{U}|\phi\rangle|0\rangle) \stackrel{(3.12)}{\approx} (\hat{U}|\psi\rangle|\psi\rangle)^\dagger(\hat{U}|\phi\rangle|\phi\rangle) \stackrel{(1)}{=} (\langle\psi| \langle\psi| \hat{U}^\dagger)(\hat{U}|\phi\rangle|\phi\rangle) = \\ \langle\psi| \langle\psi| \hat{U}^\dagger \hat{U} |\phi\rangle |\phi\rangle &= \langle\psi| \langle\psi| \hat{1} |\phi\rangle |\phi\rangle = \langle\psi| \langle\psi|\phi\rangle |\phi\rangle = (\langle\psi|\phi\rangle)^2. \end{aligned} \quad (3.14)$$

Thus, $(3.13) \approx (3.14) \leftrightarrow \langle\psi|\phi\rangle \approx (\langle\psi|\phi\rangle)^2 \leftrightarrow \langle\psi|\phi\rangle \approx 0, 1$ (i.e., almost orthogonal or nearly the same state, $|\psi\rangle \approx |\phi\rangle$, respectively) [20, p. 40]. In essence, thus, the no-cloning theorem prevents just *nonorthogonal* states from being copied.

But, if the universe is quantum mechanical [8, p. 468, l. 6] [3, p. 3, l. 25], why can classical information be copied? If classical information, in the context of *correspondence principle*, is thought as orthogonal quantum states, the apparent paradox between the ability to copy classical information bits and the no-cloning theorem, raised because classical systems must obey quantum mechanics (and its linearity) [1, p. 29, l. 4-6 & p. 30, l. 1-2 & 8-9] is resolved.

¹²In equality (2) footnote 19 cannot be used, since $|\alpha\rangle\langle\beta|$ would be an operator, but $(\langle\alpha|)(|\beta\rangle) \equiv \langle\alpha|\beta\rangle$ here is a complex number in \mathbb{C} , that is, the result of the inner product $(\cdot, \cdot) \equiv \langle\cdot|\cdot\rangle : \mathcal{H} \times \mathcal{H} \rightarrow \mathbb{C}$.

4 Quantum artificial life model

In the QAL model proposed in Ref. [7] (experimental realization) and Ref. [14] (theoretical fundamentals), *individuals* or quantum artificial living entities are composed by two *qubits* (Fig. 4.1): one of the qubits plays the role of DNA, it represents its *genotype*, genetic information which is transmitted throughout generations, and, the other, its *phenotype* [7, p. 2, l. 9-12][14, p. 1, l. 35-37], the set of observable characteristics of the genotype resulting from the individual's interaction with the environment and other living units, that is, the creature's body.

This model corresponds to the research field of QAL because individuals are encoded in the mentioned two-qubit quantum states and quantum operations are used in order to implement the following natural selection processes:

- (Section 4.1) Finite lifetime, preservation of the genetic information (genotype) in time and presence of trophic roles (predator and prey).
- (Section 4.2) Self replication (as asexual *reproduction* mechanism) that maintains genetic information partially from generation to generation. Possible presence of *mutations* due to experimental setup errors.
- (Section 4.3.1) Aging, via phenotype degradation by the environment.
- (Section 4.3.2) Inter-individual interaction.

4.1 Finite lifetime ($\langle \hat{\sigma}_z \rangle_{\hat{\rho}_p}(t)$), time constant genotype ($\langle \hat{\sigma}_z \rangle_{\hat{\rho}_g} \neq \langle \hat{\sigma}_z \rangle_{\hat{\rho}_g}(t)$) and relative trophic roles ($\langle \hat{\sigma}_z \rangle_{1 \hat{\rho}_g} \lesseqgtr \langle \hat{\sigma}_z \rangle_{2 \hat{\rho}_g}$)

In the model described in Ref. [14], the expectation value of the Pauli matrix¹³ $\hat{\sigma}_z$ [10, p. 169, Eq. (3.2.32c)] in the phenotype (p) qubit, $\langle \hat{\sigma}_z \rangle_{\hat{\rho}_p}(t)$, measures the age (spent lifetime) of the artificial living units. Note that $\langle \hat{\sigma}_z \rangle_{\hat{\rho}_p} = \langle \hat{\sigma}_z \rangle_{\hat{\rho}_p}(t)$, because the phenotype $\hat{\rho}_p$ changes [7, p. 2, l. 13-14] due to the interaction performed during time t with other individuals and the environment¹⁴, as it occurs in nature!

A different observable or set of observables could have been selected, but we have chosen $\hat{\sigma}_z$ just to make calculations simpler, since its matrix representation is diagonal in $\{|0\rangle, |1\rangle\}$, the basis given by the steady state ($\hat{\rho}_A = |0\rangle\langle 0|$) of the Lindblad master equation we use to simulate the effect of the environment or bath (Section 4.3.1).

The **finite lifetime**, characteristic of all living beings, is mimicked by the time elapsed in the evolution of $\langle \hat{\sigma}_z \rangle_{\hat{\rho}_p}(t)$ from its creation to the vicinity of an asymptotic value; here, $1 - \epsilon$, for fixed ϵ ¹⁵. In other words, [14, p. 3, l. 11-12] the death age t_d is achieved when $\langle \hat{\sigma}_z \rangle_{\hat{\rho}_p}(t = t_d) = 1 - \epsilon$, so an individual is alive if and only if $\langle \hat{\sigma}_z \rangle_{\hat{\rho}_p}(t) < 1 - \epsilon$. Then, t_d can be physically regarded as the *decoherence time* (Section 4.3.1).

¹³ $\hat{\sigma}_i$ are the Pauli matrices for $i = 1, 2, 3$ [10, p. 169, Eq. (3.2.32)], or, equivalently, $i = x, y, z$ [1, p. 65, Fig. 2.2]. Additionally, $\hat{\sigma}_0 \equiv \hat{I}_2$.

¹⁴Precisely, the phenotype qubit degrades towards $\hat{\rho}_{\text{Ancillary}} \equiv \hat{\rho}_A = |0\rangle\langle 0|$. See Section 4.3.1.

¹⁵See an example in Appendix B.1.

On the other hand, $\langle \hat{\sigma}_z \rangle_{\hat{\rho}_g}$ –the expectation value of $\hat{\sigma}_z$ in the genotype (g) qubit– determines, in addition to its lifetime (implicitly)¹⁶, its role (predator or prey) in the trophic chain [14, p. 1, l. 39]. However, contrary to the phenotype, the **genotype** remains **unchanged in time** t under the influence of any interaction, $\langle \hat{\sigma}_z \rangle_{\hat{\rho}_g} \neq \langle \hat{\sigma}_z \rangle_{\hat{\rho}_g}(t)$, again following the logic of nature!

In nature, predators or preys do not change their *trophic role* during life, so it is coherent that $\langle \hat{\sigma}_z \rangle_{\hat{\rho}_g}$ determines it. In our scenario, since predators' $\langle \hat{\sigma}_z \rangle_{\hat{\rho}_p}$ is greater, closer to the death value $1 - \epsilon$, and $\langle \hat{\sigma}_z \rangle_{\hat{\rho}_p}$ increases¹⁵ with t in the absence of feeding, they have to hunt preys in order to survive.

Let us suppose that we have $\langle \hat{\sigma}_z \rangle_{\hat{\rho}_g^\alpha} > \langle \hat{\sigma}_z \rangle_{\hat{\rho}_g^\beta}$. As logic dictates, individual α will act as a predator, since

$$\langle \hat{\sigma}_z \rangle_{\hat{\rho}_g^\alpha} > \langle \hat{\sigma}_z \rangle_{\hat{\rho}_g^\beta} \stackrel{(16)}{\rightarrow} \langle \hat{\sigma}_z \rangle_{\hat{\rho}_p^\alpha}(t_{p^\alpha}) > \langle \hat{\sigma}_z \rangle_{\hat{\rho}_p^\beta}(t_{p^\beta}), \quad (4.1)$$

so individual α is closer to death, from its birth time t_{p^α} ¹⁷. Then, individual α is the predator.

The longest-living organisms (in our example, $(4.15)|_{a=0} = \langle \hat{\sigma}_z \rangle_{\hat{\rho}_{g1}}|_{a=0} = -1$, see Fig. B.1) are herbivore. They are well adapted to environmental effects (a reflection of eating plants), but they are always preys in inter-individual relations. On the other hand, the nearly death ones (in our example, $(4.15)|_{a \approx 1} = \langle \hat{\sigma}_z \rangle_{\hat{\rho}_{g1}}|_{a \approx 1} \approx 1$), are situated on the top of the trophic pyramid.

Obviously, here, *trophic roles* are **relative**: they depend on the two individuals that interact, α and β in Eq. (4.1). The same individual can be a prey for the interaction with some living units but a prey in relation to some others. This emulates the great diversity of species in nature!

4.2 Reproduction: self-replication

Besides the three biological characteristics described in Section 4.1, reproduction is also an ability common in all alive –in our formalism, $\langle \hat{\sigma}_z \rangle_{\hat{\rho}_p}(t) < 1 - \epsilon$ – organisms. Here, *self-replication* will be our reproduction mechanism [7, p. 2, l. 16-23], although of asexual nature. It is performed following two steps based on *quantum partial cloning*, copying from a given genotype $\hat{\rho}_g$ the expectation value of a chosen observable ($\hat{\sigma}_z$, here, for reasons presented in Section 4.1, paragraph 2) into a blank or ancillary state $\hat{\rho}_A$ [7, p. 2, l. 16-17] that the environment or bath provides via the closure of the trophic cycle (Section 4.3.1).

Quantum mechanics forbids *perfect* cloning, but permits solutions for partial cloning. Here, what is copied is not the whole state, but the expectation value of a set of observables that commute [16]. Commutativity is needed so that all can be written in a common basis [11, p. 111, footnote 18]. Nevertheless, in our case, as mentioned, rather than a set we just use one observable, $\hat{\sigma}_z$.

Used as a *self-replication* protocol, partial cloning establishes a powerful simile with what happens in biological systems. For instance, in DNA replication, information is not perfectly duplicated into the

¹⁶Because $\langle \hat{\sigma}_z \rangle_{\hat{\rho}_{g_i}} = \langle \hat{\sigma}_z \rangle_{\hat{\rho}_{p_i}}(t_{p_i})$, for the i^{th} generation, $i \in \mathbb{N}$, as we will see in Eq. (4.5(2)), where $t = t_{p_i}$ is the time when phenotype $\hat{\rho}_{p_i}$ is created.

¹⁷You might think that, if the predator is created later, $t_{p^\alpha} > t_{p^\beta}$, maybe, at some time t , $\langle \hat{\sigma}_z \rangle_{\hat{\rho}_p^\alpha}(t) < \langle \hat{\sigma}_z \rangle_{\hat{\rho}_p^\beta}(t)$, but there is not contradiction in young predators feeding from old preys. The trophic role is determined by the genotype and does not change with time.

following generations, solely sequences of bases are copied [15, p. 1, l. 25-28]. Here, $\langle \hat{\sigma}_z \rangle_{\hat{\rho}_g}$ plays the role of that part of DNA transmitted via reproduction.

Our quantum partial cloning operation *entangles* the genotype $\hat{\rho}_g$ and the phenotype $\hat{\rho}_p$ with the ancillary state $\hat{\rho}_A$ [7, p. 2, l. 17-18], and this entanglement is spread across generations. By this entanglement implementation, this QAL model goes beyond the straightforward quantization of existing classical models, in contrast to Section 2.4.

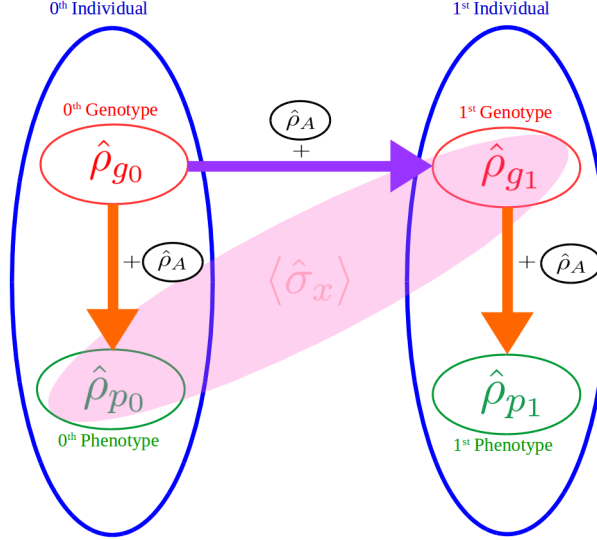


Figure 4.1: (Left) Creation of the 0th individual via $\hat{\rho}_{p0}$ **phenotype creation** from genotype $\hat{\rho}_{g0}$. (Right) Creation of the 1st individual via *self-replication* (4.2): $\hat{\rho}_{g1}$ **genotype creation** (4.2.2) from genotype $\hat{\rho}_{g0} + \hat{\rho}_{p1}$ **phenotype creation** (4.2.3) from the new genotype $\hat{\rho}_{g1}$. The pink ellipse represents the information that is conveyed, in Eq. (4.6), onto the global state of the two outputs of cloning operator \hat{U} in Eq. (4.2).

In our model, life begins from an unknown initial genotype $\hat{\rho}_{g0}$. It will be taken as the genotype of the 0th generation individual after the first **phenotype creation**, (4.10)|_{i=0} = $\hat{\rho}_{p0} = \hat{U}(\hat{\rho}_{g0} \otimes \hat{\rho}_A)\hat{U}^\dagger$. Here, from the genotype $\hat{\rho}_{g0}$, the phenotype $\hat{\rho}_{p0}$ is created, cloning $\langle \hat{\sigma}_z \rangle_{\hat{\rho}_{g0}}$ to a blank state $\hat{\rho}_A$. With this, the 0th generation living unit is born.

Then, the 0th individual and the forthcoming generations breed via **self-replication**. Self-replication is essentially the same mechanism used to create the 0th individual, with the exception that in the formation of the 0th individual, we used a given genotype, $\hat{\rho}_{g0}$. Now, however, we have to create it first. First, we create the new individual's genotype ($\hat{\rho}_{g1}$, e.g., for self-replication to create the 1st generation individual, right part of Fig. 4.1) from the progenitor's genotype ($\hat{\rho}_{g0}$, in the chosen example), and then the phenotype ($\hat{\rho}_{p1}$, in the same instance), from the new genotype ($\hat{\rho}_{g1}$). Thus, as mentioned, two events form the self-replication process:

- **Genotype creation** (4.2.2): From the i^{th} individual's genotype $\hat{\rho}_{g_i}$, $i \in \mathbb{N}$, the genotype of the $i + 1$ generation's individual, $\hat{\rho}_{g_{i+1}}$, is created, duplicating $\langle \hat{\sigma}_z \rangle$ to a blank state $\hat{\rho}_A$: $\hat{\rho}_{g_{i+1}} \stackrel{(4.10)}{=} \hat{U}(\hat{\rho}_{g_i} \otimes \hat{\rho}_A)\hat{U}^\dagger$ [7, p. 2, l. 19-20].

- **Phenotype creation** (4.2.3): From the new genotype $\hat{\rho}_{g_{i+1}}$, the phenotype of the same new individual, $\hat{\rho}_{p_{i+1}}$, is created, copying again $\langle \hat{\sigma}_z \rangle$ to a blank state $\hat{\rho}_A$: $\hat{\rho}_{p_{i+1}} \stackrel{(4.10)}{=} \hat{U} (\hat{\rho}_{g_{i+1}} \otimes \hat{\rho}_A) \hat{U}^\dagger$ [7, p. 2, l. 20-22].

4.2.1 Quantum partial cloning operator \hat{U} as self-replication operator

Quantum partial cloning, the cloning of the expectation value of a chosen *single*-qubit observable, is effectuated via the operator \hat{U} proposed in Ref. [14, p. 2, Eq. (1b) & (3c)], [15, p. 2, Eq. (7)] and [16, p. L220, l. 30]:

$$\hat{\rho}_{\text{new}} = \hat{U} (\hat{\rho}_{\text{old}} \otimes \hat{\rho}_A) \hat{U}^\dagger, \quad (4.2)$$

where, since we have chosen $\hat{\sigma}_z$ as the *single*-qubit observable to partially clone, and $\hat{\rho}_A = |0\rangle\langle 0|$ as the known ancillary qubit, $\hat{U} \stackrel{(B.9)}{=} \hat{U}_{\text{CNOT}} \equiv \hat{U}_{C_{\hat{\sigma}_z}}$ [16, p. L221, l. 37-38]. See the proof in Appendix B.2.

Eq. (4.2) has a form reminiscent of the t evolution of density operators $\hat{\rho}$: [10, p. 181, Eq. (3.4.7)]

$$\begin{aligned} \hat{\rho}(t) &\equiv \sum_i w_i |\alpha^{(i)}(t)\rangle \langle \alpha^{(i)}(t)| = \sum_i w_i |\alpha^{(i)}(t)\rangle \left(|\alpha^{(i)}(t)\rangle \right)^\dagger \\ &= \sum_i w_i \left(\hat{U}(t, t_0) |\alpha^{(i)}(t_0)\rangle \right) \left(\hat{U}(t, t_0) |\alpha^{(i)}(t_0)\rangle \right)^\dagger \\ &= \sum_i w_i \hat{U}(t, t_0) |\alpha^{(i)}(t_0)\rangle \left(|\alpha^{(i)}(t_0)\rangle \right)^\dagger \hat{U}^\dagger(t, t_0) \\ &= \hat{U}(t, t_0) \left(\sum_i w_i |\alpha^{(i)}(t_0)\rangle \langle \alpha^{(i)}(t_0)| \right) \hat{U}^\dagger(t, t_0) = \hat{U}(t, t_0) \hat{\rho}(t_0) \hat{U}^\dagger(t, t_0). \end{aligned} \quad (4.3)$$

Nevertheless, in Eq. (4.2), unitary transformation $\hat{U} \neq \hat{U}(t, t_0)$. It acts on an n -dimension initial quantum state $\hat{\rho}_{\text{old}}$ —where $n = \dim \hat{\rho}_{\text{old}} = \dim \mathcal{H}_{\hat{\rho}_{g_0}} = 2^k$, where $k \in \mathbb{N}$ is the number of qubits used in the progeny line from $\hat{\rho}_{g_0}$, because, as mentioned in Section 1, qubits are 2-level quantum systems and dimensions grow exponentially—, and copies the expectation value of a chosen set of observables ($\hat{\sigma}_z$, here) from $\hat{\rho}_{\text{old}}$ to a blank state $\hat{\rho}_A$, in order to create $\hat{\rho}_{\text{new}}$:

$$\begin{aligned} \hat{\rho}_{\text{new}} &\equiv \sum_i w_i |\alpha^{(i)}\rangle_{\text{new}} \langle \alpha^{(i)}|_{\text{new}} = \sum_i w_i |\alpha^{(i)}\rangle_{\text{new}} \left(|\alpha^{(i)}\rangle_{\text{new}} \right)^\dagger \\ &\stackrel{(3.9)}{=} \sum_i w_i \left(\hat{U} |\alpha^{(i)}\rangle_{\text{old}} |0\rangle \right) \left(\hat{U} |\alpha^{(i)}\rangle_{\text{old}} |0\rangle \right)^\dagger \\ &= \sum_i w_i \hat{U} |\alpha^{(i)}\rangle_{\text{old}} |0\rangle \left(|\alpha^{(i)}\rangle_{\text{old}} |0\rangle \right)^\dagger \hat{U}^\dagger \stackrel{(1)}{=} \sum_i w_i \hat{U} |\alpha^{(i)}\rangle_{\text{old}} |0\rangle \langle \alpha^{(i)}|_{\text{old}} \langle 0| \hat{U}^\dagger \\ &= \hat{U} \left(\sum_i w_i |\alpha^{(i)}\rangle_{\text{old}} |0\rangle \langle \alpha^{(i)}|_{\text{old}} \langle 0| \right) \hat{U}^\dagger \stackrel{(2)}{=} \hat{U} \left(\left[\sum_i w_i |\alpha^{(i)}\rangle_{\text{old}} \langle \alpha^{(i)}|_{\text{old}} \right] \otimes |0\rangle \langle 0| \right) \hat{U}^\dagger \\ &= \hat{U} (\hat{\rho}_{\text{old}} \otimes \hat{\rho}_A) \hat{U}^\dagger = (4.2), \end{aligned} \quad (4.4)$$

where in equality (1) we used $(|a\rangle \otimes |b\rangle)^\dagger = |a\rangle^\dagger \otimes |b\rangle^\dagger = \langle a| \otimes \langle b| \equiv \langle a| \langle b|$ ¹⁸ [1, p. 74, Eq. (2.53)], and, in

¹⁸We use the abbreviated notations $|v\rangle \otimes |w\rangle \equiv |v\rangle |w\rangle \equiv |v, w\rangle \equiv |vw\rangle$ [1, p. 72, l. 33], where \otimes is the tensor product.

$$(2), (\hat{A} \otimes \hat{B})(\hat{C} \otimes \hat{D}) = (\hat{A}\hat{C}) \otimes (\hat{B}\hat{D}).^{19}$$

Thus, using Eq. (4.2), from a precursor qubit $\hat{\rho}_{\text{old}}$, a new qubit $\hat{\rho}_{\text{new}}$ is created. For the instance described in Fig. 4.1, $\hat{\rho}_{\text{old}} = \hat{\rho}_{g_0}$ and $\hat{\rho}_{\text{new}} = \hat{\rho}_{g_1}$ [$\hat{\rho}_{\text{old}} = \hat{\rho}_{g_1}$ and $\hat{\rho}_{\text{new}} = \hat{\rho}_{p_1}$], for the **genotype creation** [**phenotype creation**] of the 1st individual.

Besides, as it can be seen in the two arrows that, tantamount to Fig. 1 in Ref. [15, p. 2] and Fig. 1 in Ref [16, p. L220], branch from $\hat{\rho}_{g_0}$ in Fig. 4.1, each quantum partial cloning operation has two possible outputs.

Henceforth, so that the quantum partial cloning operator \hat{U} can be considered reliable, the expectation value of the chosen observable $-\langle \hat{\sigma}_z \rangle$, here– duplicated into the two possible outputs must have the same value. In other words, a measurement of $\hat{\sigma}_z$ on either the two output qubits $\hat{\rho}_{p_i}$ and $\hat{\rho}_{g_{i+1}}$ ought to be the same as on the input qubit in the unknown input state $\hat{\rho}_i$, $i \in \mathbb{N}$: [14, p. 2, Eq. (1a)] [15, p. 1, Eq. (1)] [16, p. L220, Eq. (1)]

$$\langle \hat{\sigma}_z \rangle_{\hat{\rho}_{g_i}} \equiv \langle \hat{\sigma}_z \rangle_{\hat{\rho}_i} \stackrel{(1)}{=} \langle (\hat{\sigma}_z)_{g_{i+1}} \otimes \hat{1}_{p_i} \rangle_{\hat{\rho}_{g_{i+1}}} \equiv \langle \hat{\sigma}_z \rangle_{\hat{\rho}_{g_{i+1}}} \stackrel{(2)}{=} \langle \hat{1}_{g_{i+1}} \otimes (\hat{\sigma}_z)_{p_i} \rangle_{\hat{\rho}_{g_{i+1}}} \equiv \langle \hat{\sigma}_z \rangle_{\hat{\rho}_{p_i}}(t_{p_i}), \quad i \in \mathbb{N}, \quad (4.5)$$

where, t_{p_i} is the time, prior to any change provoked by interactions (with the environment and/or other individuals), when the phenotype $\hat{\rho}_{p_i}$ is created from the genotype $\hat{\rho}_{g_i}$.

$\hat{\rho}_{g_{i+1}}$ ²⁰ represents the system formed by two output qubits of \hat{U} , Eq. (4.10): one subspace is $\hat{\rho}_{p_i}$ and, the other, $\hat{\rho}_{g_{i+1}}$. In connection with this, operators' subscripts in Eq. (4.5) indicate the qubits ($\hat{\rho}_{g_{i+1}}$ or $\hat{\rho}_{p_i}$) they act on. In fact, definitions $\langle (\hat{\sigma}_z)_{g_{i+1}} \otimes \hat{1}_{p_i} \rangle_{\hat{\rho}_{g_{i+1}}} \equiv \langle \hat{\sigma}_z \rangle_{\hat{\rho}_{g_{i+1}}}$ and $\langle \hat{1}_{g_{i+1}} \otimes (\hat{\sigma}_z)_{p_i} \rangle_{\hat{\rho}_{g_{i+1}}} \equiv \langle \hat{\sigma}_z \rangle_{\hat{\rho}_{p_i}}(t_{p_i})$ in Eq. (4.5) follow from footnote 19. The fact that the left (right) operator acts on g_{i+1} (p_i) fits the result in Eq. (4.23).

For the particular case $i = 0$, $\hat{\rho}_0 = \hat{\rho}_{g_0}$,²⁰ we have $\langle \hat{\sigma}_z \otimes 1 \rangle_{\hat{\rho}_0} = \langle 1 \otimes \hat{\sigma}_z \rangle_{\hat{\rho}_0} = \langle \hat{\sigma}_z \rangle_{\hat{\rho}_0} \equiv \langle \hat{\sigma}_z \rangle_{\hat{\rho}_{g_0}}$. We can think of the left (right) operator in $\langle (\hat{\sigma}_z)_{g_1} \otimes \hat{1}_{p_0} \rangle_{\hat{\rho}_1} \equiv \langle \hat{\sigma}_z \rangle_{\hat{\rho}_{g_1}}$ and $\langle \hat{1}_{g_1} \otimes (\hat{\sigma}_z)_{p_0} \rangle_{\hat{\rho}_1} \equiv \langle \hat{\sigma}_z \rangle_{\hat{\rho}_{p_0}}(t_0)$ of Eq. (4.5) as acting on the qubit located in the top right (bottom left) part of Fig. 4.1.

Equality (1) in Eq. (4.5), **genotype creation** $\langle \hat{\sigma}_z \rangle_{\hat{\rho}_{g_i}} \stackrel{(1)}{=} \langle \hat{\sigma}_z \rangle_{\hat{\rho}_{g_{i+1}}}$, is necessary so that **preservation of the genetic information throughout successive generations** (as well as time, obviously) can be mimicked [14, p. 2, l. 31-32]. On the other hand, equality (2), **phenotype creation** $\langle \hat{\sigma}_z \rangle_{\hat{\rho}_{g_i}} \stackrel{(2)}{=} \langle \hat{\sigma}_z \rangle_{\hat{\rho}_{p_i}}(t_{p_i})$, ensures we have a phenotype that is a result, at least with respect to the value of $\langle \hat{\sigma}_z \rangle$, of its corresponding genotype, a crucial feature in natural selection! Withal, possible errors in the replication stage would provide this model's simile of *mutation* [7, p. 2, l. 27] [14, p. 2, l. 3-4].

Using Eq. (3.6), $\hat{\rho} = \frac{1}{2}(\hat{1}_2 + \vec{r} \cdot \vec{\sigma})$, for interpretation purposes, the action of the exposed cloning protocol can be regarded as the perfect copying of just the component r_3 of the *Bloch vector* or *Polarization vector* $\vec{r} = (r_1, r_2, r_3) = \langle \hat{\sigma}_i \rangle_{\hat{\rho}} \vec{n}_i$, $i = 1, 2, 3$, whereas the values of r_1 and r_2 are completely disregarded, since we have $\vec{\sigma} = (0, 0, \hat{\sigma}_z)$ [16, p. L222, l. 33-34]. That is, the no-cloning theorem only allows approximate cloning,

¹⁹ $(\hat{A} \otimes \hat{B})(\hat{C} \otimes \hat{D}) = (\hat{A}\hat{C}) \otimes (\hat{B}\hat{D})$ follows from defining $\hat{A} \otimes \hat{1}_B$ ($\hat{1}_A \otimes \hat{B}$) as an operator which acts solely on subspace A (B): $(\hat{A} \otimes \hat{1}_B)(\hat{1}_A \otimes \hat{B}) = \hat{A}\hat{1}_A \otimes \hat{1}_B\hat{B} = \hat{A} \otimes \hat{B}$, in a bipartite system in $\mathcal{H}_A \otimes \mathcal{H}_B$.

²⁰ $i = 0$ is the exception, where $\hat{\rho}_0 = \hat{\rho}_{g_0}$.

the cloning of a part of the Bloch vector \vec{r} . This is equivalent to copying classical information, because there is no quantum superposition in just a component of \vec{r} , and that is why the mentioned no-go theorem is not contradicted.

Our quantum partial cloning protocol is not solely capable of transmitting classical information (diagonal elements of $\hat{\rho}_{g_i}$) like $\langle \hat{\sigma}_z \rangle_{\hat{\rho}_{g_i}}$. Indeed, **quantum information** is also disseminated, associated to the coherences (off-diagonal elements of the density operator in a considered basis) belonging to $\hat{\rho}_{g_i}$.

This quantum information is related to an observable which does not commute with $\hat{\sigma}_z$, let us say $\hat{\sigma}_x$, and it is copied into to the *global state* of the outputs ($\hat{\rho}_{p_i}$ and $\hat{\rho}_{g_{i+1}}$). The quantum nature of this statistics resides in the fact that it cannot be determined which part of the information has been copied into to the output phenotype subspace $\langle \hat{\sigma}_x \rangle_{\hat{\rho}_{p_i}} \equiv \langle \hat{1} \otimes \hat{\sigma}_x \rangle_{\hat{\rho}_{i+1}}$ and which one into the output genotype $\langle \hat{\sigma}_x \rangle_{\hat{\rho}_{g_{i+1}}} \equiv \langle \hat{\sigma}_x \otimes \hat{1} \rangle_{\hat{\rho}_{i+1}}$. In other words, there is some information that belongs simultaneously (pink ellipse in Fig. 4.1) to both outputs of the quantum partial cloning operation, so they are quantumly correlated or **entangled!**

By transmitting quantum information from the genotype $\hat{\rho}_{g_i}$ to the global state, or common space of $\hat{\rho}_{p_i}$ and $\hat{\rho}_{g_{i+1}}$, we mean that the following condition is satisfied: [15, p. 2, Eq. (2)]

$$\langle \hat{\sigma}_x \rangle_{\hat{\rho}_i} = \langle \hat{\sigma}_x \otimes \hat{\sigma}_x \rangle_{\hat{\rho}_{i+1}}. \quad (4.6)$$

This means that the quantum partial cloning operator \hat{U} , apart from duplicating the expectation value of the 0th generation individual independently to its descendants, also conveys information to the offspring as a whole. The latter kind of information is related in biological systems to collective behaviors! For example, self-organization of neurons. [15, p. 2, below Theorem 1]

See an example for the case $i = 0$ (Fig. 4.1) in Eq. (4.18), which corresponds to transmission onto the global state of the first cloning operation's outputs.

4.2.2 Genotype creation

As said, the first step in the reproduction via self-replication is *partially cloning* –without violating the *no-cloning* theorem– the expectation value of a certain set of observables (only $\langle \hat{\sigma}_z \rangle_g$, in this model) belonging to a predecessor genotype ($\hat{\rho}_{g_0}$, for example, in order to start forming the 1st individual, as in Fig. 4.1) into an ancillary state $\hat{\rho}_A = |0\rangle\langle 0|$ originated (see Section 4.3.1) by the environment, so that a new genotype ($\hat{\rho}_{g_1}$, in the 1st individual example) is created.

The self-replication process must preserve the expectation value for the chosen observable, Eq. (4.5(1)). Therefore, $\langle \hat{\sigma}_z \rangle_{\hat{\rho}_g}$ will be constant both in time – $\langle \hat{\sigma}_z \rangle_{\hat{\rho}_g} \neq \langle \hat{\sigma}_z \rangle_{\hat{\rho}_g}(t)$, as mentioned in Section 4.1, paragraph 4– and from generation to generation, as said in the second paragraph below Eq. (4.10).

Example: in order to prove that $\langle \hat{\sigma}_z \rangle_{\hat{\rho}_g}$ remains constant, let us suppose that the unknown inaugural

genotype state $\hat{\rho}_0 = \hat{\rho}_{g_0}$ from which subsequent living units will be created is described by the following density operator, in the $\{|\pm\rangle_z\} \equiv \{|0\rangle, |1\rangle\}$ computational basis (as we work in a basis in which $\hat{\sigma}_z$ is diagonal [15, p. 2, l. 20-21]):²¹

$$\hat{\rho}_0 = \hat{\rho}_{g_0} \doteq \begin{pmatrix} a & b - ic \\ b + ic & 1 - a \end{pmatrix}. \quad (4.7)$$

where $a < 1$, as it can be inferred from Fig. B.1.

From this precursor genotype $\hat{\rho}_{g_0}$, Eq. (4.7), we create the genotype qubit belonging to the new individual of the 1st generation, $\hat{\rho}_{g_1}$, via the operator proposed in Eq. (4.10):²²

$$\hat{\rho}_1 \stackrel{(4.10)}{\equiv} \hat{\rho}_{g_1} = \hat{U}(\hat{\rho}_{g_0} \otimes \hat{\rho}_A)\hat{U}^\dagger \stackrel{(B.10)}{=} \begin{pmatrix} a & 0 & 0 & b - ic \\ 0 & 0 & 0 & 0 \\ 0 & 0 & 0 & 0 \\ b + ic & 0 & 0 & 1 - a \end{pmatrix}, \quad (4.8)$$

where we have used, in the $\{|0\rangle, |1\rangle\}^{\otimes 2} = \{|0\rangle, |1\rangle\} \otimes \{|0\rangle, |1\rangle\} = \{|00\rangle, |01\rangle, |10\rangle, |11\rangle\}$ ¹⁸ basis, [1, p. xxxi, l. 1]

$$\hat{U} \stackrel{(B.9)}{=} \hat{U}_{\text{CNOT}} \stackrel{(B.11)}{=} \begin{pmatrix} 1 & 0 & 0 & 0 \\ 0 & 1 & 0 & 0 \\ 0 & 0 & 0 & 1 \\ 0 & 0 & 1 & 0 \end{pmatrix}, \quad (4.9)$$

where $\hat{U}^\dagger \equiv \hat{U}_{\text{CNOT}}^\dagger = \hat{U}_{\text{CNOT}} \equiv \hat{U}$, and $\hat{U}^\dagger \equiv (\hat{U}^*)^T \stackrel{(1)}{=} \hat{U}^T$. Equality (1) is satisfied because $\hat{U} \in \mathbb{R}$. Hence, unitarity condition for quantum logic gates $\hat{U}^\dagger = \hat{U}^{-1}$ simplifies to orthogonality $\hat{U}^T = \hat{U}^{-1}$, here. Then, $\hat{U}^T \equiv \hat{U}_{\text{CNOT}}^T = \hat{U}_{\text{CNOT}} \equiv \hat{U}$. In other words, \hat{U} is a symmetric matrix, a square matrix that is equal to its transpose.

4.2.3 Phenotype creation

Then, the new phenotype is created. As in the genotype creation, the expectation value of $\hat{\sigma}_z$ from the genotype $\hat{\rho}_{g_i}$, $\langle \hat{\sigma}_z \rangle_{\hat{\rho}_{g_i}}$, is copied to an ancillary state $\hat{\rho}_A$ [14, p. 2, Eq. (3c)], without contradicting the *no-cloning* theorem [15, p. 2, l. 17-19]. With this, the i^{th} living unit is completed, $i \in \mathbb{N}$.

Genotype's $\langle \hat{\sigma}_z \rangle_{\hat{\rho}_{g_i}}$ remains constant, $\langle \hat{\sigma}_z \rangle_{\hat{\rho}_{g_i}} \neq \langle \hat{\sigma}_z \rangle_{\hat{\rho}_{g_i}}(t)$, as mentioned in Section 4.1. Conversely, the phenotype's $\langle \hat{\sigma}_z \rangle_{\hat{\rho}_{p_i}}(t)$ is prone to change because of interactions. For example, for the case of the cloning operations $i = 0, 1$ in Fig. 4.1, since they are not simultaneous ($t_{p_0} \neq t_{p_1}$; precisely, $t_{p_0} < t_{p_1}$), $\langle \hat{\sigma}_z \rangle_{\hat{\rho}_{p_0}}(t)$ has already changed by the time p_1 is created. Nevertheless, because of $\langle \hat{\sigma}_z \rangle_{\hat{\rho}_g}$'s conservation through generations, phenotypes have the same initial expectation value of $\hat{\sigma}_z$ if they have descended from a common ancestor, $\langle \hat{\sigma}_z \rangle_{\hat{\rho}_{p_i}}(t_{p_i}) = \langle \hat{\sigma}_z \rangle_{\hat{\rho}_{p_j}}(t_{p_j})$, for $i \neq j$.

²¹See on the author's page that $\hat{\rho}_{g_0}$, Eq. (4.7), satisfies the usual properties of the density operator ($\hat{\rho}$).

²²See calculations of Eq. (4.8-4.9) in Appendix B.3.

Furthering with Eq. (4.2), it can be defined in this context as

$$\hat{\rho}_{i+1} \equiv \hat{\rho}_{p_i}(t_{p_i}) = \hat{\rho}_{g_{i+1}} \stackrel{(4.2)}{=} \hat{U}(\hat{\rho}_{g_i} \otimes \hat{\rho}_A) \hat{U}^\dagger \equiv \hat{U}(\hat{\rho}_i \otimes \hat{\rho}_A) \hat{U}^\dagger, \quad i \in \mathbb{N}. \quad (4.10)$$

The first equality here is the reason why we defined, in Eq. (4.5(2)), $\langle \hat{1}_{g_{i+1}} \otimes (\hat{\sigma}_z)_{p_i} \rangle_{\hat{\rho}_{p_i}(t_{p_i})} \stackrel{(4.10)}{=} \langle \hat{1}_{g_{i+1}} \otimes (\hat{\sigma}_z)_{p_i} \rangle_{\hat{\rho}_{i+1}} \equiv \langle \hat{\sigma}_z \rangle_{\hat{\rho}_{p_i}}(t_{p_i})$.

If we wanted perfect copying $\forall \hat{\rho}_i$, that is, satisfying $\hat{\rho}_{p_i}(t_{p_i}) = \hat{\rho}_i$ apart from Eq. (4.10), as it can be deduced from Eq. (3.6), we would need $\langle \hat{\sigma}_k \rangle_{p_i}(t_{p_i}) = \langle \hat{\sigma}_k \rangle_{g_i}$, for $k = 1, 2, 3$,¹³ not just for $k = 3$. However, this is not possible since they cannot be expressed in the same basis because they do not form a set of commuting observables: $[\hat{\sigma}_k, \hat{\sigma}_l] = 2i \epsilon_{klm} \hat{\sigma}_m$ [10, p. 169, Eq. (3.2.25)].²³ Or, from another perspective, this would imply copying not just its component r_3 , but all the *Polarization vector* $\vec{r} = \langle \hat{\sigma}_i \rangle_{\hat{\rho}}$. The latter is not permitted by the no-cloning theorem.

Because of what has just been explained, $\hat{\rho}_{p_i}(t_{p_i}) \neq \hat{\rho}_i \equiv \hat{\rho}_{g_i}$. For instance, for $i = 1$, $\hat{\rho}_{p_1}(t_{p_1}) \neq \hat{\rho}_{g_1} =$ (4.8). Instead, we have: [15, p. 2, Eq. (8)]

$$\begin{aligned} \hat{\rho}_{p_1}(t_{p_1}) \stackrel{(4.10)}{=} \hat{\rho}_{g_2} \equiv \hat{\rho}_2 = \hat{U}[\hat{\rho}_1 \otimes \hat{\rho}_A] \hat{U}^\dagger \stackrel{(1)}{=} \hat{U}_1[\hat{\rho}_1 \otimes \hat{\rho}_A] \hat{U}_1^\dagger \stackrel{(4.8)}{=} \hat{U}_1 \left[\left(\hat{U}_0(\hat{\rho}_0 \otimes \hat{\rho}_A) \hat{U}_0^\dagger \right) \otimes \hat{\rho}_A \right] \hat{U}_1^\dagger \\ \stackrel{(2)}{=} \left(\hat{U}_1 \hat{U}_0 \right) (\hat{\rho}_0 \otimes \hat{\rho}_A \otimes \hat{\rho}_A) \left(\hat{U}_0^\dagger \hat{U}_1^\dagger \right) = \left(\hat{U}_1 \hat{U}_0 \right) (\hat{\rho}_0 \otimes \hat{\rho}_A \otimes \hat{\rho}_A) \left(\hat{U}_1 \hat{U}_0 \right)^\dagger, \end{aligned} \quad (4.11)$$

where in (1) we redefined Eq. (4.10) as $\hat{\rho}_{i+1} = \hat{U}_i(\hat{\rho}_i \otimes \hat{\rho}_A) \hat{U}_i^\dagger$, $i \in \mathbb{N}$, just to differentiate the $\hat{U} \equiv \hat{U}_0$ operators that belong to $\hat{\rho}_1 =$ (4.8). On the other hand, in (2) we used the remark made in footnote 19.

4.2.4 Preservation of $\langle \hat{\sigma}_z \rangle$ after self-replications

Being the condition imposed in Eq. (4.5), we will show that our self-replication protocol maintains $\langle \hat{\sigma}_z \rangle$, the expectation value taken in the two output qubits created by the action of the \hat{U} operator on $\hat{\rho}_i$: either the genotype of the next generation ($\hat{\rho}_{i+1}$) or the phenotype subspace belonging to the same generation ($\hat{\rho}_{p_i}(t_{p_i})$).

As mentioned, what it is truly conserved, both in time t and from generation to generation, is the expectation value taken in the i^{th} generation's genotype subspace, $\langle \hat{\sigma}_z \rangle_{\hat{\rho}_{g_i}}$. For the same individual, both the genotype and the phenotype subspace are created using the information of the same predecessor genotype, which has the same $\langle \hat{\sigma}_z \rangle$ that its ancestors, but then the phenotype changes with time t .

Nevertheless, what we want to prove here is that the protocol chosen is effective in the sense that the expectation value of the chosen observable is copied or preserved during the replication process, conservation described by Eq. (4.5). We will see as well that $\langle \hat{\sigma}_x \rangle$ and $\langle \hat{\sigma}_y \rangle$, instead, are not preserved by our self-replication protocol.

Starting with the 0th generation genotype, the arbitrary initial genotype $\hat{\rho}_0 \equiv \hat{\rho}_{g_0} =$ (4.7), using the definition $\langle \hat{\sigma}_k \rangle_{\hat{\rho}} = \text{Tr}(\hat{\rho} \hat{\sigma}_k)$, $k = 1, 2, 3$, [10, p. 181, Eq. (3.4.10)]

²³ ϵ_{klm} is the Levi-Civita symbol: $\epsilon_{123} = \epsilon_{231} = \epsilon_{312} = 1 = -\epsilon_{321} = -\epsilon_{213} = -\epsilon_{132}$ and $\epsilon_{klm} = 0$ if $k = l$, $l = m$ or $k = m$.

$$\langle \hat{\sigma}_z \rangle_{\hat{\rho}_{g_0}} = \text{Tr}(\hat{\rho}_{g_0} \hat{\sigma}_z) \doteq \text{Tr} \left(\begin{pmatrix} a & b - ic \\ b + ic & 1 - a \end{pmatrix} \begin{pmatrix} 1 & 0 \\ 0 & -1 \end{pmatrix} \right) = \text{Tr} \begin{pmatrix} a & ic - b \\ b + ic & a - 1 \end{pmatrix} = 2a - 1, \quad (4.12)$$

$$\langle \hat{\sigma}_x \rangle_{\hat{\rho}_{g_0}} = \text{Tr}(\hat{\rho}_{g_0} \hat{\sigma}_x) \doteq \text{Tr} \left(\begin{pmatrix} a & b - ic \\ b + ic & 1 - a \end{pmatrix} \begin{pmatrix} 0 & 1 \\ 1 & 0 \end{pmatrix} \right) = \text{Tr} \begin{pmatrix} b - ic & a \\ 1 - a & b + ic \end{pmatrix} = 2b, \quad (4.13)$$

$$\langle \hat{\sigma}_y \rangle_{\hat{\rho}_{g_0}} = \text{Tr}(\hat{\rho}_{g_0} \hat{\sigma}_y) \doteq \text{Tr} \left(\begin{pmatrix} a & b - ic \\ b + ic & 1 - a \end{pmatrix} \begin{pmatrix} 0 & -i \\ i & 0 \end{pmatrix} \right) = \text{Tr} \begin{pmatrix} bi + c & -ai \\ i - ai & c - ib \end{pmatrix} = 2c. \quad (4.14)$$

Now, in the creation of the corresponding both output qubits: the 1st generation's genotype and 0th generation's phenotype, defined by $\hat{\rho}_{g_1} = (4.8)$ and $\hat{\rho}_{p_0}$, respectively, Eq. (4.5) ought to be fulfilled.²⁴

$$\begin{cases} \langle \hat{\sigma}_z \rangle_{\hat{\rho}_{g_1}} = \langle (\hat{\sigma}_z)_{g_1} \otimes \hat{\mathbb{1}}_{p_0} \rangle_{\hat{\rho}_1} \equiv \langle \hat{\sigma}_z \otimes \hat{\mathbb{1}}_2 \rangle_{\hat{\rho}_1} \stackrel{(B.12)}{=} 2a - 1. \\ \langle \hat{\sigma}_z \rangle_{\hat{\rho}_{p_0}}(t_{p_0}) = \langle \hat{\mathbb{1}}_{g_1} \otimes (\hat{\sigma}_z)_{p_0} \rangle_{\hat{\rho}_{p_0}(t_{p_0})} \stackrel{(4.10)}{=} \langle \hat{\mathbb{1}}_{g_1} \otimes (\hat{\sigma}_z)_{p_0} \rangle_{\hat{\rho}_1} \equiv \langle \hat{\mathbb{1}}_2 \otimes \hat{\sigma}_z \rangle_{\hat{\rho}_1} \stackrel{(B.13)}{=} 2a - 1. \end{cases} \quad (4.15)$$

As it can be seen, Eq. (4.5) is satisfied: $\langle \hat{\sigma}_z \rangle_{\hat{\rho}_{g_0}} \stackrel{(4.12)}{=} 2a - 1 \stackrel{(B.12)}{=} \langle \hat{\sigma}_z \rangle_{\hat{\rho}_{g_1}} \stackrel{(B.13)}{=} \langle \hat{\sigma}_z \rangle_{\hat{\rho}_{p_0}}(t_{p_0})$. Note that this results depend on a , the diagonal element (then, classical information) of the precursor genotype $\hat{\rho}_{g_0} = (4.7)$, which has spread heretofore.

On the other hand, if we replace $\hat{\sigma}_z$ by $\hat{\sigma}_x$ and $\hat{\sigma}_y$, respectively,

$$\begin{cases} \langle \hat{\sigma}_x \rangle_{\hat{\rho}_{g_1}} \equiv \langle \hat{\sigma}_x \otimes \hat{\mathbb{1}}_2 \rangle_{\hat{\rho}_1} \stackrel{(B.14)}{=} 0. \\ \langle \hat{\sigma}_x \rangle_{\hat{\rho}_{p_0}}(t_{p_0}) \equiv \langle \hat{\mathbb{1}}_2 \otimes \hat{\sigma}_x \rangle_{\hat{\rho}_1} \stackrel{(B.15)}{=} 0. \end{cases} \quad (4.16) \quad \begin{cases} \langle \hat{\sigma}_y \rangle_{\hat{\rho}_{g_1}} \equiv \langle \hat{\sigma}_y \otimes \hat{\mathbb{1}}_2 \rangle_{\hat{\rho}_1} \stackrel{(B.16)}{=} 0. \\ \langle \hat{\sigma}_y \rangle_{\hat{\rho}_{p_0}}(t_{p_0}) \equiv \langle \hat{\mathbb{1}}_2 \otimes \hat{\sigma}_y \rangle_{\hat{\rho}_1} \stackrel{(B.17)}{=} 0. \end{cases} \quad (4.17)$$

Thus, we have proven that our reproduction mechanism conserves only $\langle \hat{\sigma}_z \rangle$, the expectation value of the chosen observable. That is, Eq. (4.5) is not obeyed for $\langle \hat{\sigma}_x \rangle$ and $\langle \hat{\sigma}_y \rangle$: $\langle \hat{\sigma}_x \rangle_{\hat{\rho}_{g_0}} \stackrel{(4.13)}{=} 2b \neq 0 \stackrel{(B.14)}{=} \langle \hat{\sigma}_x \rangle_{\hat{\rho}_{g_1}} \stackrel{(B.15)}{=} \langle \hat{\sigma}_x \rangle_{\hat{\rho}_{p_0}}(t_{p_0})$ and $\langle \hat{\sigma}_y \rangle_{\hat{\rho}_{g_0}} \stackrel{(4.14)}{=} 2c \neq 0 \stackrel{(B.16)}{=} \langle \hat{\sigma}_y \rangle_{\hat{\rho}_{g_1}} \stackrel{(B.17)}{=} \langle \hat{\sigma}_y \rangle_{\hat{\rho}_{p_0}}(t_{p_0})$.

Furthermore,

$$(4.6)|_{i=0} = \langle \hat{\sigma}_x \otimes \hat{\sigma}_x \rangle_{\hat{\rho}_1} \stackrel{(B.18)}{=} 2b \stackrel{(4.13)}{=} \langle \hat{\sigma}_x \rangle_{\hat{\rho}_0}. \quad (4.18)$$

So, as claimed, quantum information is also conveyed, even if it is duplicated into the global state, not to the independent subspaces of the output qubits. Notice that the b coefficient in Eq. (4.18) corresponds to a coherence or off-diagonal element in the initial state $\hat{\rho}_0 = (4.7)$.

4.3 Phenotype change

As explained in Section 4.1 (l. 4-5), as in nature, the phenotype $-\langle \hat{\sigma}_z \rangle_p$, here— changes by the interaction with both the environment (Section 4.3.1) and other individuals (Section 4.3.2):

²⁴See calculations pertaining to Eq. (4.15-4.17) in Appendix B.4.

4.3.1 Environment

All physical systems are subjected to external influences to a greater or lesser extent. Uncontrolled environmental interaction decoheres QCs, and pure states get mixed²⁵. Decoherence destroys quantum superpositions and entanglement, the cornerstones of QCs (Section 1), thus decreasing the probability of successful computation.

Most macroscopic systems, for example, decohere so rapidly as to make quantum superposition effects practically unobservable. The usual aim is to build systems that decohere slowly compared to the time required to do the computation. Nevertheless, here, we will take advantage of this disturbances in order to simulate the aging of living units!

Systems that approximately preserve quantum coherence (off-diagonal elements of the density matrix $\hat{\rho}$) are treated with Hamiltonian time evolution $\hat{\rho}(t) = \hat{U} \hat{\rho}(t_0) \hat{U}^\dagger$, $\hat{U} = \hat{U}(t, t_0)$ [17, p. 4604, Eq. (8)]. For those that, because of environmental effects, do not, as in our case, master equations are used [2, p. 1074, l. 55-60].

Precisely, we will model the effect of the environment, the $\hat{\rho}_{p_i}$ phenotype qubit's degradation (*aging* by dissipation) until the asymptotic state $\langle \hat{\sigma}_z \rangle_p(t = t_d) = 1 - \epsilon$ (*death*), using the *Lindblad master equation*²⁶. It will describe the environment or bath coupled with each phenotype qubit $\hat{\rho}_{p_i}$: [14, p. 2, Eq. (2)]

$$\dot{\hat{\rho}}_{p_i} = \frac{d}{dt} \hat{\rho}_{p_i}(t) = \lambda \left(\hat{\sigma} \hat{\rho}_{p_i}(t) \hat{\sigma}^\dagger - \frac{1}{2} \left\{ \hat{\sigma}^\dagger \hat{\sigma}, \hat{\rho}_{p_i}(t) \right\} \right), \quad (4.20)$$

where $\hat{\sigma} \equiv |0\rangle \langle 1| \doteq \begin{pmatrix} 0 & 1 \\ 0 & 0 \end{pmatrix}$ is the *Lindblad* or *jump* operator [7, p. 2, l. 24-25] and $\lambda \geq 0$, the eigenvalues. Its *steady state* is the ancillary (or blank) state $\hat{\rho}_A = |0\rangle \langle 0|$.

It decoheres living units' phenotypes towards the Lindbladian's steady states $\hat{\rho}_A$, as we prove in Eq. (B.25). This establishes an analogy to the aging process of phenotypes $\hat{\rho}_{p_i}$, and resembles the thermal dissipation of thermodynamical systems ($\hat{\rho}_{p_i}$, here), which fluctuate until they reach the environment's temperature ($\hat{\rho}_A$, in our case), modeled as a thermal reservoir.

These steady states $\hat{\rho}_A$ can be said to be the cadavers belonging to the living entities and, at the same time, the starting point of newborn individuals, the register where information is copied in the two events that constitute the self-replication process. Such a duality simulates the final link in the trophic chain, the role decomposers play: the closure of the cycle!

For the particular case $i = 0$, and initial condition (4.10) $|_{i=0} = \hat{\rho}_{p_0}(t_{p_0}) = \hat{\rho}_{g_1} \equiv \hat{\rho}_1$, we obtain from

²⁵Decoherence means losing off-diagonal elements in the matrix representation, for a certain basis, of the corresponding density matrix $\hat{\rho}$, known as *quantum coherences*. Then, $\hat{\rho}$ states tend to the totally mixed form $\hat{\rho} = \frac{1}{n}$, for dimension $n \in \mathbb{N} - \{0\}$.

²⁶The general, diagonal, form of the *Lindbladian*, for a system described by $\hat{\rho}$, is

$$\dot{\hat{\rho}} = \frac{d}{dt} \hat{\rho}(t) = \mathcal{L}[\hat{\rho}(t)] \equiv -\frac{i}{\hbar} [\hat{H}, \hat{\rho}(t)] + \sum_k \lambda_k \left(\hat{\sigma}_k \hat{\rho}(t) \hat{\sigma}_k^\dagger - \frac{1}{2} \left\{ \hat{\sigma}_k^\dagger \hat{\sigma}_k, \hat{\rho}(t) \right\} \right), \quad (4.19)$$

The part of master equations multiplied by λ describes the action of the environment, so setting $\lambda_k = 0$ means isolating the system, and we obtain the *quantum Liouville equation* [10, p. 185, Eq. (3.4.29)]: (4.19) $|_{\lambda_k=0} = \dot{\hat{\rho}} = -\frac{i}{\hbar} [\hat{H}, \hat{\rho}]$.

Eq. (B.29-B.33), [14, p. 3, Eq. (4)]

$$\hat{\rho}_{p_0}(t) \doteq \begin{pmatrix} a & 0 & 0 & (b-ic)e^{-\lambda t/2} \\ 0 & 0 & 0 & 0 \\ 0 & 0 & (1-a)(1-e^{-\lambda t}) & 0 \\ (b+ic)e^{-\lambda t/2} & 0 & 0 & (1-a)e^{-\lambda t} \end{pmatrix}. \quad (4.21)$$

As mentioned and the logic of nature dictates, the expectation value of the selected observable ($\hat{\sigma}_z$, here) remains constant in the genotype subspace –Eq. (4.22)–, but it is a function of time t in the phenotype subspace –Eq. (4.23)–: [14, p. 3, Eq. (5)]

$$\langle \hat{\sigma}_z \rangle_{\hat{\rho}_{g_1}} = \langle (\hat{\sigma}_z)_{g_1} \otimes \hat{\mathbb{1}}_{p_0} \rangle_{\hat{\rho}_{p_0}(t)} \equiv \langle \hat{\sigma}_z \otimes \hat{\mathbb{1}}_2 \rangle_{\hat{\rho}_{p_0}(t)} \stackrel{(B.34)}{=} 2a - 1 \stackrel{(4.15a)}{=} \langle \hat{\sigma}_z \rangle_{\hat{\rho}_{g_1}}(t_0) \neq \langle \hat{\sigma}_z \rangle_{\hat{\rho}_{g_1}}(t), \quad (4.22)$$

$$\langle \hat{\sigma}_z \rangle_{\hat{\rho}_{p_0}}(t) = \langle \hat{\mathbb{1}}_{g_1} \otimes (\hat{\sigma}_z)_{p_0} \rangle_{\hat{\rho}_{p_0}(t)} \equiv \langle \hat{\mathbb{1}}_2 \otimes \hat{\sigma}_z \rangle_{\hat{\rho}_{p_0}(t)} \stackrel{(B.35)}{=} 1 + 2e^{-\lambda t}(a-1) \neq \langle \hat{\sigma}_z \rangle_{\hat{\rho}_{p_0}}(t_{p_0}). \quad (4.23)$$

If we substitute in these equations $t = t_{p_0} = 0$, the time at when both the phenotype $\hat{\rho}_{p_0}$ and the genotype qubit $\hat{\rho}_{g_1}$ have just been created from a predecessor genotype $\hat{\rho}_{g_0}$, we recover Eq. (4.15): $\langle \hat{\sigma}_z \rangle_{\hat{\rho}_{p_0}}(t=0) \stackrel{(4.23)}{=} 1 + 2e^{-\lambda 0}(a-1) = 1 + 2a - 2 = 2a - 1 \stackrel{(4.22)}{=} \langle \hat{\sigma}_z \rangle_{\hat{\rho}_{g_1}} = (4.15)$.

4.3.2 Inter-individual interaction

This is the last biological feature we will introduce. Interactions between pairs of individuals favor the predators –individuals with a higher $\langle \hat{\sigma}_z \rangle_{\hat{\rho}_{g_i}}$, that is, a shorter life, Eq. (4.1)–. This equilibrates the predator and prey population: the former are better adapted to interaction with other living units, and the latter, to environmental effects.

We won't use the inter-individual interaction protocol belonging to Ref. [14]. Although this model, as described in Ref. [7], can be implemented on current QCs and the one we will expose cannot, with it, simulation acquires more features like giving the prey a choice to *escape* from harm when interaction occurs. See the corresponding code in Appendix A.3.

In both models, living units displace randomly through the grid, provided with PBCs, one cell at a time. The two individuals that interact sum four qubits, so the implementation is achieved by a $2^4 \times 2^4$ unitary operation –see Ref. [14, p. 4, Eq. (9)]–, which changes both phenotypes contingent upon the corresponding genotypes. That is, phenotypes are the target qubits, and the genotypes, the control ones [7, p. 2, l. 29-30]. In our model, living units cannot share the same location, and their interaction range is the Moore neighborhood.

Let us denote $\alpha \equiv$ predator and $\beta \equiv$ prey. Interaction is described by a Hamiltonian that depends on both genotypes ($\hat{\rho}_g^\alpha$ and $\hat{\rho}_g^\beta$)²⁷ $\hat{H}_{\text{int}} = \sum_k \hat{H}_k$, where

$$\hat{H}_k \equiv a_k (\hat{\sigma}_z^{\otimes 2}) + b_k \left\{ \begin{pmatrix} \hat{\sigma}_z \otimes \hat{\mathbb{1}}_2 \\ \hat{\mathbb{1}}_2 \otimes \hat{\sigma}_z \end{pmatrix} \right\}, \quad k = \left\{ \begin{matrix} \alpha \\ \beta \end{matrix} \right\}, \quad a_k, b_k \in [-1, 1]. \quad (4.24)$$

²⁷Both genotypes sum 2 qubits, so $\dim \hat{H}_{\text{int}} = 2^2$. See, for instance, Eq. (B.39).

\hat{H}_{int} is tunable in the sense that each individual can be assigned a certain a and b coefficient. If $\langle \hat{H}_{\text{int}} \rangle_{\hat{\rho}_{g_\alpha} \otimes \hat{\rho}_{g_\beta}} > 0$ (< 0) the predator hunts the prey (the prey escapes). However, predators (preys) do not necessarily have a_k and b_k values that make $\langle \hat{H}_{\text{int}} \rangle_{\hat{\rho}_{g_\alpha} \otimes \hat{\rho}_{g_\beta}}$ positive (negative), which would be the most beneficial case for them.

Nevertheless, since predators (preys) have a greater (smaller) $\langle \hat{\sigma}_z \rangle_{\hat{\rho}_g}$, Eq. (4.1), they will be more likely to have bigger (smaller) $\langle \hat{H}_{\text{int}} \rangle_{\hat{\rho}_{g_\alpha} \otimes \hat{\rho}_{g_\beta}}$ values. That is why we arbitrarily associated positive (negative) $\langle \hat{H}_{\text{int}} \rangle_{\hat{\rho}_{g_\alpha} \otimes \hat{\rho}_{g_\beta}}$ to the most beneficial interaction for them, *attraction* (*repulsion*).

If the expectation value of the interaction Hamiltonian is attractive, the predator feeds from the prey and gets more life (less age, $\langle \hat{\sigma}_z \rangle_{\hat{\rho}_p^\alpha} \downarrow$), at prey's expense ($\langle \hat{\sigma}_z \rangle_{\hat{\rho}_p^\beta} \uparrow$). Otherwise, the prey escapes and it does not get any harm.

Now, we will study the expectation value of the interaction Hamiltonian in the state $\hat{\rho}_{g_\alpha} \otimes \hat{\rho}_{g_\beta}$ as a function of a_k and b_k . Let us start by building the genotype of our living units:

$$\begin{aligned} |g_k\rangle &\stackrel{(3.2)}{=} \begin{pmatrix} \cos(\theta_k/2) \\ \sin(\theta_k/2)e^{i\varphi} \end{pmatrix} \rightarrow \hat{\rho}_g^k = |g_k\rangle\langle g_k| = \begin{pmatrix} \cos(\theta_k/2) & \\ \sin(\theta_k/2)e^{i\varphi} & \end{pmatrix} \begin{pmatrix} \cos(\theta_k/2) & \sin(\theta_k/2)e^{-i\varphi} \\ & \end{pmatrix} \\ &= \begin{pmatrix} \cos^2(\theta_k/2) & \frac{1}{2}\sin\theta_k e^{-i\varphi} \\ \frac{1}{2}\sin\theta_k e^{i\varphi} & \sin^2(\theta_k/2) \end{pmatrix}, \quad k = \alpha, \beta. \end{aligned} \quad (4.25)$$

Then, for $k = \alpha$.

$$\langle \hat{H}_k \rangle_{\hat{\rho}_g^\alpha \otimes \hat{\rho}_g^\beta} |_{k=\alpha} \stackrel{(B.41)}{=} \langle \hat{\sigma}_z \rangle_{\hat{\rho}_g^\alpha} (a_\alpha \langle \hat{\sigma}_z \rangle_{\hat{\rho}_g^\beta} - b_\alpha). \quad (4.26)$$

It is similar for $k = \beta$, with the exception that the second row of Eq. (4.24) has to be used.

If $\langle \hat{\sigma}_z \rangle_{\hat{\rho}_g^\alpha} > \langle \hat{\sigma}_z \rangle_{\hat{\rho}_g^\beta}$ ²⁸, α is a prey, according to Eq. (4.1). Then, the beneficial attitude for the prey α is the one that makes interaction *attractive*, so that it can hunt the prey β . As we defined in the paragraph below Eq. (4.24), interaction is attractive if

$$\langle \hat{H}_k \rangle_{\hat{\rho}_g^\alpha \otimes \hat{\rho}_g^\beta} |_{k=\alpha} > 0 \stackrel{(4.26)}{\leftrightarrow} \left\{ \begin{array}{l} \text{If } \langle \hat{\sigma}_z \rangle_{\hat{\rho}_g^\alpha} > 0 \rightarrow a_\alpha \langle \hat{\sigma}_z \rangle_{\hat{\rho}_g^\beta} > b_\alpha \\ \text{If } \langle \hat{\sigma}_z \rangle_{\hat{\rho}_g^\alpha} < 0 \rightarrow a_\alpha \langle \hat{\sigma}_z \rangle_{\hat{\rho}_g^\beta} < b_\alpha \end{array} \right\}. \quad (4.28)$$

4.4 Experimental implementation

We have presented a code for our QAL model in Appendix A.3. Nevertheless, it might also be interesting implementing some aspects of our model in IBM's cloud QC. Its qubit order is the following

$$|wxyz\rangle \equiv \left(|w\rangle_{g_1} |x\rangle_{p_1} \right) \left(|y\rangle_{g_2} |z\rangle_{p_2} \right) \equiv (|w\rangle_3 |x\rangle_2) (|y\rangle_1 |z\rangle_0), \quad w, x, y, z \in \{0, 1\}. \quad (4.29)$$

²⁸More precisely,

$$\langle \hat{\sigma}_z \rangle_{\hat{\rho}_g^\alpha} > \langle \hat{\sigma}_z \rangle_{\hat{\rho}_g^\beta} \stackrel{(B.40)}{\leftrightarrow} \cos\theta_\alpha > \cos\theta_\beta \leftrightarrow \theta_\alpha < \theta_\beta, \quad (4.27)$$

where the last step follows from the fact that $\cos\theta_k$ is a decreasing function for $\theta_k \in [0, \pi]$ (the range for the polar angle θ in the Bloch sphere, Fig. 3.1), $k = \alpha, \beta$.

We will employ the controlled-gate \hat{U}_{ij} , where $(i, j) = (\text{control}, \text{target})$. For example, using IBM's notation, if $|x\rangle_1 |y\rangle_0 \equiv |xy\rangle$, $\hat{U}_{10} |xy\rangle = |x\rangle |x \oplus y\rangle$ and $\hat{U}_{01} |xy\rangle = |x \oplus y\rangle |x\rangle$. Our usual definition $\hat{U}_{\text{CNOT}} \equiv (\text{B.11})$, is the one that takes the leftmost qubit as the control. Id est, for the qubit order in Eq. (4.29),²⁹

$$\hat{U}_{\text{CNOT}} = \hat{U}_{ij}, \quad i, j = 0, 1, 2, 3, \quad i > j. \quad (4.30)$$

As mentioned (last paragraph of Section 3.1.2), IBM's QC chip solely allows the experimental implementation of CNOT gates \hat{U}_{ij} in the $i > j$ direction! That is, direct implementation of \hat{U}_{ji} gates, $i > j$, is not allowed. It can be checked in the `composer`. Nevertheless, the control/target roles can be exchanged in the following way:

$$\hat{U}_{ji} \stackrel{(\text{B.9})}{=} \hat{U}_{\text{Had}}^{\otimes 2} \hat{U}_{ij} \hat{U}_{\text{Had}}^{\otimes 2} : i, j = 0, 1, 2, 3 \text{ and } i > j, \quad (4.31)$$

where the superscript $(\otimes 2)$ refers to *parallel* computation in the corresponding 2 qubits or subsystems. That is, 2 Hadamard gates operating independently on 2 qubits, in analogy with the remark in footnote 19. See the right part of Fig. 4.2.

Apart from \hat{U}_{ij} , $i > j$, and $\hat{U}_{\text{Had}} = (\text{3.7})$ in Eq. (4.31), the device we will use provides the following unitary operators: [IBM, Intro, Other single qubit gates]

$$\hat{u}_2(\varphi, \lambda) \doteq \frac{1}{\sqrt{2}} \begin{pmatrix} 1 & -e^{i\lambda} \\ e^{i\varphi} & e^{i(\varphi+\lambda)} \end{pmatrix} \quad \text{and} \quad \hat{u}_3(\theta, \varphi, \lambda) \doteq \frac{1}{\sqrt{2}} \begin{pmatrix} \cos \frac{\theta}{2} & -e^{i\lambda} \sin \frac{\theta}{2} \\ e^{i\varphi} \sin \frac{\theta}{2} & e^{i(\varphi+\lambda)} \cos \frac{\theta}{2} \end{pmatrix}. \quad (4.32)$$

4.4.1 Experimental implementation of self-replication

We will now construct the quantum circuit associated to our reproduction mechanism (4.2). From Ref. [7, p. 3, Fig. 1], we define the initial state as

$$|\psi(t_0)\rangle = (|0\rangle_{g_1} |0\rangle_{p_1}) (|0\rangle_{g_2} |0\rangle_{p_2}) \equiv (|0\rangle_3 |0\rangle_2) (|0\rangle_1 |0\rangle_0), \quad (4.33)$$

where the right-hand side refers to IBM's qubit order (4.29).

• $t = t_1$: We initialize the genotype g_1 [g_2] in the state (3.2) $|_{(\varphi=0, \theta=\pi/4)} = \frac{1}{\sqrt{2}}(\cos(\pi/8) |0\rangle + \sin(\pi/8) |1\rangle)$ [(3.2) $|_{(\varphi=0, \theta=3\pi/4)} = \frac{1}{\sqrt{2}}(\cos(3\pi/8) |0\rangle + \sin(3\pi/8) |1\rangle)$] by the following operations: [7, p. 3, l. 5]

$$\begin{aligned} |\psi(t_1)\rangle &= (\hat{u}_3(\pi/4, 0, 0) |0\rangle_3 |0\rangle_2) (\hat{u}_3(3\pi/4, 0, 0) |0\rangle_1 |0\rangle_0) \\ &\stackrel{(4.32)}{=} \left(\frac{1}{\sqrt{2}} \begin{pmatrix} \cos \frac{\pi}{8} & \sin \frac{\pi}{8} \\ \sin \frac{\pi}{8} & \cos \frac{\pi}{8} \end{pmatrix} |0\rangle_3 |0\rangle_2 \right) \left(\frac{1}{\sqrt{2}} \begin{pmatrix} \cos \frac{3\pi}{8} & \sin \frac{3\pi}{8} \\ \sin \frac{3\pi}{8} & \cos \frac{3\pi}{8} \end{pmatrix} |0\rangle_1 |0\rangle_0 \right) \\ &\doteq \left(\frac{1}{\sqrt{2}} \begin{pmatrix} \cos \frac{\pi}{8} \\ \sin \frac{\pi}{8} \end{pmatrix}_3 |0\rangle_2 \right) \left(\frac{1}{\sqrt{2}} \begin{pmatrix} \cos \frac{3\pi}{8} \\ \sin \frac{3\pi}{8} \end{pmatrix}_1 |0\rangle_0 \right), \text{ or} \end{aligned} \quad (4.34)$$

$$|\psi(t_1)\rangle \stackrel{(4.34)}{=} \frac{1}{2} \left(\cos \frac{\pi}{8} \cos \frac{3\pi}{8} |0000\rangle + \cos \frac{\pi}{8} \sin \frac{3\pi}{8} |0010\rangle + \sin \frac{\pi}{8} \cos \frac{3\pi}{8} |1000\rangle + \sin \frac{\pi}{8} \sin \frac{3\pi}{8} |1010\rangle \right). \quad (4.35)$$

²⁹Proof in Appendix B.8.

- $t = t_2$: Afterwards, individual 1 (2) is completed copying the genotype g_1 (g_2) into $\hat{\rho}_A$: [7, p. 3, l. 5-7]

$$\begin{aligned}
|\psi(t_2)\rangle &\stackrel{(4.34)}{=} \hat{U}_{32} \left(\frac{1}{\sqrt{2}} \begin{pmatrix} \cos \frac{\pi}{8} \\ \sin \frac{\pi}{8} \end{pmatrix}_3 \otimes \begin{pmatrix} 1 \\ 0 \end{pmatrix}_2 \right) \hat{U}_{10} \left(\frac{1}{\sqrt{2}} \begin{pmatrix} \cos \frac{3\pi}{8} \\ \sin \frac{3\pi}{8} \end{pmatrix}_1 \otimes \begin{pmatrix} 1 \\ 0 \end{pmatrix}_0 \right) \\
&= \left(\begin{pmatrix} 1 & & \\ & 1 & \\ & & 1 \end{pmatrix} \frac{1}{\sqrt{2}} \begin{pmatrix} \cos \frac{\pi}{8} \\ 0 \\ \sin \frac{\pi}{8} \end{pmatrix} \right) \left(\begin{pmatrix} 1 & & \\ & 1 & \\ & & 1 \end{pmatrix} \frac{1}{\sqrt{2}} \begin{pmatrix} \cos \frac{3\pi}{8} \\ 0 \\ \sin \frac{3\pi}{8} \end{pmatrix} \right) \\
&= \frac{1}{\sqrt{2}} \begin{pmatrix} \cos \frac{\pi}{8} \\ 0 \\ 0 \\ \sin \frac{\pi}{8} \end{pmatrix} \frac{1}{\sqrt{2}} \begin{pmatrix} \cos \frac{3\pi}{8} \\ 0 \\ 0 \\ \sin \frac{3\pi}{8} \end{pmatrix} \\
&= \frac{1}{\sqrt{2}} \left(\cos \frac{\pi}{8} |0\rangle_3 |0\rangle_2 + \sin \frac{\pi}{8} |1\rangle_3 |1\rangle_2 \right) \frac{1}{\sqrt{2}} \left(\cos \frac{3\pi}{8} |0\rangle_1 |0\rangle_0 + \sin \frac{3\pi}{8} |1\rangle_1 |1\rangle_0 \right), \text{ or}
\end{aligned} \tag{4.36}$$

$$|\psi(t_2)\rangle \stackrel{(4.36)}{=} \frac{1}{2} \left(\cos \frac{\pi}{8} \cos \frac{3\pi}{8} |0000\rangle + \cos \frac{\pi}{8} \sin \frac{3\pi}{8} |0011\rangle + \sin \frac{\pi}{8} \cos \frac{3\pi}{8} |1100\rangle + \sin \frac{\pi}{8} \sin \frac{3\pi}{8} |1111\rangle \right), \tag{4.37}$$

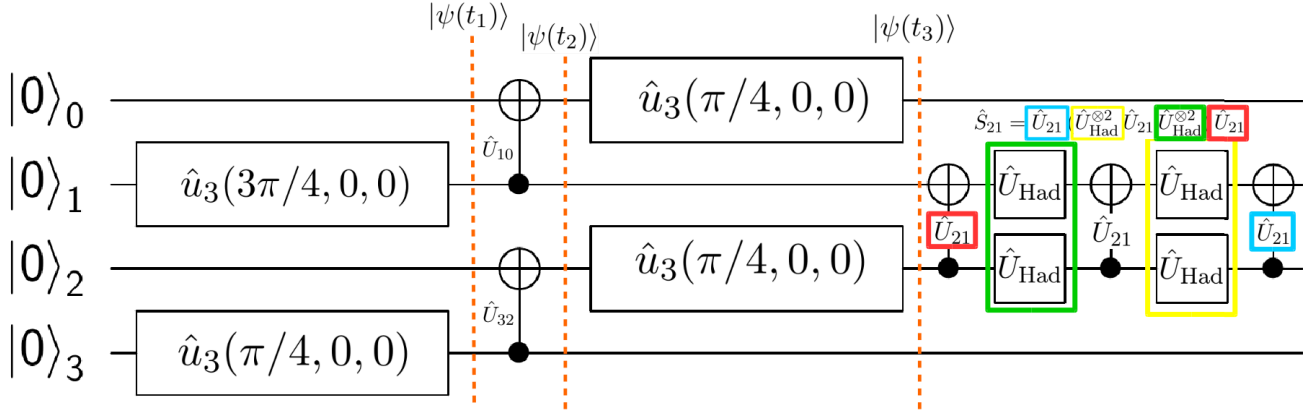


Figure 4.2: ($t_0 \rightarrow t_2$) Creation of the genotypes (4.34) and phenotypes (4.36) in order to create two individuals. ($t_2 \rightarrow t_3$) Simulation of environmental effects on the phenotypes (4.4.2). (t_3) Swap operator created using Eq. (4.31), as an illustrative example. Figure created using Qiskit.

4.4.2 Experimental implementation of environment's decoherence

Finally, the environment's influence, decoherence towards $\hat{\rho}_A$ described in Section 4.3.1, cannot be directly simulated in our device. The alternative is considering projections to $|0\rangle_p$ as rotations along OY , $e^{i\hat{\sigma}_y \theta}$, [7, p. 2, l. 37-40] in each phenotype's Bloch sphere per *discrete* t step, where, obviously, θ is inversely proportional to decoherence or death time, t_d .

5 Conclusions

We chose the topic of Artificial Life because it can describe a wide range of systems, some of them stated in Section 1.2, paragraph 2. Besides, we aimed to prove that the behavior of these systems is better described by QCs rather than conventional ones. Maybe the best approach to describe, for instance, the origin of life is quantum physics, after all.

To this end, in a nutshell, we first presented, Section 2.2, and programmed, Appendix A.1, GoL. We later, Section 2.4, showed that including here fundamental principles of quantum mechanics in order to describe cell's states and transition rules –along with a relative phase difference $e^{i\phi}$, Section 2.4.3– more complex AL scenarios, behaviors previously unseen in classical GoL, arise. One of the most remarkable results is that this semi-classical cells, can move faster than the purely classical ones³⁰.

Then, in our QAL model, we emphasized shallowly the path started by Ref. [7], [14] and [15]. They lead to minimal but consistent simulations of Darwinian scenarios in quantum platforms, establishing analogies between the a priori unconnected fields of artificial life and quantum mechanics: living units capable of reproducing depending on a process of selection that allows the better adapted survive and, thus –since self-replicating probability is equal for all alive organisms–, produce more offspring.

Apart from that, in the aforementioned QAL model, we implemented not solely superposition, but also entanglement. This enabled dissemination of not just classical, but also quantum information: respectively, $\langle \hat{\sigma}_z \rangle_{\hat{\rho}_i}$ and $\langle \hat{\sigma}_x \rangle_{\hat{\rho}_i}$, coherences of $\hat{\rho}_i$ transmitted to the global state of the outputs of the quantum partial cloning operator \hat{U} .

We have not included in our work the experimental realization of the inter-individual interaction protocol described in Ref. [7], due to space and understanding issues. However, we tried to demonstrate, at least for the self-replication protocol and aging, that a minimal biological behavior can be achieved with current technology.

By the way, taking our bachelor perspective a bit beyond its horizons, we emphasized the requirement, usual in research, of adapting theoretical models to experimental constraints. In this case, these limitations were the uniqueness in the control-target direction of \hat{U}_{CNOT} quantum logic gates and the impossibility of attaching a quantum channel that gradually, and with high fidelity, projected the system to state $|0\rangle$ in order to simulate aging.

Regarding model's design, it could be enriched including, for example, spatial information, that is, implementation of more realistic grids with non-homogeneous effects on individuals: less self-replication probability and faster decoherence for more *rugged* zones –e.g. extreme climate ecosystems–. Faster decoherence would mean a greater coupling constant $\lambda = \lambda(x, y)$ in the Lindbladian. Genotype (DNA) recombinations via sexual reproduction could also be introduced, and the complexity of the model would be increased by selecting a larger set of observables to *transmit* into the global state of successive generations [7, p. 2, l. 30-33]. Nevertheless, $\hat{\sigma}_z$ is the only observable that can be *copied* in this model, $\hat{U} = \hat{U}_{\text{CNOT}}$ and $\hat{\rho}_A = |0\rangle\langle 0|$.

In addition, this thesis covered different approaches: along with pure theoretical work –concepts related

³⁰See the wick's example in Appendix A.2.2, code line 27. The output is on the author's [page](#). Here, because of display problems, death cell's are represented by black squares.

to Quantum information and QAL were previously unseen–, numerous calculations (Appendix B), programs (Appendix A, via *GNU Octave*) and even experimental implementations, using IBM’s device, subject to the restrictions mentioned, have been carried out.

With all this, we can claim we have reflected how QCs, due to the exponential growth of the Hilbert space dimension with the number of individuals, may outperform conventional ones in the field of AL simulations. At the same time, we have deepened a bit our very basic knowledge relative to the field of quantum information, a very interdisciplinary topic, carrying out a work more closer to the nature of research activities we absolutely ignored hitherto.

Bibliography

- [1] M. A. Nielsen & I. L. Chuang, *Quantum Computation and Quantum Information* (Cambridge University Press, Cambridge, United Kingdom, 2010).
- [2] S. Lloyd, *Universal quantum simulators*, *Science*, vol. **273**, p. 1073 (1996).
- [3] P. W. Shor, *Polynomial time algorithms for prime factorization and discrete logarithms on a quantum computer*, *SIAM J. Sci. Statist. Comput.*, vol. **26**, p. 1484 (1997).
- [4] Ricard Solé, *Vidas Sintéticas* (Tusquets Editores, Barcelona, Spain, 2012).
- [5] M. Gardner, *Mathematical games: The fantastic combinations of John Conway's new solitaire game Life*, *Scientific American*, vol. **223**(10), p. 120 (1970).
- [6] A. Adamatzky (Ed.), *Game of Life Cellular Automata* (Springer-Verlag London Limited, London, United Kingdom, 2010).
- [7] U. Alvarez-Rodriguez, M. Sanz, L. Lamata & E. Solano, *Quantum Artificial Life in an IBM Quantum Computer*, *Scientific Reports*, vol. **8**, p. 14793 (2018).
- [8] R. P. Feynman, *Simulating physics with computers*, *Int. J. Theor. Phys.*, vol. **21**, p. 467 (1982).
- [9] A. P. Flitney & D. Abbott, *A semi-quantum version of the game of Life*, *arXiv: 0208149* (2002).
- [10] J. J. Sakurai & Jim J. Napolitano, *Modern Quantum Mechanics* (Addison-Wesley Publishing Company, San Francisco, United States, 2010).
- [11] D. J. Griffiths, *Introduction to Quantum Mechanics* (Pearson Education International, United States, 2004).
- [12] L. K. Grover, *A fast quantum mechanical algorithm for database search*, *Proceedings of the 28th Annual ACM Symposium on the Theory of Computing (STOC)*, p. 212 (1996).
- [13] R. Shankar, *Principles of Quantum Mechanics* (Plenum Press, New York, United States, 1994).
- [14] U. Alvarez-Rodriguez, M. Sanz, L. Lamata & E. Solano, *Artificial Life in Quantum Technologies*, *Scientific Reports*, vol. **6**, p. 20956 (2016).
- [15] U. Alvarez-Rodriguez, M. Sanz, L. Lamata & E. Solano, *Biomimetic Cloning of Quantum Observables*, *Scientific Reports*, vol. **4**, p. 4910 (2014).
- [16] A. Ferraro, A. Galbiati, & M. Paris, *Cloning of observables*, *J. Phys. A: Math. Gen.*, vol. **39**, p. L219 (2006).
- [17] D. P. DiVincenzo, *Quantum computation and spin physics*, *J. Appl. Phys.* **81**, p. 4602 (1997).
- [18] T. Rowland, *Unitary Matrix*, Mathworld – A Wolfram Web Resource, <http://mathworld.wolfram.com/UnitaryMatrix.html>.
- [19] D. E. Deutsch, *Quantum computational networks*, *Proc. Royal Soc. Lond.*, vol. **A 425**, p. 73 (1989).
- [20] N. D. Mermin, *Quantum Computer Science: An Introduction*, (Cambridge University Press, Cambridge, United Kingdom, 2007).

A Codes

A.1 Game of life implementation

Figures belonging to Section 2.3.2 are obtained from the following code. See an enlightening example for the module function (mod) in code line 82 on the author's [page](#).

```
1  % ----- INITIAL CONDITION -----
2  % Dimensions of the 2-D lattice:
3  n_row= 10;
4  n_column= 12;
5
6  % "steps" = number of steps,
7  steps=30;
8
9  % "grid" = initial grid or lattice. 0="alive" cells and 1="death" ones.
10
11 % Initial condition Example 1:
12 % Uncomment (remove "%") the following to fill the "grid" (matrix) randomly with 0 or 1:
13 %grid = randi([0 1],n_row,n_column);
14
15 % Fill the grid with death(=1) cells, in order to deploy the following examples.
16 for i= 1:n_row
17     for j = 1:n_column
18         grid(i,j)=1;
19     endfor
20 endfor
21
22 % Initial condition Example 2: Glider (fixed shape that moves across the grid). Useful in
23     order to see the periodic boundary conditions (PBCs)
24 grid(4,2)=grid(5,2)=grid(5,4)=grid(6,2)=grid(6,3)=0;
25
26 % Initial condition Example 3: "Tetromino" (shape formed by four connected alive cells)
27     that becomes a "beehive" ("still-life" or stable figure) on the fourth generation.
28 %grid(4,4)=grid(5,4)=grid(5,5)=grid(5,6)=0;
29
30 % Initial condition Example 4: "Tetromino" that after the tenth generation becomes four
31     isolated periodical blinkers.
32 %grid(4,5)=grid(5,4)=grid(5,5)=grid(5,6)=0;
33
34
35
36 % ----- INITIAL CONDITION DISPLAY -----
37 colormap gray; % Image traversing black to white in shades of gray.
38 imagesc(grid);
```

```

39
40 % Notable when n_row >> n_column or n_row << n_column, not to stretch the cells and
    keep the square shape, we apply the following:
41 axis equal tight
42 drawnow
43
44 % Intrinsic function that pauses the GIF for (argument) seconds, in order to visualize
    each generation:
45 pause(0.1)
46
47
48 % ----- MAIN PROGRAM -----
49 % "n_row" and "n_column" will be referenced later by "size(grid,1)" and "size(grid,2)",
    respectively, where the intrinsic function size() gives the following array if the
    argument is "grid": size(grid) = [n_row n_column].
50 % For a general A matrix: size(A) = [size(A,1) size(A,2)].
51
52 % Originally, we used the concatenated matrix grid_boundary=[grid grid grid; grid grid
    grid; grid grid grid] as a reference to apply the PBCs, but it was expensive in terms
    of memory.
53
54 for t=1:steps % t indexes the number of time steps.
55
56 % First, we create the environment that will be updated at time t + 1 ("grid_next")
    according to the lattice at the previous generation or time t ("grid").
57 grid_next=grid;
58
59 % If we used "grid" both as a reference and as the environment we change for the same
    time t, as the analysis of the neighborhood of each cell can only be computed
    individually, we would not follow "Conway's Game of Life" rule that states that, at
    each generation or time step, all the grid ought to be changed or updated
    synchronously, and not cell by cell.
60
61 % We use i and j to index the grid spatially.
62 % i goes from (1) to (n_row); i.e., from (1) to (size(grid,1))
63 % j goes from (1) to (n_column); i.e., from (1) to (size(grid,2))
64
65 % Matrix indexing starts from integer 1 by default. That is why we used i= 1:size(grid
    ,1) (j= 1:size(grid,2)) instead of i= 0:(size(grid,1)-1) (j= 0:(size(grid,2)-1)).
66
67 for i= 1:size(grid,1) % size(grid,1)=n_row
68     for j= 1:size(grid,2) % size(grid,2)=n_column
69         x=0; % x = counter of alive "Moore neighbors"
70
71
72 % For i=1 or size(grid,1) and/or j=1 or size(grid,2) —id est, when we are analyzing a
    cell on the border of the grid— PBCs have to be applied.
73

```

```

74 % We implement PBCs using the intrinsic function mod(a,b), which gives the remainder
    of a/b. Hence, it can be used to create "modulo operation".
75
76 % As stated (code l. 65), since matrix indexing starts from integer 1, in order to
    prevent "mod" from starting the period from 0, instead of mod(a,b), we will use
    mod(a-1,b)+1, where b=size(grid,1) (b=size(grid,2)) if a=i (a=j).
77
78 % There are 8 cells in the Moore neighborhood, so 8 conditions have to be fulfilled.
    This conditions are expressed gradually SIMPLER in Appendix A.2, code lines 54-65,
    and Appendix A.3, code line 122!
79
80 if (grid([mod((i+1)-1,size(grid,1))+1],j)==0)
81     x=x+1;
82 endif
83 if (grid([mod((i-1)-1,size(grid,1))+1],j)==0)
84     x=x+1;
85 endif
86 if (grid(i,[mod((j+1)-1,size(grid,2))+1])==0)
87     x=x+1;
88 endif
89 if (grid(i,[mod((j-1)-1,size(grid,2))+1])==0)
90     x=x+1;
91 endif
92 if (grid([mod((i+1)-1,size(grid,1))+1],[mod((j+1)-1,size(grid,2))+1])==0)
93     x=x+1;
94 endif
95 if (grid([mod((i+1)-1,size(grid,1))+1],[mod((j-1)-1,size(grid,2))+1])==0)
96     x=x+1;
97 endif
98 if (grid([mod((i-1)-1,size(grid,1))+1],[mod((j+1)-1,size(grid,2))+1])==0)
99     x=x+1;
100 endif
101 if (grid([mod((i-1)-1,size(grid,1))+1],[mod((j-1)-1,size(grid,2))+1])==0)
102     x=x+1;
103 endif
104
105 % We first used:
106 %if (grid(i+1,j)==1) || (grid(i-1,j)==1) || (grid(i,j+1)==1) || ...
107 % If we use the latter (| = or), or, equivalently, if we use "elif", we won't pass
    by all the conditions once one of them is satisfied.
108
109 % GoL rules (see Introduction)
110 if grid(i,j)==0 && (x<2 || x>3)           % "&" = "and " ;   "==" = "is equal to
111     grid_next(i,j)=1;
112 elseif grid(i,j)==1 && x==3
113     grid_next(i,j)=0;
114 endif
115

```



```

116     endfor % end the cycle relative to column index "j".
117 endfor % end the cycle relative to row index "i".
118
119 % ----- DISPLAY -----
120 colormap gray;
121 imagesc(grid_next);
122 axis equal tight
123 drawnow
124 pause(0.1)
125 % -----
126
127 grid=grid_next; % To use "grid" as the lattice at time t and "grid_next" as the
    lattice in the next time step t+1.
128 endfor % end the cycle relative to the number of time steps ("t").

```

A.2 Quantum GoL implementation

A.2.1 Quantum GoL without phase $e^{i\phi}$

As stated at the end of Section 2.4.2, we obtain the same results as in Section 2.3.2. Because of its similarity with the code in Sections A.1 and A.2.2, we put it on the author's [page](#).

A.2.2 Quantum GoL with phase $e^{i\phi}$

Section 2.4.3 can be implemented using the following code. See the wick example's output on the author's [page](#).

```

1 n_row= 10;      % Dimensions of the 2D lattice
2 n_column= 12;
3 steps=30;      % "steps" = number of steps,
4
5 % In semiquantum GoL, cell states are not numbers, but 2-level vectors: |\psi>=a|ket{1}>+b
    |ket{0}>=a|ket{alive}>+b|ket{dead}>
6 % Then, in the {|1>,|0>} basis, |\psi>=[a;b] : |a|^2 + |b|^2 =1.
7
8 for m= 1:n_row      % Fill the grid with death cells
9     for n = 1:n_column % m,n instead of i,j to avoid confusion with imaginary number i.
10        % 3D matrix = matrix(row,column,page), where in each "page" there is an ordinary 2D
            matrix!
11        grid(m,n,1)=0; % grid(m,n,1) = a (|1> state coef.)
12        grid(m,n,2)=1; % grid(m,n,2) = b (|0> state coef.)
13        phi(m,n)=exp(i*theta); % phi=e^{i\phi}, phase of the cell.
14    endfor
15 endfor

```

```

16
17 % Initial condition Example 1: Glider. To check that, WITHOUT PHASE, we obtain the
    CLASSICAL results!
18 %grid(4,2,1)=grid(5,2,1)=grid(5,4,1)=grid(6,2,1)=grid(6,3,1)=1;
19 %grid(4,2,2)=grid(5,2,2)=grid(5,4,2)=grid(6,2,2)=grid(6,3,2)=0;
20
21 % Initial condition Example 2: Destructive interference
22 % A block with a cell with |1> out of phase by \pi.
23 %phi(2,2)=e^(i*pi);
24 %grid(1,1,1)=grid(1,2,1)=grid(2,1,1)=grid(2,2,1)=1;
25 %grid(1,1,2)=grid(1,2,2)=grid(2,1,2)=grid(2,2,2)=0;
26
27 %Initial condition Example 3: a "wick" that burns at the speed of light (one cell per
    time step).
28 phi(4,1)=e^(i*pi/2);
29 for m = 3:(n_column-2)
30     if rem(m,2)~=0
31         phi(4,m)=e^(i*pi);
32     endif
33 endfor
34 for l=1:(n_column-2)
35     grid(4,l,1)=1; grid(4,l,2)=0;
36 endfor
37
38 disp(['Grid, in the following ', num2str(steps),' steps'])
39 % ----- INITIAL CONDITION DISPLAY -----
40 colormap gray; % Image traversing black to white in shades of gray.
41 imagesc(grid(:,:,1)); % Only display |1> coef.)
42 axis equal tight % To keep the square shape
43 drawnow
44 pause(0.1) % Pauses the GIF for (argument) seconds
45
46 % ----- MAIN PROGRAM -----
47 for t=1:steps
48 % grid at time t + 1 = "grid_next"; grid at the previous generation or time t = "grid".
49 grid_next=grid; % No-cloning theorem forbids this. Hence, synchronous application of
    GoL rules is NOT realizable in a QC!
50
51 for m= 1:size(grid,1) % size(grid,1)=n_row
52     for n= 1:size(grid,2) % size(grid,2)=n_column
53         % x = counter of Moore neighbors' "health" = \sum_{i=1}^8 a_i*e^{i\phi} = a_M, with
            PBCs
54         x= grid([mod((m+1)-1,size(grid,1))+1],n,1)*phi([mod((m+1)-1,size(grid,1))+1],n) ...
55             +grid([mod((m-1)-1,size(grid,1))+1],n,1)*phi([mod((m-1)-1,size(grid,1))+1],n) ...
56             +grid(m,[mod((n+1)-1,size(grid,2))+1],1)*phi(m,[mod((n+1)-1,size(grid,2))+1]) ...
57             +grid(m,[mod((n-1)-1,size(grid,2))+1],1)*phi(m,[mod((n-1)-1,size(grid,2))+1]) ...
58             +grid([mod((m+1)-1,size(grid,1))+1],[mod((n+1)-1,size(grid,2))+1],1)* ...
59             phi([mod((m+1)-1,size(grid,1))+1],[mod((n+1)-1,size(grid,2))+1]) ...

```

```

60     +grid([mod((m+1)-1,size(grid,1))+1],[mod((n-1)-1,size(grid,2))+1],1)* ...
61     phi([mod((m+1)-1,size(grid,1))+1],[mod((n-1)-1,size(grid,2))+1]) ...
62     +grid([mod((m-1)-1,size(grid,1))+1],[mod((n+1)-1,size(grid,2))+1],1)* ...
63     phi([mod((m-1)-1,size(grid,1))+1],[mod((n+1)-1,size(grid,2))+1]) ...
64     +grid([mod((m-1)-1,size(grid,1))+1],[mod((n-1)-1,size(grid,2))+1],1)* ...
65     phi([mod((m-1)-1,size(grid,1))+1],[mod((n-1)-1,size(grid,2))+1]);
66
67     % Birth, Death and Survival operators
68     B=[grid(m,n,1),grid(m,n,2)*phi(m,n); 0,0]/[abs(grid(m,n,1)+grid(m,n,2)*phi(m,n))]^2;
69     D=[0,0; grid(m,n,1)*phi(m,n),grid(m,n,2)]/[abs(grid(m,n,1)*phi(m,n)+grid(m,n,2))]^2;
70     S=[1,0; 0,1];
71
72     if (0<=abs(x)) && (abs(x)<=1) % G function
73         G=D;
74     endif
75     if (1<abs(x)) && (abs(x)<=2)
76         G=(sqrt(2)+1)*(2-abs(x))*D+(abs(x)-1)*S;
77     endif
78     if (2<abs(x)) && (abs(x)<=3)
79         G=(sqrt(2)+1)*(3-abs(x))*S+(abs(x)-2)*B;
80     endif
81     if (3<abs(x)) && (abs(x)<=4)
82         G=(sqrt(2)+1)*(4-abs(x))*B+(abs(x)-3)*D;
83     endif
84     if (abs(x)>4)
85         G=D;
86     endif
87
88     cell_next=G*[grid(m,n,1); grid(m,n,2)]; % Apply the rules.
89     % Resulting grid, where cell_next=[cell_next(1,1); cell_next(2,1)]
90     grid_next(m,n,1)=cell_next(1,1); grid_next(m,n,2)=cell_next(2,1);
91
92     endfor % end the loop of column index "j".
93 endfor % end the loop of row index "i".
94
95 % ----- DISPLAY -----
96 colormap gray;
97 imagesc(grid(:,:,1));
98 axis equal tight
99 drawnow
100 pause(0.1)
101 % -----
102
103 grid=grid_next; % Resulting grid becomes the reference one in the next time step.
104 endfor % end the cycle relative to the number of time steps ("t").

```

A.3 Quantum artificial life code

Self-replication is not implemented here, they all correspond to the $i = 0$ generation. See the output of this code on the author's [page](#).

```

1 % Definition of useful expressions:
2 ket_0=[1 0]; % = |0>, in the {|0>,|1>} computational basis.
3 ket_1=[0 1]; % = |1>
4 rho_A= kron(ket_0,ket_0'); % = |0>\otimes<0|= |0><0|, where kron(A,B)= A \otimes B, and
   ket_0'= (|0>)\dagger = <0|.
5 sigma_x=[0 1; 1 0];
6 sigma_z=[1 0; 0 -1];
7 % CNOT = |0><0|\otimes 1_2 + |1><1|\otimes sigma_x :
8 CNOT= kron( kron(ket_0,ket_0'), eye(2) ) + kron( kron(ket_1,ket_1'), sigma_x );
9
10 % Variable parameters.
11 n_indiv=3; % Number of individuals.
12 epsilon=0.3; % , for instance. <sigma_z>_p(t_d) = 1-epsilon = "death age", where t_d =
   t_death.
13 harm=0.1; % Harm= %10, e.g., of <H_int>_genotypes*prey's life.
14
15
16 alive_labels=[];
17 for i=1:n_indiv;
18   alive_labels(i)=i;
19 endfor;
20
21
22 % -----Initial "age" of n individuals-----
23 % Each initial (t=0) individual's pheno. will be described by a density matrix of the
   form, for instance, of Eq. (4.7):
24 for i=1:n_indiv % per individual
25   a=(-1:0.1:(2-epsilon)/2)([randi([1 size(-1:0.1:(2-epsilon)/2, 2)])]); % Eq. (4.15b) =
   2a-1 = 1-epsilon -> to obtain the maximum value of a.
26   % where, (-1:0.1:1)=[-1 -0.9 ... 0.9 1]; randi([min max])= random integer in [min,
   max]; size(A,2) = number of columns of the matrix A.
27   % That is, we randomly choose an element. For example, (-1:0.1:1)(2)=-0.9; (-1:0.1:1)
   (3)=-0.8; (-1:0.1:1)(4)=-0.7; ...
28   b=0.7; % For example. For the moment where are interested just in a, because lifetime
   depends on it. See Eq. (4.15b)
29   c=0.5; % For example.
30
31   % 3D matrix = matrix(row, column, page), the i th page, for the i th individual. On
   each page, there is a conventional 2D matrix.
32   rho_g0(:,:,i)=[a, b-j*c; b+j*c, 1-a]; % j = imaginary number i. Eq. (4.7)
33   rho_p0(:,:,i)= CNOT*kron(rho_g0(:,:,i),rho_A)*CNOT'; % Eq. (4.8). It would be rho_g1
   (:,:,i) as well, but we are not implementing self-replication, for now.

```

```

34 expectation_sigma_z_p0(i)=trace(rho_p0(:,:,i)*kron(eye(2),sigma_z)); % Eq. (4.5(2)).
    Instead, for the rho_g1 subspace it would be kron(sigma_z,eye(2))).
35 expectation_sigma_z_g0(i)=expectation_sigma_z_p0(i); % At t=0, <sigma_z>_p0=<sigma_z>
    _g0.
36 endfor
37
38
39 % For the interaction Hamiltonian H_int:
40 for i=1:n_indiv
41     a_k(i)=(-1:0.01:1)([randi([1 size(-1:0.01:1, 2)])]); % a_k coef. in Eq. (4.24).
42     b_k(i)=(-1:0.01:1)([randi([1 size(-1:0.01:1, 2)])]); % b_k " " " " .
43 endfor
44
45
46
47 % Dimensions of the 2-D lattice.
48 n_row= 3;
49 n_column=4;
50 % Fill the grid with 0s. 0 = no indiv.
51 for i=1:n_row;
52     for j=1:n_column;
53         grid(i,j)=0;
54     endfor
55 endfor
56
57
58 % Individuals get born in a random location of the grid.
59 % x_pos= [x position of the 1 st indiv., ..., x position of the n th indiv.])
60 for i=1:n_indiv
61     y_pos(i)=randi(n_row); % randi(max) = random integer from 1 to max.
62     x_pos(i)=randi(n_column);
63     while grid(y_pos(i),x_pos(i))!=0 % 2 indiv. or more cannot be born in the same cell.
64         y_pos(i)=randi(n_row); x_pos(i)=randi(n_column);
65     endwhile
66     grid(y_pos(i),x_pos(i))=i; % We represent the i th individual in the grid by the
        integer i.
67 endfor
68
69 disp(['-----GRID at t=0-----'
70     ]) %disp() = display string.
71 disp(grid); disp(' '); disp(' '); disp(' '); disp(' '); disp(' '); disp(' '); disp(' ');
72
73
74 for t=0:0.1:1 % per time step
75     disp(['-----At t=',num2str(t),'
76         -----'])
77     disp(' '); disp(' ')

```

```

77
78
79 % CHECK if there is any DEAD individual.
80 dead_labels=[]; % Individuals that die at this t step.
81 for i=1:size(alive_labels,2) % per alive individual.
82     if (expectation_sigma_z_p0(alive_labels(i))>= 1-epsilon)
83         disp(['Individual ', num2str(alive_labels(i)), ' has DIED!    (Death age=', num2str(1-
            epsilon), ')'])
84         grid(y_pos(alive_labels(i)), x_pos(alive_labels(i)))=0; % The indiv. disappears from
            the grid.
85         disp(['Then, individual ', num2str(alive_labels(i)), ' disappears from the grid:']);
            disp(grid); disp(' ')
86         % To avoid problems ("index out of bounds") erasing labels from "alive_labels":
87         dead_labels=cat(2, dead_labels, alive_labels(i)); % cat(dim,A,B) concatenates B to the
            end of A along dimension dim. dim=2=column.
88     endif
89 endfor
90 % Remove common elements from arrays "alive_labels" and "dead_labels":
91 alive_labels=setdiff(alive_labels, dead_labels); % setdiff(A,B) returns the data in A
            that is not in B.
92
93 if size(alive_labels,1)==0==size([],1), where [] is an empty array.
94     disp('ALL individuals are dead, program ENDS!')
95     break % Program ends.
96 endif
97
98 disp(' ')
99 disp(['-----AGE-----'])
100 eta=1-exp(-t); % Time in \lambda*t units: \lambda*t=t
101 M_0=[1 0; 0 sqrt(1-eta)]; M_1=[0 sqrt(eta); 0 0]; % Eq. (B.22)
102 for i=1:size(alive_labels,2) % per alive individual.
103     % Careful, alive_labels(i) is the label of the alive individual, not i!
104     rho_p0(:, :, alive_labels(i))=kron(eye(2), M_0)*rho_p0(:, :, alive_labels(i))*kron(eye(2),
            M_0)'+ kron(eye(2), M_1)*rho_p0(:, :, alive_labels(i))*kron(eye(2), M_1)'; % 1_2
            otimes M_1 to act on pheno. subspace.
105     expectation_sigma_z_p0(alive_labels(i))=trace(rho_p0(:, :, alive_labels(i))*kron(eye(2)
            , sigma_z));
106     disp([' ', num2str(alive_labels(i)), ': <sigma_z>_p0=', num2str(
            expectation_sigma_z_p0(alive_labels(i)))]])
107 endfor
108 disp(' '); disp(' ');
109
110
111 disp(['-----Random MOVEMENT-----'])
112 for i=1:size(alive_labels,2) % per alive individual.
113     if t==0
114         disp('    NO movement at t=0.')
115         break % At t=0 individuals interact, but do not move until the next t step.

```

```

116     endif
117     x=randi([-1 1]); % movement in x axis.
118     y=randi([-1 1]); %      "      " y      "      .
119     disp(['If individual ', num2str(alive_labels(i)), ' moves in direction (x,y)=(',
120           num2str(x), ',', num2str(y), '):'])
121     if (x!=0) || (y!=0) % = if the individual moves:
122         % There is a - in ...(y_pos(alive_labels(i))-y)..., because row index y_pos()
123         % increases towards the negative direction of y:
124         if (grid(mod((y_pos(alive_labels(i))-y)-1, n_row)+1, mod((x_pos(i)+x)-1, n_column)
125             +1)!=0) % Cannot move to a cell where there already is an individual.
126             disp(['Individual ', num2str(alive_labels(i)), ' canNOT move there, that cell is
127                 already occupied by individual ', num2str(grid(mod((y_pos(alive_labels(i))-y)
128                     -1, n_row)+1, mod((x_pos(alive_labels(i))+x)-1, n_column)+1)), '.'])
129         else
130             grid(mod((y_pos(alive_labels(i))-y)-1, n_row)+1, mod((x_pos(alive_labels(i))+x)-1,
131                 n_column)+1)=grid(y_pos(alive_labels(i)), x_pos(alive_labels(i)));
132             grid(y_pos(alive_labels(i)), x_pos(alive_labels(i)))=0; % The indiv. disappears
133             % from the previous position.
134             y_pos(alive_labels(i))=mod((y_pos(alive_labels(i))-y)-1, n_row)+1; % new position
135             % 's row index.
136             x_pos(alive_labels(i))=mod((x_pos(alive_labels(i))+x)-1, n_column)+1; % new
137             % position's column index.
138         endif
139     endif
140     disp(grid)
141 endfor
142 disp(' '); disp(' ')
143
144 disp(['----- INTERACTION -----'])
145 disp('<sigma_z>_p(t=0)=<sigma_z>_g=trophic role'); disp(' ');
146 pred_prej_total=[]; % = [predator_label, prey_label], to clean later the repeated
147 % interactions. We will add a row per interaction.
148 for i=1:size(alive_labels,2) % per alive individual.
149     for x_interac=-1:1 % Interaction range (Moore) in the x axis.
150         for y_interac=-1:1 %      "      "      "      " y      "      .
151             if (x_interac!=0) || (y_interac!=0) % Not to include the current indiv., where (
152                 x_interac,y_interac)=(0,0).
153                 %disp(['The cell at the (x,y)=(', num2str(x_interac), ',', num2str(y_interac), ')
154                     % part of the ', num2str(i), ' th indiv is: ', num2str(grid(mod((y_pos(i)-
155                         y_interac)-1, n_row)+1, mod((x_pos(i)+x_interac)-1, n_column)+1))]
156                 % There is a - in ...(y_pos(alive_labels(i))-y_interac)..., because row index
157                 % y_pos() increases towards the negative direction of y:
158                 if (grid(mod((y_pos(alive_labels(i))-y_interac)-1, n_row)+1, mod((x_pos(
159                     alive_labels(i))+x_interac)-1, n_column)+1)!=0)
160                     interac_indiv=grid(mod((y_pos(alive_labels(i))-y_interac)-1, n_row)+1, mod((
161                         x_pos(alive_labels(i))+x_interac)-1, n_column)+1); % label of the
162                     % individual that interacts with the i th one.
163                     disp(['Individual ', num2str(alive_labels(i)), ' interacts with individual ',

```

```

147         num2str(interac_indiv),'.')]
148     disp(['      ',num2str(alive_labels(i)),': <sigma_z>_p0(t=0)=' ,num2str(
        expectation_sigma_z_g0(alive_labels(i)))]
149     disp(['      ', num2str(interac_indiv),': <sigma_z>_p0(t=0)=' ,num2str(
        expectation_sigma_z_g0(interac_indiv))]
150     if ( expectation_sigma_z_g0(alive_labels(i)) > expectation_sigma_z_g0(
        interac_indiv) )
151         disp(['      Thus, here: ', num2str(alive_labels(i)),'=predator; ', num2str(
        interac_indiv),'=prey.']); disp(' ')
152         pred_prej_total=[pred_prej_total; [alive_labels(i), interac_indiv]];
153     elseif ( expectation_sigma_z_g0(alive_labels(i)) < expectation_sigma_z_g0(
        interac_indiv) )
154         disp(['      Thus, here: ', num2str(interac_indiv),'=predator; ', num2str(
        alive_labels(i)),'=prey.']); disp(' ')
155         pred_prej_total=[pred_prej_total; [interac_indiv, alive_labels(i)]];
156     else % same level in the trophic pyramid.
157         disp(['      Thus, here, both are predators or both preys, they do NOT
        interact!.']); disp(' ')
158         % Thus, here, we do not append a row to the matrix pred_prej_total.
159     endif
160     endif
161     endfor
162 endfor
163 endfor
164
165 % Clean the repeated interactions.
166 pred_prej_not_repeated=unique(pred_prej_total,'rows'); % Return the unique rows.
167 disp(' '); disp(' '); disp(' '); disp('EFFECTS:'); disp(' ');
168 for i=1:size(pred_prej_not_repeated,1) % Each row is an (unrepeated per t step)
        interaction.
169     disp(['If ', num2str(pred_prej_not_repeated(i,1)),'=predator; ', num2str(
        pred_prej_not_repeated(i,2)),'=prey:'])
170
171     % Interaction Hamiltonian H_int
172     H_pred=a_k(pred_prej_not_repeated(i,1))*kron(sigma_z,sigma_z)+b_k(
        pred_prej_not_repeated(i,1))*kron(sigma_z,eye(2));
173     H_prej=a_k(pred_prej_not_repeated(i,2))*kron(sigma_z,sigma_z)+b_k(
        pred_prej_not_repeated(i,2))*kron(eye(2),sigma_z);
174     H_int=H_pred+H_prej;
175     % <H_int>_kron(rho_g_pred,rho_g_prej):
176     expectation_H_int_genotypes=trace( kron(rho_g0(:,:,pred_prej_not_repeated(i,1)),
        rho_g0(:,:,pred_prej_not_repeated(i,2))) * H_int);
177     disp(['      <H_int>_genotypes = ', num2str(expectation_H_int_genotypes)])
178     if (expectation_H_int_genotypes>0) % The predator HUNTs the prey. Harm is
        proportional to <H_int>_genotypes and prey's life:
179         % Predator's age decreases, beneficial for it. Note the abs(), age can be negative.
180         expectation_sigma_z_p0(pred_prej_not_repeated(i,1))= expectation_sigma_z_p0(

```



```

    pred_prey_not_repeated(i,1) - harm*expectation_H_int_genotypes* abs(
    expectation_sigma_z_p0(pred_prey_not_repeated(i,2)));
181 % Prey's age increases by the same amount (feeding) predator's age decreases.
    Harmful for the prey.
182 expectation_sigma_z_p0(pred_prey_not_repeated(i,2))= expectation_sigma_z_p0(
    pred_prey_not_repeated(i,2)) + harm*expectation_H_int_genotypes* abs(
    expectation_sigma_z_p0(pred_prey_not_repeated(i,2)));
183 disp(['    The predator (' ,num2str(pred_prey_not_repeated(i,1)),') HUNTS the prey (
    ' ,num2str(pred_prey_not_repeated(i,2)),'):    <sigma_z>_p0^pred=',num2str(
    expectation_sigma_z_p0(pred_prey_not_repeated(i,1))),';    <sigma_z>_p0^prey=',
    num2str(expectation_sigma_z_p0(pred_prey_not_repeated(i,2))),'.'])
184 else % prey escapes
185     disp(['    The prey (' ,num2str(pred_prey_not_repeated(i,2)),') ESCAPES from the
    prey (' ,num2str(pred_prey_not_repeated(i,2)),'), so it does NOT get any harm!'
    ])
186     endif
187     disp(' ')
188 endfor
189 disp(' '); disp(' '); disp(' '); disp(' '); disp(' '); disp(' '); disp(' '); disp(' ');
    disp(' '); disp(' ');
190
191 endfor % End of time t iterations.

```

B Calculations

B.1 Why did we choose $t \uparrow$, $\langle \hat{\sigma}_z \rangle_{\hat{\rho}_p} \uparrow$?

- Example:

$$(4.23) = \langle \hat{\sigma}_z \rangle_{\hat{\rho}_{p_0}}(t) = 1 + 2e^{-\lambda t}(a - 1) \quad (B.1)$$

$$\diamond \langle \hat{\sigma}_z \rangle_{\hat{\rho}_{p_0}}(t=0) \stackrel{(4.23)}{=} 1 + 2e^{-\lambda 0}(a - 1) = 1 + 2a - 2 = 2a - 1 \stackrel{(4.22)}{=} \langle \hat{\sigma}_z \rangle_{\hat{\rho}_{g_1}} = (4.15).$$

$$\diamond \langle \hat{\sigma}_z \rangle_{\hat{\rho}_{p_0}}(t=\infty) \stackrel{(4.23)}{=} 1 + 2e^{-\lambda \infty} = 1 + 0 = 1 = \langle \hat{\sigma}_z \rangle(t=t_d) \leftrightarrow \epsilon = 0.$$

$$\text{So, } \langle \hat{\sigma}_z \rangle(t=t_d) > \langle \hat{\sigma}_z \rangle_{\hat{\rho}_{p_0}}(t=0) \leftrightarrow 1 > 2a - 1 \leftrightarrow a < 1.$$

- In general, for $t = \infty$, $\langle \hat{\sigma}_z \rangle_{\hat{\rho}_{p_i}}(t)|_{t=\infty} \stackrel{(B.25)}{=} \langle \hat{\sigma}_z \rangle_{\hat{\rho}_A} = \text{Tr}(\hat{\rho}_A \hat{\sigma}_z) = 1.$

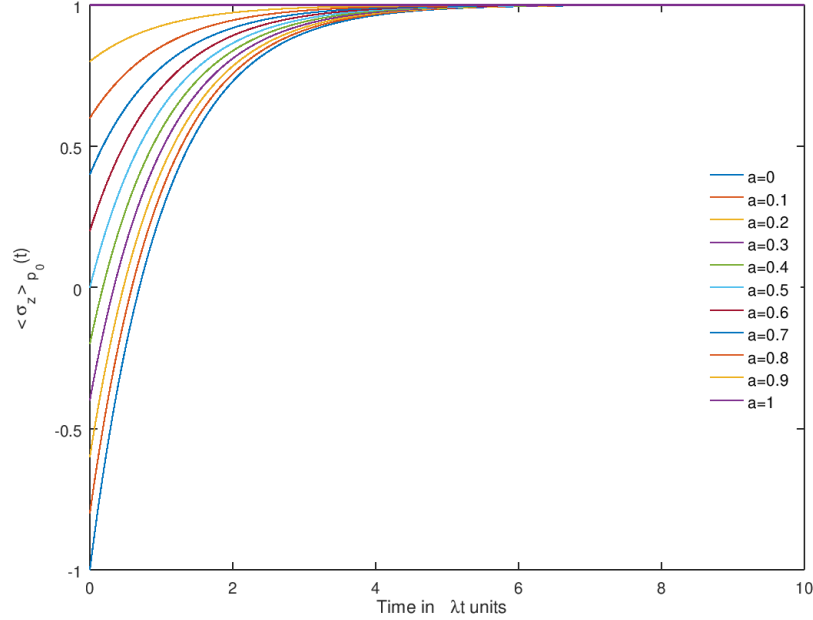


Figure B.1: Plot of $(4.23) = \langle \hat{\sigma}_z \rangle_{\hat{\rho}_{p_0}}(t) = 1 + 2e^{-\lambda t}(a - 1)$ as a function of λt , for several values of $a < 1$. $a > 1$ is forbidden, because $\langle \hat{\sigma}_z \rangle_{\hat{\rho}_{p_i}}(t)$ must be an increasing function. For $a_1 > a_2$, $t_d(a_1) < t_d(a_2)$.

B.2 If $\hat{\sigma}_z$ is the observable whose expectation value in the genotype subspace is chosen to be preserved by Eq. (4.2), and $\hat{\rho}_A = |0\rangle\langle 0|$, why $\hat{U} = \hat{U}_{\text{CNOT}}$?

Let us suppose we have a unitary operator of the following form, in the $\{|0\rangle, |1\rangle\}$ basis,

$$\hat{U} \doteq \begin{pmatrix} A & e & f & g \\ e^* & B & h & i \\ f^* & h^* & C & j \\ g^* & i^* & j^* & d \end{pmatrix}, \quad A, B, C, d \in \mathbb{R}. \quad (\text{B.2})$$

For $\hat{\rho}_{g_0} = (4.7)$, $\langle \hat{\sigma}_z \rangle_{\hat{\rho}_{g_0}} \stackrel{(4.12)}{=} 2a - 1$. We want Eq. (4.5) to be satisfied. Then,

$$\begin{cases} \langle \hat{\sigma}_z \otimes \hat{1}_2 \rangle_{\hat{\rho}_1} = 2a - 1. \\ \langle \hat{1}_2 \otimes \hat{\sigma}_z \rangle_{\hat{\rho}_1} = 2a - 1. \end{cases}, \quad \text{where} \quad (\text{B.3})$$

$$\begin{aligned} \hat{\rho}_1 &= \hat{U} (\hat{\rho}_{g_0} \otimes \hat{\rho}_A) \hat{U}^\dagger \stackrel{(\text{B.10-B.2})}{=} \hat{U} \begin{pmatrix} a & 0 & b - ic & 0 \\ 0 & 0 & 0 & 0 \\ b + ic & 0 & 1 - a & 0 \\ 0 & 0 & 0 & 0 \end{pmatrix} \begin{pmatrix} A & e & f & g \\ e^* & B & h & i \\ f^* & h^* & C & j \\ g^* & i^* & j^* & d \end{pmatrix} \\ &= \begin{pmatrix} A & e & f & g \\ e^* & B & h & i \\ f^* & h^* & C & j \\ g^* & i^* & j^* & D \end{pmatrix} \begin{pmatrix} aA + f^*(b - ic) & ae + h^*(b - ic) & af + C(b - ic) & ag + j(b - ic) \\ 0 & 0 & 0 & 0 \\ A(b + ic) + f^*(1 - a) & e(b + ic) + h^*(1 - a) & f(b + ic) + C(1 - a) & g(b + ic) + j(1 - a) \\ 0 & 0 & 0 & 0 \end{pmatrix} \\ &= \begin{pmatrix} aA^2 + 2A\text{Re}(f(b + ic)) + |f|^2(1 - a); & Aae + Ah^*(b - ic) + ef(b + ic) + fh^*(1 - a); & Aaf + AC(b - ic) + f^2(b + ic) + fC(1 - a); & Aag + Aj(b - ic) + fg(b + ic) + fj(1 - a); \\ e^*aA + e^*f^*(b - ic) + hA(b + ic) + hf^*(1 - a); & a|e|^2 + 2\text{Re}(he(b + ic)) + |h|^2(1 - a); & e^*af + e^*C(b - ic) + hf(b + ic) + hC(1 - a); & e^*ag + e^*j(b - ic) + hg(b + ic) + hj(1 - a); \\ f^*aA + (f^*)^2(b - ic) + CA(b + ic) + Cf^*(1 - a); & f^*ae + f^*h^*(b - ic) + Ce(b + ic) + Ch^*(1 - a); & a|f|^2 + 2C\text{Re}(f(b + ic)) + C^2(1 - a); & f^*ag + f^*j(b - ic) + Cg(b + ic) + Cj(1 - a); \\ g^*aA + g^*f^*(b - ic) + j^*A(b + ic) + j^*f^*(1 - a); & g^*ae + g^*h^*(b - ic) + j^*e(b + ic) + j^*h^*(1 - a); & g^*af + g^*C(b - ic) + j^*f(b + ic) + j^*C(1 - a); & a|g|^2 + 2\text{Re}(gj^*(b + ic)) + |j|^2(1 - a); \end{pmatrix}. \quad (\text{B.4}) \end{aligned}$$

• Normalization condition for density operators, $\text{Tr } \hat{\rho}_1 = 1$, is obeyed if, and only if,

$$\begin{aligned} 1 &= [aA^2 + 2A\text{Re}(f(b + ic)) + |f|^2(1 - a)] + [a|e|^2 + 2\text{Re}(he(b + ic)) + |h|^2(1 - a)] \\ &\quad + [a|f|^2 + 2C\text{Re}(f(b + ic)) + C^2(1 - a)] + [a|g|^2 + 2\text{Re}(gj^*(b + ic)) + |j|^2(1 - a)]. \end{aligned} \quad (\text{B.5})$$

• From Eq. (B.3a),

$$\begin{aligned} 2a - 1 &= \langle \hat{\sigma}_z \otimes \hat{1}_2 \rangle_{\hat{\rho}_1} = \text{Tr} \left(\hat{\rho}_1 \begin{pmatrix} 1 & & & \\ & 1 & & \\ & & -1 & \\ & & & -1 \end{pmatrix} \right) \\ &\stackrel{(\text{B.5})}{=} [aA^2 + 2A\text{Re}(f(b + ic)) + |f|^2(1 - a)] + [a|e|^2 + 2\text{Re}(he(b + ic)) + |h|^2(1 - a)] \\ &\quad - [a|f|^2 + 2C\text{Re}(f(b + ic)) + C^2(1 - a)] - [a|g|^2 + 2\text{Re}(gj^*(b + ic)) + |j|^2(1 - a)] \\ &\stackrel{(\text{B.5})}{=} 2 [aA^2 + 2A\text{Re}(f(b + ic)) + |f|^2(1 - a)] + 2 [a|e|^2 + 2\text{Re}(he(b + ic)) + |h|^2(1 - a)] - 1 \\ &\leftrightarrow a = [aA^2 + 2A\text{Re}(f(b + ic)) + |f|^2(1 - a)] + [a|e|^2 + 2\text{Re}(he(b + ic)) + |h|^2(1 - a)]. \end{aligned} \quad (\text{B.6})$$

where in (1) we used Eq. (B.4) and the fact that we are only interested in its diagonal elements. We claim the latter because multiplying by $\hat{\sigma}_z \otimes \hat{1}_2$ just makes Eq. (B.4) change in sign and we are evaluating the trace, the sum of the diagonal elements, of this matrix product.

- From Eq. (B.3b),

$$\begin{aligned}
2a - 1 &= \langle \hat{1}_2 \otimes \hat{\sigma}_z \rangle_{\hat{\rho}_1} = \text{Tr} \left(\hat{\rho}_1 \begin{pmatrix} 1 & & & \\ & -1 & & \\ & & 1 & \\ & & & -1 \end{pmatrix} \right) \\
&\stackrel{\text{(B.4)}}{=} [aA^2 + 2A\text{Re}(f(b+ic)) + |f|^2(1-a)] - [a|e|^2 + 2\text{Re}(he(b+ic)) + |h|^2(1-a)] \\
&\quad + [a|f|^2 + 2C\text{Re}(f(b+ic)) + C^2(1-a)] - [a|g|^2 + 2\text{Re}(gj^*(b+ic)) + |j|^2(1-a)] \\
&\stackrel{\text{(B.5)}}{=} 2[aA^2 + 2A\text{Re}(f(b+ic)) + |f|^2(1-a)] + 2[a|f|^2 + 2C\text{Re}(f(b+ic)) + C^2(1-a)] - 1 \\
&\leftrightarrow a = [aA^2 + 2A\text{Re}(f(b+ic)) + |f|^2(1-a)] + [a|f|^2 + 2C\text{Re}(f(b+ic)) + C^2(1-a)].
\end{aligned} \tag{B.7}$$

- (B.6)–(B.7) = $a - a = 0 = [a|e|^2 + 2\text{Re}(he(b+ic)) + |h|^2(1-a)] - [a|f|^2 + 2C\text{Re}(f(b+ic)) + C^2(1-a)]$.

- Then, Eq. (B.5),

$$\begin{aligned}
1 &= [aA^2 + 2A\text{Re}(f(b+ic)) + |f|^2(1-a)] + 2[a|e|^2 + 2\text{Re}(he(b+ic)) + |h|^2(1-a)] \\
&\quad + [a|g|^2 + 2\text{Re}(gj^*(b+ic)) + |j|^2(1-a)] \leftrightarrow e, f, g, h = 0 \text{ (to remove } b, c) \text{ and } A = j = 1.
\end{aligned} \tag{B.8}$$

- Now, from Eq. (B.7), $a = a - C^2(1-a) \leftrightarrow C = 0$.

Hence, Eq. (B.2),

$$\hat{U} \doteq \begin{pmatrix} A & e & f & g \\ e^* & B & h & i \\ f^* & h^* & C & j \\ g^* & i^* & j^* & d \end{pmatrix} = \begin{pmatrix} 1 & & & \\ & 1 & & \\ & & & 1 \\ & & & & 1 \end{pmatrix} \stackrel{\text{(3.8)}}{\doteq} \hat{U}_{\text{CNOT}} \equiv \hat{U}_{C_{\hat{\sigma}_x}}. \tag{B.9}$$

B.3 Calculations of $\hat{\rho}_{g_1}$, Eq. (4.8), and \hat{U}_{CNOT} , Eq. (4.9)

$$\begin{aligned}
\hat{\rho}_{g_1} &\equiv \hat{U}(\hat{\rho}_{g_0} \otimes \hat{\rho}_A)\hat{U}^\dagger = \hat{U}(\hat{\rho}_{g_0} \otimes |0\rangle\langle 0|)\hat{U}^\dagger \doteq \begin{pmatrix} 1 & 0 & 0 & 0 \\ 0 & 1 & 0 & 0 \\ 0 & 0 & 0 & 1 \\ 0 & 0 & 1 & 0 \end{pmatrix} \left(\begin{pmatrix} a & b-ic \\ b+ic & 1-a \end{pmatrix} \otimes \begin{pmatrix} 1 & 0 \\ 0 & 0 \end{pmatrix} \right) \begin{pmatrix} 1 & 0 & 0 & 0 \\ 0 & 1 & 0 & 0 \\ 0 & 0 & 0 & 1 \\ 0 & 0 & 1 & 0 \end{pmatrix}^T \\
&= \begin{pmatrix} 1 & 0 & 0 & 0 \\ 0 & 1 & 0 & 0 \\ 0 & 0 & 0 & 1 \\ 0 & 0 & 1 & 0 \end{pmatrix} \begin{pmatrix} a \begin{pmatrix} 1 & 0 \\ 0 & 0 \end{pmatrix} & (b-ic) \begin{pmatrix} 1 & 0 \\ 0 & 0 \end{pmatrix} \\ (b+ic) \begin{pmatrix} 1 & 0 \\ 0 & 0 \end{pmatrix} & (1-a) \begin{pmatrix} 1 & 0 \\ 0 & 0 \end{pmatrix} \end{pmatrix} \begin{pmatrix} 1 & 0 & 0 & 0 \\ 0 & 1 & 0 & 0 \\ 0 & 0 & 0 & 1 \\ 0 & 0 & 1 & 0 \end{pmatrix} \\
&= \begin{pmatrix} 1 & 0 & 0 & 0 \\ 0 & 1 & 0 & 0 \\ 0 & 0 & 0 & 1 \\ 0 & 0 & 1 & 0 \end{pmatrix} \begin{pmatrix} a & 0 & b-ic & 0 \\ 0 & 0 & 0 & 0 \\ b+ic & 0 & 1-a & 0 \\ 0 & 0 & 0 & 0 \end{pmatrix} \begin{pmatrix} 1 & 0 & 0 & 0 \\ 0 & 1 & 0 & 0 \\ 0 & 0 & 0 & 1 \\ 0 & 0 & 1 & 0 \end{pmatrix} = \begin{pmatrix} 1 & 0 & 0 & 0 \\ 0 & 1 & 0 & 0 \\ 0 & 0 & 0 & 1 \\ 0 & 0 & 1 & 0 \end{pmatrix} \begin{pmatrix} a & 0 & 0 & b-ic \\ 0 & 0 & 0 & 0 \\ b+ic & 0 & 0 & 1-a \\ 0 & 0 & 0 & 0 \end{pmatrix} \\
&= \begin{pmatrix} a & 0 & 0 & b-ic \\ 0 & 0 & 0 & 0 \\ 0 & 0 & 0 & 0 \\ b+ic & 0 & 0 & 1-a \end{pmatrix}, \text{ where}
\end{aligned} \tag{B.10}$$

$$\begin{aligned}
\hat{U} \stackrel{\text{(B.9)}}{=} \hat{U}_{\text{CNOT}} &\equiv |0\rangle\langle 0| \otimes \hat{1}_2 + |1\rangle\langle 1| \otimes \hat{\sigma}_x \doteq \begin{pmatrix} 1 & 0 \\ 0 & 0 \end{pmatrix} \otimes \begin{pmatrix} 1 & 0 \\ 0 & 1 \end{pmatrix} + \begin{pmatrix} 0 & 0 \\ 0 & 1 \end{pmatrix} \otimes \begin{pmatrix} 0 & 1 \\ 1 & 0 \end{pmatrix} \\
&= \begin{pmatrix} 1 \begin{pmatrix} 1 & 0 \\ 0 & 1 \end{pmatrix} & 0 \begin{pmatrix} 1 & 0 \\ 0 & 1 \end{pmatrix} \\ 0 \begin{pmatrix} 1 & 0 \\ 0 & 1 \end{pmatrix} & 0 \begin{pmatrix} 1 & 0 \\ 0 & 1 \end{pmatrix} \end{pmatrix} + \begin{pmatrix} 0 \begin{pmatrix} 0 & 1 \\ 1 & 0 \end{pmatrix} & 0 \begin{pmatrix} 0 & 1 \\ 1 & 0 \end{pmatrix} \\ 0 \begin{pmatrix} 0 & 1 \\ 1 & 0 \end{pmatrix} & 1 \begin{pmatrix} 0 & 1 \\ 1 & 0 \end{pmatrix} \end{pmatrix} = \begin{pmatrix} 1 & 0 & 0 & 0 \\ 0 & 1 & 0 & 0 \\ 0 & 0 & 0 & 0 \\ 0 & 0 & 0 & 0 \end{pmatrix} + \begin{pmatrix} 0 & 0 & 0 & 0 \\ 0 & 0 & 0 & 0 \\ 0 & 0 & 0 & 1 \\ 0 & 0 & 1 & 0 \end{pmatrix} \\
&= \begin{pmatrix} 1 & 0 & 0 & 0 \\ 0 & 1 & 0 & 0 \\ 0 & 0 & 0 & 1 \\ 0 & 0 & 1 & 0 \end{pmatrix}.
\end{aligned} \tag{B.11}$$

where the partial cloning operation for the two qubits implied is the CNOT gate ($\hat{U} = \hat{U}_{\text{CNOT}}$) because of Appendix B.2.

B.4 Calculations of Eq. (4.15-4.17)

$$\begin{aligned}
\bullet \langle \hat{\sigma}_z \rangle_{\hat{\rho}_{g_1}} &= \langle (\hat{\sigma}_z)_{g_1} \otimes \hat{1}_{p_0} \rangle_{\hat{\rho}_1} \equiv \langle \hat{\sigma}_z \otimes \hat{1}_2 \rangle_{\hat{\rho}_1} = \text{Tr}(\hat{\rho}_1(\hat{\sigma}_z \otimes \hat{1}_2)) \doteq \text{Tr} \left(\hat{\rho}_1 \left(\begin{pmatrix} 1 & 0 \\ 0 & -1 \end{pmatrix} \otimes \begin{pmatrix} 1 & 0 \\ 0 & 1 \end{pmatrix} \right) \right) \\
&= \text{Tr} \left(\begin{pmatrix} a & 0 & 0 & b-ic \\ 0 & 0 & 0 & 0 \\ 0 & 0 & 0 & 0 \\ b+ic & 0 & 0 & 1-a \end{pmatrix} \begin{pmatrix} 1 & 0 & 0 & 0 \\ 0 & 1 & 0 & 0 \\ 0 & 0 & -1 & 0 \\ 0 & 0 & 0 & -1 \end{pmatrix} \right) = \text{Tr} \begin{pmatrix} a & 0 & 0 & ic-b \\ 0 & 0 & 0 & 0 \\ 0 & 0 & 0 & 0 \\ b+ic & 0 & 0 & a-1 \end{pmatrix} = 2a-1.
\end{aligned} \tag{B.12}$$

- $$\begin{aligned}
\langle \hat{\sigma}_z \rangle_{\hat{\rho}_{p_0}}(t_{p_0}) &= \langle \hat{1}_{g_1} \otimes (\hat{\sigma}_z)_{p_0} \rangle_{\hat{\rho}_1} \equiv \langle \hat{1}_2 \otimes \hat{\sigma}_z \rangle_{\hat{\rho}_1} = \text{Tr}(\hat{\rho}_1(\hat{1}_2 \otimes \hat{\sigma}_z)) \doteq \text{Tr} \left(\hat{\rho}_1 \left(\begin{pmatrix} 1 & 0 \\ 0 & 1 \end{pmatrix} \otimes \begin{pmatrix} 1 & 0 \\ 0 & -1 \end{pmatrix} \right) \right) \\
&= \text{Tr} \left(\begin{pmatrix} a & 0 & 0 & b-ic \\ 0 & 0 & 0 & 0 \\ 0 & 0 & 0 & 0 \\ b+ic & 0 & 0 & 1-a \end{pmatrix} \begin{pmatrix} 1 & 0 & 0 & 0 \\ 0 & -1 & 0 & 0 \\ 0 & 0 & 1 & 0 \\ 0 & 0 & 0 & -1 \end{pmatrix} \right) = \text{Tr} \begin{pmatrix} a & 0 & 0 & ic-b \\ 0 & 0 & 0 & 0 \\ 0 & 0 & 0 & 0 \\ b+ic & 0 & 0 & a-1 \end{pmatrix} = 2a-1.
\end{aligned}
\tag{B.13}$$

- $$\begin{aligned}
\langle \hat{\sigma}_x \rangle_{\hat{\rho}_{g_1}} &= \langle (\hat{\sigma}_x)_{g_1} \otimes \hat{1}_{t_{p_0}} \rangle_{\hat{\rho}_1} \equiv \langle \hat{\sigma}_x \otimes \hat{1}_2 \rangle_{\hat{\rho}_1} = \text{Tr}(\hat{\rho}_1(\hat{\sigma}_x \otimes \hat{1}_2)) \doteq \text{Tr} \left(\hat{\rho}_1 \left(\begin{pmatrix} 0 & 1 \\ 1 & 0 \end{pmatrix} \otimes \begin{pmatrix} 1 & 0 \\ 0 & 1 \end{pmatrix} \right) \right) \\
&= \text{Tr} \left(\begin{pmatrix} a & 0 & 0 & b-ic \\ 0 & 0 & 0 & 0 \\ 0 & 0 & 0 & 0 \\ b+ic & 0 & 0 & 1-a \end{pmatrix} \begin{pmatrix} 0 & 0 & 1 & 0 \\ 0 & 0 & 0 & 1 \\ 1 & 0 & 0 & 0 \\ 0 & 1 & 0 & 0 \end{pmatrix} \right) = \text{Tr} \begin{pmatrix} 0 & b-ic & a & 0 \\ 0 & 0 & 0 & 0 \\ 0 & 0 & 0 & 0 \\ 0 & 1-a & b+ic & 0 \end{pmatrix} = 0.
\end{aligned}
\tag{B.14}$$

- $$\begin{aligned}
\langle \hat{\sigma}_x \rangle_{\hat{\rho}_{p_0}}(t_{p_0}) &= \langle \hat{1}_{g_1} \otimes (\hat{\sigma}_x)_{p_0} \rangle_{\hat{\rho}_1} \equiv \langle \hat{1}_2 \otimes \hat{\sigma}_x \rangle_{\hat{\rho}_1} = \text{Tr}(\hat{\rho}_1(\hat{1}_2 \otimes \hat{\sigma}_x)) \doteq \text{Tr} \left(\hat{\rho}_1 \left(\begin{pmatrix} 1 & 0 \\ 0 & 1 \end{pmatrix} \otimes \begin{pmatrix} 0 & 1 \\ 1 & 0 \end{pmatrix} \right) \right) \\
&= \text{Tr} \left(\begin{pmatrix} a & 0 & 0 & b-ic \\ 0 & 0 & 0 & 0 \\ 0 & 0 & 0 & 0 \\ b+ic & 0 & 0 & 1-a \end{pmatrix} \begin{pmatrix} 0 & 1 & 0 & 0 \\ 1 & 0 & 0 & 0 \\ 0 & 0 & 0 & 1 \\ 0 & 0 & 1 & 0 \end{pmatrix} \right) = \text{Tr} \begin{pmatrix} 0 & a & b-ic & 0 \\ 0 & 0 & 0 & 0 \\ 0 & 0 & 0 & 0 \\ 0 & b+ic & 1-a & 0 \end{pmatrix} = 0.
\end{aligned}
\tag{B.15}$$

- $$\begin{aligned}
\langle \hat{\sigma}_y \rangle_{\hat{\rho}_{g_1}} &= \langle (\hat{\sigma}_y)_{g_1} \otimes \hat{1}_{p_0} \rangle_{\hat{\rho}_1} \equiv \langle \hat{\sigma}_y \otimes \hat{1}_2 \rangle_{\hat{\rho}_1} = \text{Tr}(\hat{\rho}_1(\hat{\sigma}_y \otimes \hat{1}_2)) \doteq \text{Tr} \left(\hat{\rho}_1 \left(\begin{pmatrix} 0 & -i \\ i & 0 \end{pmatrix} \otimes \begin{pmatrix} 1 & 0 \\ 0 & 1 \end{pmatrix} \right) \right) \\
&= \text{Tr} \left(\begin{pmatrix} a & 0 & 0 & b-ic \\ 0 & 0 & 0 & 0 \\ 0 & 0 & 0 & 0 \\ b+ic & 0 & 0 & 1-a \end{pmatrix} \begin{pmatrix} 0 & 0 & -i & 0 \\ 0 & 0 & 0 & -i \\ i & 0 & 0 & 0 \\ 0 & i & 0 & 0 \end{pmatrix} \right) = \text{Tr} \begin{pmatrix} 0 & c+ib & -ai & 0 \\ 0 & 0 & 0 & 0 \\ 0 & 0 & 0 & 0 \\ 0 & i-ai & c-ib & 0 \end{pmatrix} = 0.
\end{aligned}
\tag{B.16}$$

- $$\begin{aligned}
\langle \hat{\sigma}_y \rangle_{\hat{\rho}_{p_0}}(t_{p_0}) &= \langle \hat{1}_{g_1} \otimes (\hat{\sigma}_y)_{p_0} \rangle_{\hat{\rho}_1} \equiv \langle \hat{1}_2 \otimes \hat{\sigma}_y \rangle_{\hat{\rho}_1} = \text{Tr}(\hat{\rho}_1(\hat{1}_2 \otimes \hat{\sigma}_y)) \doteq \text{Tr} \left(\hat{\rho}_1 \left(\begin{pmatrix} 1 & 0 \\ 0 & 1 \end{pmatrix} \otimes \begin{pmatrix} 0 & -i \\ i & 0 \end{pmatrix} \right) \right) \\
&= \text{Tr} \left(\begin{pmatrix} a & 0 & 0 & b-ic \\ 0 & 0 & 0 & 0 \\ 0 & 0 & 0 & 0 \\ b+ic & 0 & 0 & 1-a \end{pmatrix} \begin{pmatrix} 0 & -i & 0 & 0 \\ i & 0 & 0 & 0 \\ 0 & 0 & 0 & -i \\ 0 & 0 & i & 0 \end{pmatrix} \right) = \text{Tr} \begin{pmatrix} 0 & -ai & c+ib & 0 \\ 0 & 0 & 0 & 0 \\ 0 & 0 & 0 & 0 \\ 0 & c-ib & i-ai & 0 \end{pmatrix} = 0.
\end{aligned}
\tag{B.17}$$

- $$\begin{aligned}
\langle \hat{\sigma}_x \otimes \hat{\sigma}_x \rangle_{\hat{\rho}_1} &= \text{Tr}(\hat{\rho}_1(\hat{\sigma}_x \otimes \hat{\sigma}_x)) \doteq \text{Tr} \left(\hat{\rho}_1 \left(\begin{pmatrix} 0 & 1 \\ 1 & 0 \end{pmatrix} \otimes \begin{pmatrix} 0 & 1 \\ 1 & 0 \end{pmatrix} \right) \right) \\
&= \text{Tr} \left(\begin{pmatrix} a & 0 & 0 & b-ic \\ 0 & 0 & 0 & 0 \\ 0 & 0 & 0 & 0 \\ b+ic & 0 & 0 & 1-a \end{pmatrix} \begin{pmatrix} 0 & 0 & 0 & 1 \\ 0 & 0 & 1 & 0 \\ 0 & 1 & 0 & 0 \\ 1 & 0 & 0 & 0 \end{pmatrix} \right) = \text{Tr} \begin{pmatrix} b-ic & 0 & 0 & a \\ 0 & 0 & 0 & 0 \\ 0 & 0 & 0 & 0 \\ 1-a & 0 & 0 & b+ic \end{pmatrix} = 2b.
\end{aligned}
\tag{B.18}$$

B.5 Why is $\hat{\rho}_A$ the steady state of our Lindbladian?

Let us substitute in Eq. (4.20) a density operator of the form $\hat{\rho}(t) \doteq \begin{pmatrix} a & b \\ b^* & 1-a \end{pmatrix}$, $a = a(t)$, $b = b(t)$.

$$\begin{aligned} \frac{d}{dt}\hat{\rho}(t) &= \lambda \left(\hat{\sigma} \hat{\rho}(t) \hat{\sigma}^\dagger - \frac{1}{2} \{ \hat{\sigma}^\dagger \hat{\sigma}, \hat{\rho}(t) \} \right) \doteq \lambda \begin{pmatrix} 0 & 1 \\ 0 & 0 \end{pmatrix} \begin{pmatrix} a & b \\ b^* & 1-a \end{pmatrix} \begin{pmatrix} 0 & 0 \\ 1 & 0 \end{pmatrix} - \lambda \frac{1}{2} \left\{ \begin{pmatrix} 0 & 0 \\ 1 & 0 \end{pmatrix} \begin{pmatrix} 0 & 1 \\ 0 & 0 \end{pmatrix}, \hat{\rho}(t) \right\} \\ &= \lambda \begin{pmatrix} 0 & 1 \\ 0 & 0 \end{pmatrix} \begin{pmatrix} b & 0 \\ 1-a & 0 \end{pmatrix} - \lambda \frac{1}{2} \begin{pmatrix} 0 & 0 \\ 0 & 1 \end{pmatrix} \begin{pmatrix} a & b \\ b^* & 1-a \end{pmatrix} - \lambda \frac{1}{2} \begin{pmatrix} a & b \\ b^* & 1-a \end{pmatrix} \begin{pmatrix} 0 & 0 \\ 0 & 1 \end{pmatrix} \\ &= \lambda \begin{pmatrix} 1-a & 0 \\ 0 & 0 \end{pmatrix} - \lambda \frac{1}{2} \begin{pmatrix} 0 & 0 \\ b^* & 1-a \end{pmatrix} - \lambda \frac{1}{2} \begin{pmatrix} 0 & b \\ 0 & 1-a \end{pmatrix} = -\lambda \begin{pmatrix} a-1 & b/2 \\ b^*/2 & 1-a \end{pmatrix}. \end{aligned} \quad (\text{B.19})$$

Hence, if we define $a(t=0) \equiv a_0$ and $b(t=0) \equiv b_0$,

$$\begin{aligned} \bullet \quad \frac{d}{dt} [\hat{\rho}(t)]_{11} &= \frac{da}{dt} = \lambda(1-a) \quad \rightarrow \quad \frac{da}{1-a} = \lambda dt \quad \rightarrow \quad -\ln(1-a) + C_1 = \lambda t \quad \xrightarrow{t=0} \\ &-\ln(1-a_0) + C_1 = 0 \quad \rightarrow \quad \ln\left(\frac{1-a}{1-a_0}\right) = -\lambda t \quad \rightarrow \quad a = a(t) = 1 + e^{-\lambda t}(a_0 - 1), \end{aligned} \quad (\text{B.20})$$

$$\bullet \quad \frac{d}{dt} [\hat{\rho}(t)]_{12} = \frac{db}{dt} = -\lambda b/2 \rightarrow \frac{db}{b} = -\frac{\lambda}{2} dt \quad \rightarrow \quad \ln\left(\frac{b}{b_0}\right) = -\frac{\lambda}{2} t \quad \rightarrow \quad b = b(t) = b_0 e^{-\lambda t/2}. \quad (\text{B.21})$$

These solutions –more generally, the behavior of an open quantum system– can be viewed as $\hat{\rho}(t) = \sum_{k=0}^1 \hat{M}_k \hat{\rho}(0) \hat{M}_k^\dagger$, where $\eta \equiv 1 - e^{-\lambda t}$ and the operation elements³¹ are [1, p. 388, Eq. (8.144-8.146)]

$$\hat{M}_0 \doteq \begin{pmatrix} 1 & 0 \\ 0 & \sqrt{1-\eta} \end{pmatrix}, \quad \text{and} \quad \hat{M}_1 \doteq \begin{pmatrix} 0 & \sqrt{\eta} \\ 0 & 0 \end{pmatrix}. \quad (\text{B.22})$$

That is,

$$\begin{aligned} \hat{\rho}(t) &= \sum_k \hat{M}_k \hat{\rho}(0) \hat{M}_k^\dagger = \hat{M}_0 \hat{\rho}(0) \hat{M}_0^\dagger + \hat{M}_1 \hat{\rho}(0) \hat{M}_1^\dagger \doteq \begin{pmatrix} 1 & 0 \\ 0 & \sqrt{1-\eta} \end{pmatrix} \begin{pmatrix} a_0 & b_0 \\ b_0^* & 1-a_0 \end{pmatrix} \begin{pmatrix} 1 & 0 \\ 0 & \sqrt{1-\eta} \end{pmatrix} + \\ &\begin{pmatrix} 0 & \sqrt{\eta} \\ 0 & 0 \end{pmatrix} \begin{pmatrix} a_0 & b_0 \\ b_0^* & 1-a_0 \end{pmatrix} \begin{pmatrix} 0 & 0 \\ \sqrt{\eta} & 0 \end{pmatrix} = \begin{pmatrix} 1 & 0 \\ 0 & \sqrt{1-\eta} \end{pmatrix} \begin{pmatrix} a_0 & b_0\sqrt{1-\eta} \\ b_0^* & (1-a_0)\sqrt{1-\eta} \end{pmatrix} + \begin{pmatrix} 0 & \sqrt{\eta} \\ 0 & 0 \end{pmatrix} \begin{pmatrix} b_0\sqrt{\eta} & 0 \\ (1-a_0)\sqrt{\eta} & 0 \end{pmatrix} \\ &= \begin{pmatrix} a_0 & b_0\sqrt{1-\eta} \\ b_0^*\sqrt{1-\eta} & (1-a_0)(1-\eta) \end{pmatrix} + \begin{pmatrix} (1-a_0)\eta & 0 \\ 0 & 0 \end{pmatrix} = \begin{pmatrix} a_0 + (1-a_0)\eta & b_0\sqrt{1-\eta} \\ b_0^*\sqrt{1-\eta} & (1-a_0)(1-\eta) \end{pmatrix}. \end{aligned} \quad (\text{B.23})$$

³¹(B.22) is said to be a normalized set of so called *Kraus operators* since

$$\sum_k \hat{M}_k^\dagger \hat{M}_k = \hat{M}_0^\dagger \hat{M}_0 + \hat{M}_1^\dagger \hat{M}_1 \doteq \begin{pmatrix} 1 & 0 \\ 0 & \sqrt{1-\eta} \end{pmatrix} \begin{pmatrix} 1 & 0 \\ 0 & \sqrt{1-\eta} \end{pmatrix} + \begin{pmatrix} 0 & 0 \\ \sqrt{\eta} & 0 \end{pmatrix} \begin{pmatrix} 0 & \sqrt{\eta} \\ 0 & 0 \end{pmatrix} = \begin{pmatrix} 1 & 0 \\ 0 & 1-\eta \end{pmatrix} + \begin{pmatrix} 0 & 0 \\ 0 & \eta \end{pmatrix} = \hat{1}_2.$$

- For $t = 0 \rightarrow \eta = 1 - e^{-\lambda 0} = 1 - 1 = 0$ we recover the initial state $\hat{\rho}(t = 0)$,

$$\hat{\rho}(t = 0) \doteq \begin{pmatrix} a_0 + (1 - a_0)0 & b_0\sqrt{1 - 0} \\ b_0^*\sqrt{1 - 0} & (1 - a_0)(1 - 0) \end{pmatrix} = \begin{pmatrix} a_0 & b_0 \\ b_0^* & 1 - a_0 \end{pmatrix}. \quad (\text{B.24})$$

- For $t = \infty \rightarrow \eta = 1 - e^{-\lambda\infty} = 1 - 0 = 1$, conversely,

$$\hat{\rho}(t = \infty) \doteq \begin{pmatrix} a + (1 - a)1 & b\sqrt{1 - 1} \\ b^*\sqrt{1 - 1} & (1 - a)(1 - 1) \end{pmatrix} = \begin{pmatrix} 1 & 0 \\ 0 & 0 \end{pmatrix} \doteq |0\rangle\langle 0| \equiv \hat{\rho}_A. \quad (\text{B.25})$$

Thus, regardless of the initial state $\hat{\rho}(t = 0)$, the Lindbladian pushes the system towards its steady state $|0\rangle$, by destroying all coherences (off-diagonal elements in the matrix representation of the density operator $\hat{\rho}$).

B.6 Calculations of $\hat{\rho}_{p_0}(t)$, Eq. (4.21)

Here, we use $\hat{\sigma} = \hat{1}_2 \otimes |0\rangle\langle 1|$ instead of $\hat{\sigma} = |0\rangle\langle 1|$ in Eq. (4.21) in order to act just on the subspace corresponding to the phenotype qubit, following footnote 19. Despite dropping the subscripts to avoid cumbersome notation, rigorously $\hat{\sigma} = \hat{1}_2 \otimes |0\rangle\langle 1|$ would be $\hat{\sigma}_p$, where subscript p denotes that it acts on the phenotype subspace.

$$\hat{\sigma} = \hat{1}_2 \otimes |0\rangle\langle 1| \doteq \begin{pmatrix} 1 & 0 \\ 0 & 1 \end{pmatrix} \otimes \begin{pmatrix} 0 & 1 \\ 0 & 0 \end{pmatrix} = \begin{pmatrix} 1 \begin{pmatrix} 0 & 1 \\ 0 & 0 \end{pmatrix} & 0 \begin{pmatrix} 0 & 1 \\ 0 & 0 \end{pmatrix} \\ 0 \begin{pmatrix} 0 & 1 \\ 0 & 0 \end{pmatrix} & 1 \begin{pmatrix} 0 & 1 \\ 0 & 0 \end{pmatrix} \end{pmatrix} = \begin{pmatrix} 0 & 1 & & \\ & 0 & & \\ & & 0 & 1 \\ & & 0 & 0 \end{pmatrix}, \quad (\text{B.26})$$

$$\text{and } \hat{\sigma}^\dagger = (\hat{1}_2 \otimes |0\rangle\langle 1|)^\dagger \stackrel{(1)}{=} (\hat{1}_2)^\dagger \otimes (|0\rangle\langle 1|)^\dagger \stackrel{(2)}{=} \hat{1}_2 \otimes |1\rangle\langle 0| \doteq \begin{pmatrix} 1 & 0 \\ 0 & 1 \end{pmatrix} \otimes \begin{pmatrix} 0 & 0 \\ 1 & 0 \end{pmatrix} = \begin{pmatrix} 0 & 0 & & \\ 1 & 0 & & \\ & & 0 & 0 \\ & & 1 & 0 \end{pmatrix}, \quad (\text{B.27})$$

where in equality (B.27(1)) we used Ref. [1, p. 74, Eq. (2.53)]: $(\hat{A} \otimes \hat{B})^T = \hat{A}^T \otimes \hat{B}^T$, and $(\hat{A} + \hat{B})^* = \hat{A}^* \otimes \hat{B}^*$. Therefore, since $\hat{A}^\dagger \equiv (\hat{A}^*)^T \equiv (\hat{A}^T)^*$, $(\hat{A} + \hat{B})^\dagger = \hat{A}^\dagger \otimes \hat{B}^\dagger$. We additionally used, in equality (B.27(2)), $(\hat{1}_2)^\dagger \doteq \begin{pmatrix} 1 & 0 \\ 0 & 1 \end{pmatrix}^\dagger = \begin{pmatrix} 1 & 0 \\ 0 & 1 \end{pmatrix} \doteq \hat{1}_2$.

Then,

$$\begin{aligned} \dot{\hat{\rho}}_1 &= \lambda \left(\hat{\sigma} \hat{\rho}_1 \hat{\sigma}^\dagger - \frac{1}{2} \hat{\sigma}^\dagger \hat{\sigma} \hat{\rho}_1 - \frac{1}{2} \hat{\rho}_1 \hat{\sigma}^\dagger \hat{\sigma} \right) \stackrel{(4.8)}{=} \lambda \hat{\sigma} \begin{pmatrix} a & 0 & 0 & b-ic \\ 0 & 0 & 0 & 0 \\ 0 & 0 & 0 & 0 \\ b+ic & 0 & 0 & 1-a \end{pmatrix} \begin{pmatrix} 0 & 0 \\ 1 & 0 \\ & 0 & 0 \\ & & 1 & 0 \end{pmatrix} \\ &- \lambda \frac{1}{2} \hat{\sigma}^\dagger \begin{pmatrix} 0 & 1 \\ 0 & 0 \\ & 0 & 1 \\ & & 0 & 0 \end{pmatrix} \begin{pmatrix} a & 0 & 0 & b-ic \\ 0 & 0 & 0 & 0 \\ 0 & 0 & 0 & 0 \\ b+ic & 0 & 0 & 1-a \end{pmatrix} - \lambda \frac{1}{2} \hat{\rho}_{p_0} \begin{pmatrix} 0 & 0 \\ 1 & 0 \\ & 0 & 0 \\ & & 1 & 0 \end{pmatrix} \begin{pmatrix} 0 & 1 \\ 0 & 0 \\ & 0 & 1 \\ & & 0 & 0 \end{pmatrix} \\ &= \lambda \begin{pmatrix} 0 & 1 \\ 0 & 0 \\ & 0 & 1 \\ & & 0 & 0 \end{pmatrix} \begin{pmatrix} 0 & 0 & b-ic & 0 \\ 0 & 0 & 0 & 0 \\ 0 & 0 & 0 & 0 \\ 0 & 0 & 1-a & 0 \end{pmatrix} - \lambda \frac{1}{2} \begin{pmatrix} 0 & 0 \\ 1 & 0 \\ & 0 & 0 \\ & & 1 & 0 \end{pmatrix} \begin{pmatrix} 0 & 0 & 0 & 0 \\ 0 & 0 & 0 & 0 \\ b+ic & 0 & 0 & 1-a \\ 0 & 0 & 0 & 0 \end{pmatrix} \\ &- \lambda \frac{1}{2} \begin{pmatrix} a & 0 & 0 & b-ic \\ 0 & 0 & 0 & 0 \\ 0 & 0 & 0 & 0 \\ b+ic & 0 & 0 & 1-a \end{pmatrix} \begin{pmatrix} 0 & 0 \\ 0 & 1 \\ & 0 & 0 \\ & & 0 & 1 \end{pmatrix} = \lambda \begin{pmatrix} 0 & 0 & 0 & 0 \\ 0 & 0 & 0 & 0 \\ 0 & 0 & 1-a & 0 \\ 0 & 0 & 0 & 0 \end{pmatrix} - \lambda \frac{1}{2} \begin{pmatrix} 0 & 0 & 0 & 0 \\ 0 & 0 & 0 & 0 \\ 0 & 0 & 0 & 0 \\ b+ic & 0 & 0 & 1-a \end{pmatrix} \\ &- \lambda \frac{1}{2} \begin{pmatrix} 0 & 0 & 0 & b-ic \\ 0 & 0 & 0 & 0 \\ 0 & 0 & 0 & 0 \\ 0 & 0 & 0 & 1-a \end{pmatrix} = -\lambda \frac{1}{2} \begin{pmatrix} 0 & 0 & 0 & b-ic \\ 0 & 0 & 0 & 0 \\ 0 & 0 & -2(1-a) & 0 \\ b+ic & 0 & 0 & 2(1-a) \end{pmatrix}. \end{aligned} \quad (\text{B.28})$$

Then, we solve Eq. (B.28) element by element in order to obtain Eq. (4.21). We use times a lot sooner ($t \ll 1$) than death or decoherence time t_d when $\hat{\rho}_{p_0}(t_d) = \hat{\rho}_A$.

- $\frac{d}{dt}(\hat{\rho}_{p_0}(t))_{11} = 0 \rightarrow (\hat{\rho}_{p_0}(t))_{11} = C_1 \xrightarrow{t=0} (\hat{\rho}_{p_0}(t=0))_{11} = C_1 \stackrel{(4.8)}{=} a \rightarrow (\hat{\rho}_{p_0}(t))_{11} = a. \quad (\text{B.29})$

- $\frac{d}{dt}(\hat{\rho}_{p_0}(t)) \begin{Bmatrix} 14 \\ 41 \end{Bmatrix} = -\lambda \frac{1}{2}(b \mp ic) \rightarrow (\hat{\rho}_{p_0}(t)) \begin{Bmatrix} 14 \\ 41 \end{Bmatrix} = -\lambda \frac{1}{2}(b \mp ic)t + C_2 \xrightarrow{t=0} (\hat{\rho}_{p_0}(t=0)) \begin{Bmatrix} 14 \\ 41 \end{Bmatrix} = C_2 \stackrel{(4.8)}{=} b \mp ic \rightarrow$
 $(\hat{\rho}_{p_0}(t)) \begin{Bmatrix} 14 \\ 41 \end{Bmatrix} = (b \mp ic) \left(-\lambda \frac{t}{2} + 1\right) \overset{t \ll 1}{\approx} (b \mp ic) e^{-\lambda \frac{t}{2}}. \quad (\text{B.30})$

- $\frac{d}{dt}(\hat{\rho}_{p_0}(t))_{44} = -\lambda(1-a) \rightarrow (\hat{\rho}_{p_0}(t))_{44} = -\lambda(1-a)t + C_4 \xrightarrow{t=0} (\hat{\rho}_{p_0}(t=0))_{44} = C_4 \stackrel{(4.8)}{=} 1-a \rightarrow$
 $(\hat{\rho}_{p_0}(t))_{44} = (1-\lambda t)(1-a) \underset{t \ll 1}{\approx} e^{-\lambda t}(1-a). \quad (\text{B.31})$

- $\frac{d}{dt}(\hat{\rho}_{p_0}(t))_{33} = \lambda(1-a) \rightarrow (\hat{\rho}_{p_0}(t))_{33} = \lambda(1-a)t + C_3 \xrightarrow{t=0} (\hat{\rho}_{p_0}(t=0))_{33} = C_3 \stackrel{(4.8)}{=} 0 \rightarrow$
 $(\hat{\rho}_{p_0}(t))_{33} = \lambda(1-a)t = (1-1+\lambda t)(1-a) = (1-(1-\lambda t))(1-a) \underset{t \ll 1}{\approx} (1-e^{-\lambda t})(1-a). \quad (\text{B.32})$

- Otherwise, (for $(\hat{\rho}_{p_0}(t))_{ij} : ij = 12, 13, 21, 22, 23, 24, 31, 32, 34, 42, 43$)

$$\frac{d}{dt}(\hat{\rho}_{p_0}(t))_{ij} = 0 \rightarrow (\hat{\rho}_{p_0}(t))_{ij} = C_5 \xrightarrow{t=0} (\hat{\rho}_{p_0}(t=0))_{ij} = C_5 \stackrel{(4.8)}{=} 0 \rightarrow (\hat{\rho}_{p_0}(t))_{ij} = 0. \quad (\text{B.33})$$

B.7 Calculations of Eq. (4.22-4.23)

- $$\begin{aligned}
\langle \hat{\sigma}_z \rangle_{g_1} &= \langle (\hat{\sigma}_z)_{g_1} \otimes \hat{1}_{p_0} \rangle_{\hat{\rho}_1(t)} \equiv \langle \hat{\sigma}_z \otimes \hat{1}_2 \rangle_{\hat{\rho}_1(t)} = \text{Tr}(\hat{\rho}_1(t) (\hat{\sigma}_z \otimes \hat{1}_2)) \doteq \text{Tr} \left(\hat{\rho}_1(t) \left(\begin{pmatrix} 1 & 0 \\ 0 & -1 \end{pmatrix} \otimes \begin{pmatrix} 1 & 0 \\ 0 & 1 \end{pmatrix} \right) \right) \\
&\stackrel{(4.21)}{=} \text{Tr} \left(\begin{pmatrix} a & 0 & 0 & (b-ic)e^{-\lambda t/2} \\ 0 & 0 & 0 & 0 \\ 0 & 0 & (1-a)(1-e^{-\lambda t}) & 0 \\ (b+ic)e^{-\lambda t/2} & 0 & 0 & (1-a)e^{-\lambda t} \end{pmatrix} \begin{pmatrix} 1 & 0 & 0 & 0 \\ 0 & 1 & 0 & 0 \\ 0 & 0 & -1 & 0 \\ 0 & 0 & 0 & -1 \end{pmatrix} \right) \\
&= \text{Tr} \begin{pmatrix} a & 0 & 0 & (ic-b)e^{-\lambda t/2} \\ 0 & 0 & 0 & 0 \\ 0 & 0 & (a-1)(1-e^{-\lambda t}) & 0 \\ (b+ic)e^{-\lambda t/2} & 0 & 0 & (a-1)e^{-\lambda t} \end{pmatrix} \\
&= a + a - ae^{-\lambda t} - 1 + e^{-\lambda t} + ae^{-\lambda t} - e^{-\lambda t} = 2a - 1 \neq \langle \hat{\sigma}_z \rangle_{g_1}(t).
\end{aligned}$$

(B.34)

- $$\begin{aligned}
\langle \hat{\sigma}_z \rangle_{p_0}(t) &= \langle \hat{1}_{g_1} \otimes (\hat{\sigma}_z)_{p_0} \rangle_{\hat{\rho}_1(t)} \equiv \langle \hat{1}_2 \otimes \hat{\sigma}_z \rangle_{\hat{\rho}_1(t)} = \text{Tr}(\hat{\rho}_1(t) (\hat{1}_2 \otimes \hat{\sigma}_z)) \doteq \text{Tr} \left(\hat{\rho}_1(t) \left(\begin{pmatrix} 1 & 0 \\ 0 & 1 \end{pmatrix} \otimes \begin{pmatrix} 1 & 0 \\ 0 & -1 \end{pmatrix} \right) \right) \\
&\stackrel{(4.21)}{=} \text{Tr} \left(\begin{pmatrix} a & 0 & 0 & (b-ic)e^{-\lambda t/2} \\ 0 & 0 & 0 & 0 \\ 0 & 0 & (1-a)(1-e^{-\lambda t}) & 0 \\ (b+ic)e^{-\lambda t/2} & 0 & 0 & (1-a)e^{-\lambda t} \end{pmatrix} \begin{pmatrix} 1 & 0 & 0 & 0 \\ 0 & -1 & 0 & 0 \\ 0 & 0 & 1 & 0 \\ 0 & 0 & 0 & -1 \end{pmatrix} \right) \\
&= \text{Tr} \begin{pmatrix} a & 0 & 0 & (ic-b)e^{-\lambda t/2} \\ 0 & 0 & 0 & 0 \\ 0 & 0 & (1-a)(1-e^{-\lambda t}) & 0 \\ (b+ic)e^{-\lambda t/2} & 0 & 0 & (a-1)e^{-\lambda t} \end{pmatrix} \\
&= a + 1 - e^{-\lambda t} - a + ae^{-\lambda t} + ae^{-\lambda t} - e^{-\lambda t} = 1 + 2e^{-\lambda t}(a-1).
\end{aligned}$$

(B.35)

B.8 Proof of Eq. (4.30)

We use the qubit order of IBM's computer, Eq. (4.29). For example, for $i = 2, j = 1$: $|xy\rangle \equiv |x\rangle_2 |y\rangle_1$, $x, y \in \{0, 1\}$.

- For \hat{U}_{ij} , $i > j$, and $i = 2, j = 1$,

$$\begin{aligned}
& \hat{U}_{21} (a |00\rangle + b |01\rangle + c |10\rangle + d |11\rangle) = a |00\rangle + b |01\rangle + c |11\rangle + d |10\rangle \doteq \\
& \hat{U}_{21} \begin{pmatrix} a \\ b \\ c \\ d \end{pmatrix} = \begin{pmatrix} a \\ b \\ d \\ c \end{pmatrix} \leftrightarrow \hat{U}_{21} \doteq \begin{pmatrix} 1 & & & \\ & 1 & & \\ & & & 1 \\ & & 1 & \end{pmatrix} = \begin{pmatrix} \hat{1}_2 & \\ & \hat{\sigma}_x \end{pmatrix} \equiv \hat{U}_{C\hat{\sigma}_x} = \hat{U}_{\text{CNOT}} = \hat{U}_{ij}. \quad \text{QED} \tag{B.36}
\end{aligned}$$

- On the other hand, for \hat{U}_{ji} , $i > j$, and $i = 2, j = 1$,

$$\begin{aligned}
& \hat{U}_{12} (a |00\rangle + b |01\rangle + c |10\rangle + d |11\rangle) = a |00\rangle + b |11\rangle + c |10\rangle + d |01\rangle \doteq \\
& \hat{U}_{12} \begin{pmatrix} a \\ b \\ c \\ d \end{pmatrix} = \begin{pmatrix} a \\ d \\ c \\ b \end{pmatrix} \leftrightarrow \hat{U}_{12} \doteq \begin{pmatrix} 1 & & & \\ & & & 1 \\ & & 1 & \\ & 1 & & \end{pmatrix} = \hat{U}_{ji}, \tag{B.37}
\end{aligned}$$

B.9 Proof of Eq. (4.31)

For $i > j$ and $i, j = 0, 1, 2, 3$, in the notation of Eq. (4.29),

$$\begin{aligned}
\hat{U}_{ji} &= \hat{U}_{\text{Had}}^{\otimes 2} \hat{U}_{ij} \hat{U}_{\text{Had}}^{\otimes 2} = \left(\frac{1}{\sqrt{2}} \begin{pmatrix} 1 & 1 \\ 1 & -1 \end{pmatrix} \otimes \frac{1}{\sqrt{2}} \begin{pmatrix} 1 & 1 \\ 1 & -1 \end{pmatrix} \right) \hat{U}_{ij} \hat{U}_{\text{had}}^{\otimes 2} \\
&\stackrel{(4.30)}{=} \frac{1}{2} \begin{pmatrix} 1 & 1 & 1 & 1 \\ 1 & -1 & 1 & -1 \\ 1 & 1 & -1 & -1 \\ 1 & -1 & -1 & 1 \end{pmatrix} \begin{pmatrix} 1 & & & \\ & 1 & & \\ & & & 1 \\ & & 1 & \end{pmatrix} \hat{U}_{\text{Had}}^{\otimes 2} \\
&= \frac{1}{2} \begin{pmatrix} 1 & 1 & 1 & 1 \\ 1 & -1 & -1 & 1 \\ 1 & 1 & -1 & -1 \\ 1 & -1 & 1 & -1 \end{pmatrix} \frac{1}{2} \begin{pmatrix} 1 & 1 & 1 & 1 \\ 1 & -1 & 1 & -1 \\ 1 & 1 & -1 & -1 \\ 1 & -1 & -1 & 1 \end{pmatrix} = \frac{1}{4} \begin{pmatrix} 4 & & & \\ & 4 & & \\ & & 4 & \\ & & & 4 \end{pmatrix} = \begin{pmatrix} 1 & & & \\ & 1 & & \\ & & 1 & \\ & & & 1 \end{pmatrix}. \tag{B.38}
\end{aligned}$$

B.10 Calculations of $\langle \hat{H}_k \rangle_{\hat{\rho}_g^\alpha \otimes \hat{\rho}_g^\beta} |_{k=\alpha}$, Eq. (4.26)

$$\begin{aligned}
\langle \hat{H}_\alpha \rangle_{\hat{\rho}_g^\alpha \otimes \hat{\rho}_g^\beta} &= \text{Tr} \left[\left(\hat{\rho}_g^\alpha \otimes \hat{\rho}_g^\beta \right) \hat{H}_\alpha \right] \stackrel{(4.24)}{=} \text{Tr} \left[\left(\hat{\rho}_g^\alpha \otimes \hat{\rho}_g^\beta \right) \left(a_\alpha (\hat{\sigma}_z^{\otimes 2}) + b_\alpha (\hat{\sigma}_z \otimes \hat{1}_2) \right) \right] \\
&= \text{Tr} \left[\left(\hat{\rho}_g^\alpha \otimes \hat{\rho}_g^\beta \right) a_\alpha (\hat{\sigma}_z^{\otimes 2}) \right] + \text{Tr} \left[\left(\hat{\rho}_g^\alpha \otimes \hat{\rho}_g^\beta \right) b_\alpha (\hat{\sigma}_z \otimes \hat{1}_2) \right] \\
&\stackrel{(4.25)}{=} \text{Tr} \left[\left(\begin{pmatrix} \cos^2(\theta_\alpha/2) & \frac{1}{2} \sin \theta_\alpha e^{-i\varphi} \\ \frac{1}{2} \sin \theta_\alpha e^{i\varphi} & \sin^2(\theta_\alpha/2) \end{pmatrix} \otimes \begin{pmatrix} \cos^2(\theta_\beta/2) & \frac{1}{2} \sin \theta_\beta e^{-i\varphi} \\ \frac{1}{2} \sin \theta_\beta e^{i\varphi} & \sin^2(\theta_\beta/2) \end{pmatrix} \right) a_\alpha (\hat{\sigma}_z^{\otimes 2}) \right] \\
&+ \text{Tr} \left[\left(\hat{\rho}_g^\alpha \otimes \hat{\rho}_g^\beta \right) b_\alpha \left(\begin{pmatrix} 1 & 0 \\ 0 & -1 \end{pmatrix} \otimes \begin{pmatrix} 1 & 0 \\ 0 & 1 \end{pmatrix} \right) \right] \\
&= a_\alpha \text{Tr} \left[\begin{pmatrix} \cos^2(\theta_\alpha/2) \cos^2(\theta_\beta/2); & \frac{1}{2} \cos^2(\theta_\alpha/2) \sin \theta_\beta e^{-i\varphi}; & \frac{1}{2} \sin \theta_\alpha e^{-i\varphi} \cos^2(\theta_\beta/2); & \frac{1}{4} \sin \theta_\alpha \sin \theta_\beta e^{-2i\varphi}; \\ \frac{1}{2} \cos^2(\theta_\alpha/2) \sin \theta_\beta e^{i\varphi}; & \cos^2(\theta_\alpha/2) \sin^2(\theta_\beta/2); & \frac{1}{4} \sin \theta_\alpha \sin \theta_\beta; & \frac{1}{2} \sin \theta_\alpha e^{-i\varphi} \sin^2(\theta_\beta/2); \\ \frac{1}{2} \sin \theta_\alpha e^{i\varphi} \cos^2(\theta_\beta/2); & \frac{1}{4} \sin \theta_\alpha \sin \theta_\beta; & \sin^2(\theta_\alpha/2) \cos^2(\theta_\beta/2); & \frac{1}{2} \sin^2(\theta_\alpha/2) \sin \theta_\beta e^{-i\varphi}; \\ \frac{1}{4} \sin \theta_\alpha \sin \theta_\beta e^{2i\varphi}; & \frac{1}{2} \sin \theta_\alpha e^{i\varphi} \sin^2(\theta_\beta/2); & \frac{1}{2} \sin^2(\theta_\alpha/2) \sin \theta_\beta e^{i\varphi}; & \sin^2(\theta_\alpha/2) \sin^2(\theta_\beta/2) \end{pmatrix} \begin{pmatrix} 1 & 0 \\ 0 & -1 & & \\ & & -1 & 0 \\ & & & 0 & 1 \end{pmatrix} \right] \\
&+ b_\alpha \text{Tr} \left[\begin{pmatrix} \cos^2(\theta_\alpha/2) \cos^2(\theta_\beta/2); & \frac{1}{2} \cos^2(\theta_\alpha/2) \sin \theta_\beta e^{-i\varphi}; & \frac{1}{2} \sin \theta_\alpha e^{-i\varphi} \cos^2(\theta_\beta/2); & \frac{1}{4} \sin \theta_\alpha \sin \theta_\beta e^{-2i\varphi}; \\ \frac{1}{2} \cos^2(\theta_\alpha/2) \sin \theta_\beta e^{i\varphi}; & \cos^2(\theta_\alpha/2) \sin^2(\theta_\beta/2); & \frac{1}{4} \sin \theta_\alpha \sin \theta_\beta; & \frac{1}{2} \sin \theta_\alpha e^{-i\varphi} \sin^2(\theta_\beta/2); \\ \frac{1}{2} \sin \theta_\alpha e^{i\varphi} \cos^2(\theta_\beta/2); & \frac{1}{4} \sin \theta_\alpha \sin \theta_\beta; & \sin^2(\theta_\alpha/2) \cos^2(\theta_\beta/2); & \frac{1}{2} \sin^2(\theta_\alpha/2) \sin \theta_\beta e^{-i\varphi}; \\ \frac{1}{4} \sin \theta_\alpha \sin \theta_\beta e^{2i\varphi}; & \frac{1}{2} \sin \theta_\alpha e^{i\varphi} \sin^2(\theta_\beta/2); & \frac{1}{2} \sin^2(\theta_\alpha/2) \sin \theta_\beta e^{i\varphi}; & \sin^2(\theta_\alpha/2) \sin^2(\theta_\beta/2) \end{pmatrix} \begin{pmatrix} 1 & 0 \\ 0 & 1 & & \\ & & -1 & 0 \\ & & & 0 & -1 \end{pmatrix} \right] \tag{B.39} \\
&= a_\alpha \text{Tr} \begin{pmatrix} \cos^2(\theta_\alpha/2) \cos^2(\theta_\beta/2); & -\frac{1}{2} \cos^2(\theta_\alpha/2) \sin \theta_\beta e^{-i\varphi}; & -\frac{1}{2} \sin \theta_\alpha e^{-i\varphi} \cos^2(\theta_\beta/2); & \frac{1}{4} \sin \theta_\alpha \sin \theta_\beta e^{-2i\varphi}; \\ \frac{1}{2} \cos^2(\theta_\alpha/2) \sin \theta_\beta e^{i\varphi}; & -\cos^2(\theta_\alpha/2) \sin^2(\theta_\beta/2); & -\frac{1}{4} \sin \theta_\alpha \sin \theta_\beta; & \frac{1}{2} \sin \theta_\alpha e^{-i\varphi} \sin^2(\theta_\beta/2); \\ \frac{1}{2} \sin \theta_\alpha e^{i\varphi} \cos^2(\theta_\beta/2); & -\frac{1}{4} \sin \theta_\alpha \sin \theta_\beta; & -\sin^2(\theta_\alpha/2) \cos^2(\theta_\beta/2); & \frac{1}{2} \sin^2(\theta_\alpha/2) \sin \theta_\beta e^{-i\varphi}; \\ \frac{1}{4} \sin \theta_\alpha \sin \theta_\beta e^{2i\varphi}; & -\frac{1}{2} \sin \theta_\alpha e^{i\varphi} \sin^2(\theta_\beta/2); & -\frac{1}{2} \sin^2(\theta_\alpha/2) \sin \theta_\beta e^{i\varphi}; & \sin^2(\theta_\alpha/2) \sin^2(\theta_\beta/2) \end{pmatrix} \\
&+ b_\alpha \text{Tr} \begin{pmatrix} \cos^2(\theta_\alpha/2) \cos^2(\theta_\beta/2); & \frac{1}{2} \cos^2(\theta_\alpha/2) \sin \theta_\beta e^{-i\varphi}; & -\frac{1}{2} \sin \theta_\alpha e^{-i\varphi} \cos^2(\theta_\beta/2); & -\frac{1}{4} \sin \theta_\alpha \sin \theta_\beta e^{-2i\varphi}; \\ \frac{1}{2} \cos^2(\theta_\alpha/2) \sin \theta_\beta e^{i\varphi}; & \cos^2(\theta_\alpha/2) \sin^2(\theta_\beta/2); & -\frac{1}{4} \sin \theta_\alpha \sin \theta_\beta; & -\frac{1}{2} \sin \theta_\alpha e^{-i\varphi} \sin^2(\theta_\beta/2); \\ \frac{1}{2} \sin \theta_\alpha e^{i\varphi} \cos^2(\theta_\beta/2); & \frac{1}{4} \sin \theta_\alpha \sin \theta_\beta; & -\sin^2(\theta_\alpha/2) \cos^2(\theta_\beta/2); & -\frac{1}{2} \sin^2(\theta_\alpha/2) \sin \theta_\beta e^{-i\varphi}; \\ \frac{1}{4} \sin \theta_\alpha \sin \theta_\beta e^{2i\varphi}; & \frac{1}{2} \sin \theta_\alpha e^{i\varphi} \sin^2(\theta_\beta/2); & -\frac{1}{2} \sin^2(\theta_\alpha/2) \sin \theta_\beta e^{i\varphi}; & -\sin^2(\theta_\alpha/2) \sin^2(\theta_\beta/2) \end{pmatrix} \\
&= a_\alpha \cos^2(\theta_\alpha/2) [\cos^2(\theta_\beta/2) - \sin^2(\theta_\beta/2)] + a_\alpha \sin^2(\theta_\alpha/2) [-\cos^2(\theta_\beta/2) + \sin^2(\theta_\beta/2)] \\
&+ b_\alpha \cos^2(\theta_\alpha/2) [\cos^2(\theta_\beta/2) + \sin^2(\theta_\beta/2)] - b_\alpha \sin^2(\theta_\alpha/2) [\cos^2(\theta_\beta/2) + \sin^2(\theta_\beta/2)] \\
&= a_\alpha \cos^2(\theta_\alpha/2) \cos \theta_\beta + a_\alpha \sin^2(\theta_\alpha/2) (-\cos \theta_\beta) + b_\alpha \cos \theta_\alpha = a_\alpha \cos \theta_\alpha \cos \theta_\beta - b_\alpha \cos \theta_\alpha \\
&= \cos \theta_\alpha (a_\alpha \cos \theta_\beta - b_\alpha).
\end{aligned}$$

$$\begin{aligned}
\bullet \quad \langle \hat{\sigma}_z \rangle_{\hat{\rho}_g^k} &= \text{Tr} \left[\hat{\rho}_g^k \hat{\sigma}_z \right] \stackrel{(4.25)}{=} \text{Tr} \left[\begin{pmatrix} \cos^2(\theta_k/2) & \frac{1}{2} \sin \theta_k e^{-i\varphi} \\ \frac{1}{2} \sin \theta_k e^{i\varphi} & \sin^2(\theta_k/2) \end{pmatrix} \begin{pmatrix} 1 & 0 \\ 0 & -1 \end{pmatrix} \right] \\
&= \text{Tr} \begin{pmatrix} \cos^2(\theta_k/2) & -\frac{1}{2} \sin \theta_k e^{-i\varphi} \\ \frac{1}{2} \sin \theta_k e^{i\varphi} & -\sin^2(\theta_k/2) \end{pmatrix} = \cos^2(\theta_k/2) - \sin^2(\theta_k/2) = \cos \theta_k.
\end{aligned} \tag{B.40}$$

Hence,

$$\langle \hat{H}_\alpha \rangle_{\hat{\rho}_g^\alpha \otimes \hat{\rho}_g^\beta} \stackrel{(B.39)}{=} \cos \theta_\alpha (a_\alpha \cos \theta_\beta - b_\alpha) \stackrel{(B.40)}{=} \langle \hat{\sigma}_z \rangle_{\hat{\rho}_g^\alpha} (a_\alpha \langle \hat{\sigma}_z \rangle_{\hat{\rho}_g^\beta} - b_\alpha). \tag{B.41}$$